12-15-2007

Development of Novel Liquid Chromatography-Electrospray Tandem Mass Spectrometry Approaches for the Structural Characterization of Brevetoxins Including in vitro Metabolites

Weiqun Wang
University of New Orleans

Development of Novel Liquid Chromatography-Electrospray Tandem Mass Spectrometry Approaches for the Structural Characterization of Brevetoxins Including in vitro Metabolites

A Dissertation

Submitted to the Graduate Faculty of the
University of New Orleans
in the partial fulfillment of the
requirements for the degree of

Doctor of Philosophy
in
The Department of Chemistry

by

Weiqun Wang

B.S. Nankai University, China, 1989
M.S. University of New Orleans, 2004

December 2007

ACKNOWLEGEMENTS

I am very grateful to the Department of Chemistry and Graduate School of the University of New Orleans for offering me the great chance to study and work at this great place.

I must thank my advisor: Dr. Richard B. Cole, who took a chance on me and kept me company during my long journey towards PhD degree. I learned a lot from him throughout my graduate studies. Without his patience and encouragement, I can never imagine being able to finish this program.

I would like to thank Dr. Guangdi Wang, who included me in their metabolism studies projects on cannabinoid receptor ligands, provided their HPLC instrument to our group for research, and included my name in their three publications.

I would like to thank current and former committee members: Dr. Yang Cai, Dr. Matthew A. Tarr, Dr. Ronald F. Evilia and Dr. Zeev Rosenzweig, they took their busy time to read my reports and dissertation and provided their valuable suggestions whenever I came to them. I especially thank Dr. Cai for hosting our whole group in his lab after Hurricane Katrina.

I would like to thank my colleagues: Kan Chen, Dr. Bing Guan, former member Yanjie Jiang, and Dr. Yan Li. My colleagues at Xavier University: Qiang Zhang and Peng Ma.

I would like to take this opportunity to thank Lexicon Pharmaceuticals for offering me current position after Hurricane Katrina, made it possible for me to finish my graduate program. I also want to thank all the people would help me during the aftermath of Hurricane Katrina.

Finally, I would like to thank my family for their endless love and support.

TABLE OF CONTENTS

ABSTRACT

Brevetoxins are natural neurotoxins that are produced by “red tide” algae. In this study, brevetoxin-1 and brevetoxin-2 were incubated with rat liver hepatocytes and rat liver microsomes, respectively. After clean-up steps, samples were analyzed by liquid chromatography-electrospray mass spectrometry (LC-ES-MS). Two metabolites were found for brevetoxin-1: brevetoxin-1-M1 (MW 900 Da), formed by converting one double bond in the E or F ring into a diol; and brevetoxin-1-M2 (MW 884 Da), a hydrolysis product of brevetoxin-1 involving opening of the lactone ring. The incubation study of brevetoxin-2 found two metabolites. Brevetoxin-2-M1 (MW 912 Da) was elucidated by negative mode LC-MS/MS to be the hydrolysis product of brevetoxin-2. The second metabolite (brevetoxin-2-M2, MW 896 Da) was deduced to be brevetoxin-3.

All brevetoxins have high affinities for sodium ions. Attempts to obtain informative product ions from the collision induced decomposition (CID) of $[M + Na]^+$ brevetoxin precursor ions only resulted in uninformative sodium ion signals. In our nano-electrospray experiments, the addition of ammonium fluoride resulted in the formation of the ammonium adduct or protonated brevetoxin with a concomitant decrease of the sodium adduct peak. Product ion spectra of $[M + NH_4]^+$ and $[M + H]^+$ were similar and provided useful structural information. The optimal values for ammonium fluoride concentration and the cone voltage were experimentally determined. In negative mode electrospray, without additives, deprotonated molecules of brevetoxins do not appear in high abundances, and thus are not well-suited for CID experiments. Several anions were tested for their abilities to form brevetoxin-anion adducts by mixing ammonium salts of these anions with brevetoxin-2 and brevetoxin-3. Under CID, $[M + Cl]^-$, $[M + Br]^-$, $[M + OAc]^-$, $[M + HCOO]^-$, $[M + NO_3]^-$ adducts all produced only the respective anions in CID experiments,

and thus, gave no structural information. In contrast, upon CID, both $[M + F]^-$ and $[M + HCO_3]^-$ precursor adducts gave structurally-informative fragment peaks that exhibited similarities to those of $[M - H]^-$ ions; the detailed fragmentation mechanisms are discussed. In comparison, fluoride is a better choice to study brevetoxins in negative ES-MS by the anionic adduct approach.

Key Words

Mass spectrometry, Brevetoxins, electrospray, liquid chromatography-mass spectrometry, metabolite, nano-electrospray, cationic adducts, anionic adducts

INTRODUCTION

A Brief History of Electrospray Mass Spectrometry

As an important analytical technique, mass spectrometry has a history of nearly one hundred years. J. J. Thomson won the Nobel Prize for his pioneering research in mass spectrometry. The first practical ionization source is electron impact or electron ionization (EI) source, which was first used by Dempster [1] and later developed by Nier [2]. For a long time, EI has been a standard ionization method for mass spectrometry. In 1966, Munson and Field [3] introduced chemical ionization (CI) to ionize molecules. Instead of by electron impact, the new technique generates characteristic ions of sample by ion-molecule reactions, a "softer" way of ionization. However, both methods require analyte to be volatile, limiting the technique to only a small fraction of organic compounds.

A revolution of mass spectrometry took place in the 1980's, electrospray ionization (ESI) [4]and matrix assistance laser desorption ionization (MALDI) [5, 6] were developed and widely accepted. ESI makes it practical to couple liquid chromatography with mass spectrometry (LC-MS). A wide range of compounds, from a hundred Dalton (small molecules) to macromolecules like proteins, can be introduced into the mass spectrometer by this ionization technique.

Electrospray as a phenomenon was observed long time ago. As early as the 1910's, physicist John Zeleny already reported a solution could be sprayed from a capillary when high voltage was applied [7, 8]. Malcom Dole and coworkers made the first attempt to couple this method with a

mass spectrometer [9]. Dole showed that it was possible to electrospray solutions of polystyrene with an average mass of 51k Da, and the desolvated ions could be measured based on their mass over charge ratio (m/z).

However, after Dole's work, research on electrospray as an ionization source became dormant. The real breakthrough came in 1980's, John Fenn, by then close to his retirement age at Yale's Department of Engineering and Applied Science, began to investigate ESI as an ion source for LC/MS interface, a great work that later lead to his receiving the Noble Prize. Fenn introduced bath gas into the ESI source to promote the desolvation of analyte solution droplets. He started with smaller molecules, but eventually achieved success with biomolecules, instead of the polymers that Dole used as study subjects [10, 11]. While John Fenn successfully developed electrosray ionization source in the US, at almost the same time, a group of Russian scientists also developed their ESI source independently [12].

In the 1990's, several attempts were made to combine ESI to several different mass analyzers. Besides John Fenn's established ESI-quadrupole arrangement, McLafferty and co-workers developed the ESI-FTICR interface; this combination allows high resolution and high mass range analysis. Larsen and McEwen [13, 14] developed an ESI/magnetic sector mass spectrometer, there are also several reports on ESI-TOF system[15-17], a combination that offers "unlimited" mass range and high mass accuracy at relatively low cost, and ESI coupling with the ion trap instrument [18, 19], a system that can perform multi-stage MS^n experiments.

Today, ESI has become one of the most important mass spectrometry ionization techniques and it has been applied to a wide range of research areas, from small molecules like pharmaceutical ingredients[20], organmetallic compounds [21] to macromolecules like polymers[22] and proteins[23].

Mechanistic Aspects of Electrospray

In electrospray, when a positive potential is applied to the solution in a capillary, driven by the electrophoresis of electrolytes, cations will migrate towards the outlet while anions will move in the opposite direction, thus, accumulating a net positive charge at the outlet tip. When the electrostatic forces and the surface tension reach a balance, the liquid will form a fully conical shape towards the counter electrode at the outlet, i.e., the so-called "Taylor cone"[24].The solution is dispersed into droplets from the cone tip, carrying net positive charges (in negative mode, the net charge is negative)[25]. The excess charges will be distributed on the surface of the droplet due to repulsive coulombic forces[26, 27].In the mean time, analyte molecules are also moving towards the surface until the partition between analytes on the surface and those inside the droplet reaches the equilibrium[28-31]. The surface activity of an analyte is an important factor to affect its electrospray signal in ESI-MS[32-35].

The behavior of charged droplets was studied by Lord Rayleigh as early as 1882[36]. Rayleigh developed his theory that predicts a droplet becoming unstable when the net charge of the droplet exceeds the limit, now known as the "Rayleigh limit". Such a limit can be reached by either

shrinking the droplet by evaporation or by applying excess charge. Once the net charge is above the limit, the droplet will break up into fine droplets, a process referred to as a "Rayleigh discharge" or "Coulomb fission"[37, 38].

The detailed mechanism of a droplet's evolution during its voyage from the liquid phase to the gas phase to finally generate the solute ion has been the subject of a large number of investigations and discussions, and even debates [37, 39, 40]. Two main theories have been proposed to explain the process. The ion evaporation model (IEM) and the charged residue model (CRM). Introduced by Iribarne and Thomson, the ion evaporation model predicts that the electric field on a droplet surface increases during droplet evaporation, and becomes strong enough to overcome the solvation forces and finally desorb solute ions from droplet surface into the gas phase[41-43]. The charged residue model, first proposed by Dole and co-workers, on the other hand, assumes that solvent evaporation will yield Coulomb fission due to Rayleigh instability. Such fission will repeat over and over and result in an ultimate droplet, containing only one molecule of solute, which in the end retains the droplet's charge when the last solvent molecule evaporates [9, 44]. These two models each have supporting evidence and they cannot rule each other out. In general, the formation of small molecule ions is more likely via ion evaporation model[45], while that of macromolecule ion is more likely via the charged residue model[46, 47].

In the gas phase, ion clusters, gaseous ions, neutral molecules and clusters are still under atmospheric pressure condition and will undergo a lot of low-energy collision. A molecule can be protonated or deprotonated by proton transfer reaction. The proton affinity of an analyte can

be defined as the negative of the enthalpy change of its protonation reaction. A protonated molecule may lose its proton to another molecule if the latter one has higher proton affinity [48-51].

Electrospray and LC/MS

Electrospray also has made it convenient interface to couple reversed phase high performance liquid chromatography (RP-HPLC) with mass spectrometry. Coupling chromatographic techniques and mass spectrometry will combine both the power of separation and the capability of structure identification, which makes it a versatile combination. GC-MS is the first practical instrument to use this concept. However, the majority of organic compounds are not volatile and can only be analyzed by liquid chromatography rather than gas chromatography. When EI and CI were the only ionization techniques available, LC-MS was quite challenging due to the difficulty to introduce LC eluant into a high vacuum EI or CI source. It was not until the 1970s that LC-MS drew more and more research interest. Scott et al. introduced the concept of moving-wire interface[52], and later on, the first commercial LC-MS with moving belt interface was marketed by Finnigan Instrument (now part of Thermo-Fisher)[53, 54]. Such interfacing provided the capability of generating EI or CI spectra; EI is advantageous for library structure searching. However, the interface is quite expensive and technically demanding, and still requires a narrow range of volatility for analytes: compounds with low volatility are difficult to remove from the belt; highly volatile compounds, on the other hand, may be lost from the belt before entering the instrument[55].

The development of electrospray ionization provided a new approach for LC-MS interfacing. It can ionize non-volatile analytes under relatively low temperature, a quite desirable ionization technique for the majority of biomedical samples, which are usually polar and thermally-labile. One difficulty to combine LC with ESI-MS directly is the difference between the high flow rate of LC (1 mL/min from a conventional LC column) and the low flow rate of ESI (2-10 μL/min). Bruins introduced pneumatically-assisted electrospray technique (commercialized as IonSpray®) to accommodate higher flow rates[56, 57]. With the support of a stream of coaxial inert gas, usually nitrogen, such a design can hold a flow rate of up to 0.2 mL/min, which is compatible with 2 mm ID LC column and still offers a stable spray[58-60]. If an additional heating device is introduced around the spray capillary that heats the surrounding air to about 250 °C, the flow rate can be as high as 2 mL/min[61].

In addition, instrument companies also develop techniques (under different trade names) to get rid of most of the large droplets and only allow a small part of charged droplets to reach the first vacuum stage of the mass spectrometer (for example, Z-Spray® by Micomass/Waters), which is a different approach to accommodate high flow rates. Nowadays, LC-ESI-MS has become one of the most widely applied techniques in biomedical research [62-64].

Nano-electrospray

One challenge faced by analysts in proteomics studies is the small amounts of analyte in biological samples, in some cases, less then ten micro-liters. While the optimum flow rate for conventional ESI is usually 2-10 μL/min, such amounts of sample would not provide analysis time long enough to accomplish tuning and data acquisition, and diluting the sample to obtain a larger volume usually would not solve the problem either.

In 1994, Emmet and Caprioli developed a "micro-electrospray" device, using a fused silica capillary with a smaller inner diameter. It can reduce the sample flow rate to 0.1 μL/min[65]. Later, the real innovation called "nano-electrospray" (nano-ESI) came in 1996, made by Wilm and Mann, they used disposable glass capillary tips as electrospray emitters, which are drawn out at one end to give orifices of 1-10 μm in diameter. Metal films (e.g., gold) are usually coated on the outside of the emitter to get sufficient conductivity. The emitters are loaded with sample from 1-5 μL by a special gel loader tip. When high voltage is applied, the electric field will generate an electrospray flow of 20-50 nL/min; sometimes a low back pressure to the emitter is helpful to initiate the flow. Therefore, a 1 μL sample can last for 20 minutes or even longer, which is sufficient to record positive and negative signals and conduct MS/MS, even MS^n experiments.

Unlike micro-electrospray, which is more or less a low-flow conventional electrospray, nano-electrospray shows some fundamental advantages. Since nano-ESI starts with the droplets much

smaller than those made by conventional ESI (0.1-0.2 μm vs 1-2 μm in diameter), therefore, unlike conventional ESI, where droplets undergo solvent evaporation, then uneven fission, yielding second generation droplets, the droplets produced by nano-ESI can be one generation less than those produced by conventional ESI, which helps to obtain good signals from complicated biological samples [66]. Juraschek et al reported that nano-electrospray gave satisfactory results for insulin samples containing 10 mM NaCl, while using conventional ESI, no useful data was obtained[67].

Physiological Effects of Brevetoxins.

Brevetoxins are natural toxins that are produced from a single cell dinoflagellate *Karenia brevis* that is responsible for blooms of "red tide" algae[68], red tide can cause massive fish kills and human health hazard. The physiological effects of brevetoxins are mainly neurotoxic symptoms in animals and humans. This type of toxin can induce central depression of respiratory and cardiac functions, spontaneous muscle contractions, spasms and rhinorrhea[69]. The toxicity of brrevetoxins stems from the fact that they bind to a specific receptor site in the voltage sensitive sodium channel (VSSC) in the cell membrane[70]. Binding involves a complicated series of association-dissociation events, and the whole binding process may need several hours to reach equilibrium [71]. It is hypothesized that the binding of brevetoxins to this VSSC receptor site will push the channel in favor of its open conformation, thus shifting the channel activation voltage and prolonging the activation duration time, while inhibiting its inactivation function[72]. Over time, cells can no longer conduct their functions properly, and many

symptoms such as hypertension and arrhythmia will occur. In clinical animal trials, the symptoms could lead to death[69].

Microsomes and Hepatocytes

Because liver is the major organ for toxic chemical biotransformations, it is the tissue of choice for metabolism and toxicity studies. Due to the limited availability of human liver tissue, rat, a species that may genetically approximate humans, is widely used in the pharmaceutical industry for *in vivo* metabolism studies and its liver tissue used in *in vitro* metabolism screening [73]. The metabolite profile of a drug obtained *in vitro* generally reflects the *in vivo* metabolite pattern, although results are limited to qualitative aspects[74]. Because of this, *in vitro* metabolism techniques involving liver tissue, including isolated liver hepatocytes and microsomes, have been developed[75]. Liver microsomes are prepared by homogenization of livers (fresh or frozen), followed by centrifugation of the homogenate at 9,000-10,000 times the force of gravity (9,000-10,000 g) to precipitate the unbroken cells, nuclei and mitochondria, yield a supernatant subcellular fraction (also known as S9 or S10); further centrifugation such fraction at about 100,000 g will yield a microsome pellet [76]. Microsomes contain many xenobiotic-metabolizing enzymes, the most prominent group of enzymes is the family of cytochrome P450 (CYPs). These enzymes play a key role in the metabolism of a variety of chemically diverse compounds.

Like liver microsomes, hepatocytes are also widely employed in *in vitro* metabolism studies. Hepatocytes are isolated from liver by so-called two-step collagenase digestion procedures. A freshly isolated liver is perfused first with an isotonic buffer solution containing a calcium chelating agent to clear the blood and to loosen cell-cell junctions, followed by a collagenase solution to dissociate the hepatocytes from the liver parenchyma [77]. Cryopreserved hepatocytes are also available, but some enzyme reactivity (including P450) might be lower than that of freshly isolated hepatocytes, and both types lose enzyme activity fairly rapidly with time. Due to this, and the commercial shortage of fresh liver, many laboratories favor liver microsomes since they can be prepared and purchased in large batches and preserved at –80 °C for many months with little loss of P450 activity [78]. However, hepatocytes are an integrated cellular system, which is closer to the real situation, and can demonstrate both phase I metabolism (oxidation, reduction or hydrolysis) and phase II metabolism (conjugate reactions of the parent or the metabolites from phase I), an advantage over microsomal systems since the latter can only provide information on phase I metabolism [79].

REFERENCES

1. Dempster AJ: **Positive Ray Analysis of Lithium and Magnesium**. *Phys Rev* 1921, **18**(6):415-422.
2. Nier AO: **A Mass Spectrometer for Isotope and Gas Analysis**. *Rev Sci Instrum* 1947, **18**(12):398-411.
3. Munson MSB, Field FH: **Chemical Ionization Mass Spectrometry. I. General Introduction**. *J Am Chem Soc* 1966, **88**(12):2621-2630.
4. Fenn JB, Mann M, Meng CK, Wong SF, Whitehouse CM: **Electrospray ionization for mass spectrometry of large biomolecules.** *Science* 1989, **246**(64-71).
5. Karas M, Hillenkamp F: **Laser Desorption ionization of proteins with molecular masses exceeding 10, 000 Daltons**. *Anal Chem* 1988, **60**(20):2299-2301.
6. Tanaka K, Waki H, Ido Y, Akita S, Yoshida Y, Yoshida T: **Protein and polymer analyses up to m/z 100,000 by laser ionization time-of-flight mass spectrometry.** *Rapid Commun Mass Spectrom* 1988, **2**:151-153.
7. Zeleny J: **The Electrical Discharge from Liquid Points, and a Hydrostatic Method of Measuring the Electric Intensity at Their Surfaces.** *Phys Rev* 1914, **1914**(3):69-91.
8. Zeleny J: **Instability of Electrified Liquid Surfaces**. *Phys Rev* 1917, **10**(1):1-6.
9. Dole M, Mack LL, Hines RL, Mobley RC, Ferguson LD, Alice MB: **Molecular Beams of Macroions.** *J Chem Phys* **1968**, **49**(5):2240-2249.
10. Yamashita M, Fenn J: **Electrospray Ion Source. Another Variation on the Free-Jet Theme.** *J Phys Chem* **1984**, **88**:4451-4459.

11. Yamashita M, Fenn J: **Negative Ion Production with the Electrospray Ion Source.** *J Phys Chem* 1984, **88**:4671-4675.

12. Aleksandrov ML, Gall LN, Krasnov VN, Nikolaev VI, Pavlenko VA, Shkurov VA: **Ion extraction from solutions at atmospheric pressure - a method for mass-spectrometric analysis of bioorganic substances**. *Dokl, Akad, Nauk SSSR* 1984, **277**:379-383.

13. Larson BS, McEwen CN: **An electrospray ion source for magnetic sector mass spectrometers**. *J Am Soc Mass Spectrom* 1991, **2**:205-211.

14. Meng CK, McEwen CN, Larson BS: **Electrospray ionization on a high-performance magnetic-sector mass spectrometer**. *Rapid Commun Mass Spectrom* 1990, **4**(5):147-150.

15. Boyle JG, Whitehouse CM: **Time-of-Flight Mass Spectrometry with an Electrospray Ion Beam.** *Anal Chem* **1992**, **64**:2084-2089.

16. Zhao J, Zhu J, Lubman DM: **Liquid sample injection using an atmospheric pressure direct current glow discharge ionization source**. *Anal Chem* 1992, **64**(13):1426-1433.

17. Verentchikov AN, Ens W, Standing KG: **Reflecting time-of-flight mass spectrometer with an electrospray ion source and orthogonal extraction**. *Anal Chem* 1994, **66**(1):126-133.

18. Van Berkel GJ, Glish GL, McLuckey SA: **Electrospray ionization combined with ion-trap mass spectrometry** *Anal Chem* 1990, **62**(13):1284-1295.

19. Schwartz JC, Syka JEP, Jardine I: **High resolution on a quadrupole ion trap mass spectrometer** *J AM Soc Mass Spectrom* 1991, **2**(5):198-204.

20. Wickremsinhe ER, Singh G, Ackermann BL, Gillespie TA, Chaudhary AK: **A review of nanoelectrospray ionization applications for drug metabolism and pharmacokinetics.** *Current Drug Metaolism* 2006, **7**(8):913-928.

21. Plattner DA: **Electrospray mass spectrometry beyond analytical chemistry: studies of organometallic catalysis in the gas phase.** *International Journal of Mass Spectrometry* 2001, **207**(3):125-144.

22. Barner-Kowollik C, Davis TP, Stenzel MH: **Probing mechanistic features of conventional, catalytic and living free radical polymerizations using soft ionization mass spectrometric techniques**. *Polymer* 2004, **45**(23):7791-7805.

23. Konermann L, Pan J, Wilson DJ: **Protein folding mechanisms studied by time-resolved electrospray mass spectrometry.** *BioTechniques* 2006, **40**(2):135-141.

24. Taylor GI: **Disintegration of Water Drops in an Electric Field.** *Proc R Soc London* **1964**, **A280**:383-397.

25. Pfeifer RJ, Hendricks CD: **Parametric Studies of Electrohydrodynamic Spraying.** *AIAA Journal* **1968**, **6**: 496-502.

26. Fenn JB: **Ion Formation from Charged Droplets: Roles of Geometry, Energy, and Time.** *J AM Soc Mass Spectrom* **1993**, **4**:524-535.

27. Karplus PA: **Hydrophobicity regained**. *Protein Sci* 1996, **6**:1302-1307.

28. Cech NB, Enke CG: **The effect of affinity for charged droplet surfaces on the fraction of analyte charged in the electrospray process.** *Anal Chem* 2001, **73**:4632-4639.

29. Cech NB, Enke CG: **Relating electrospray ionization response to non-polar character of small peptides.** *Anal Chem* 2000, **72**:2717-2723.

30. Tang K, Smith RD: **Physical/chemical separations in the break-up of highly charged droplets from electrosprays**. *J Am Chem Soc* 2001, **12**:343-347.

31. Enke CG: **A Predictive Model for Matrix and Analyte Effects in Electrospray Ionization of Singly-Charged Ionic Analytes.** *Anal Chem* **1997**, **69**:4885-4893.

32. Cech NB, Krone JR, Enke CG: **Predicting electrospray response from chromatographic retention time**. *Anal Chem* 2001, **73**(208-213).

33. Constantopoulos TL, Jackson GS, Enke CG: **Effects of salt concentration on analyte response using electrospray ionization mass spectrometry**. *J Am Soc Mass Spectrom* 1999, **10**:625-634.

34. Constantopoulos TL, Jackson GS, Enke CG: **Challenges in acheiving a fundamental model for ESI**. *Anal Chim Act* 2000, **406**:37-52.

35. Sjoberg PJR, Bokman CF, Bylund D, Markides KE: **A method for determination of ion distribution within electrosprayed droplets.** *Anal Chem* 2001, **73**:23-28.

36. Rayleigh L: **On the Equilibrium of Liquid Conducting Masses Charged with Electricity.** *Philos Mag* **1882**, **14**:184.

37. Kebarle P: **A brief overview of the present status of the mechanisms involved in electrospray mass spectrometry**. *J Mass Spectrom* 2000, **35**(7):804-817.

38. Gomez A, Tang K: **Charge and Fission of Droplets in Electrostatic Sprays.** *Phys Fluids* **1994**, **6**: 404-414.

39. Cole RB: **Some tenets pertaining to electrospray ionization mass spectrometry**. *J Mass Spectrom* 2000, **35(7)**:763-772.

40. Fernandez De la Mora J, Van Berkel GJ, Enke CG, Cole RB, Martinez-Sanchez M, Fenn JB: **Electrochemical processes in electrospray ionization mass spectrometry**. *J Mass Spectrom* 2000, **35(8)**:939-952.

41. Iribarne JV, Thomson BA: **On the Evaporation of Small Ions from Charged Droplets.** *J Chem Phys* **1976**, **64**:2287-2294.

42. Iribarne JV, Dziedzic PJ, Thomson BA: **Atmospheric pressure ion evaporation-mass spectrometry**. *Int J Mass Spectrom Ion Phys* 1983, **50**:331-347.

43. Thomson BA, Iribarne JV: **Field Induced Ion Evaporation from Liquid Surfaces at Atmospheric Pressure.** *J Chem Phys* **1979**, **71**:4451-4463.

44. Mack LL, Kralik P, Rheude A, Dole M: *J Chem Phys* 1970, **52**:4977.

45. Kebarle P, Peschke M: **On the mechanisms by which the charged droplets produced by electrospray lead to gas phase ions**. *Anal Chim Acta* 2000, **406**(1):11-35.

46. Wang G, Cole RB: **Solvation Energy and Gas-Phase Stability Influences on Alkali Metal Cluster Ion Formation in Electrospray Ionization Mass Spectrometry.** *Anal Chem* **1998**, **70**:873-881.

47. Wang G, Cole RB: **Charged Residue vs Ion Evaporation for Formation of Alkali Metal Halide Cluster Ions in ESI.** *Anal Chim Acta* 2000, **406**:53-65.

48. Stephenson JL, McLuckey SA: **Ion/ion proton transfer reactions for protein mixture analyis.** *Anal Chem* 1996, **68**:4026.

49. Amad MaH, Cech NB, Jackson GS, Enke CG: **Importance of gas-phase proton affinities in determining the electrospray ionization response for analytes and solvents**. *J Mass Spctrom* 2000, **35**(7):784-789.

50. Zhou S, Hamburger M: **Effects of solvent composition of molecular ion response in electrospray mass spectrometry: investigation of the ionization process.** *Rapid Commun Mass Spectrom* 1995, **9**:1516-1521.

51. Yen T-Y, Charles MJ, Voyksner RD: **Processes that affect electrospray ionization-mass spectrometry of nucleobases and nucleosides.** *J Am Soc Mass Spectrom* 1996, **4**:596-603.

52. Scott RPW, Scott CG, Munroe M, Hess J: **Interface for on-line liquid chromatography—mass spectroscopy analysis**. *J Chromatogr* 1974, **99**:395-405.

53. McFadden WH, Schwartz HL, Evans S: **Direct analysis of liquid chromatographic effluents**. *J Chromatogr* 1976, **122**:389-396.

54. Arpino PJ: **Ten years of liquid chromatography-mass spectrometry.** *J Chromatogr* 1985, **323**(1):3-11.

55. Arpino P: **Coupling techniques in LC/MS and SFC/MS.** *Fresenius' Journal of Analytical Chemistry* 1990, **337**(6):667-685.

56. Bruins AP, Covey TR, Henion JD: **Ion Spray Interface for Combined Liquid Chromatography/Atmospheric Pressure Ionization Mass Spectrometry.** *Anal Chem* **1987**, **59**:2642-2646.

57. Bruins AP: **Atmospheric-pressure-ionization mass spectrometry. I. Instrumentation and ionization techniques**. *Trends in Analytical Chemistry* 1994, **13**(1):37-43.

58. Ikonomou MG, Blades AT, Kebarle P: **Electrospray-Ion Spray: A Comparison of Mechanisms and Performance.** *Anal Chem* **1991**, **63**:1989-1998.

59. Dulcks T, Juraschek R: **Electrospray as an ionization method for mass spectrometry.** *Journal of Aerosol Science* 1999, **30**(7):927-943.

60. Ikonomou MG, Blades AT, Kebarle P: **Investigations of the Electrospray Interface for Liquid Chromatography/Mass Spectrometry.** *Anal Chem* **1990**, **62**:957-967.

61. Huang EC, Wachs T, Couboy JJ, Henion JD: **Atmospheric Pressure Ionization Mass Spectrometry.** *Anal Chem* **1990**, **62**:713A-725A.

62. Chen J, Korfmacher WA, Hsieh Y: **Chiral liquid chromatography-tandem mass spectrometric methods for stereoisomeric pharmaceutical determinations.** *J Chromatogr B* 2005, **820**(1):1-8.

63. Delahunty C, Yates JR, III.: **Protein identification using 2D-LC-MS/MS.** *Methods (San Diego, CA, United States)* 2005, **35**(3):248-255.

64. Backer LC, Fleming LE, Rowan A, Cheng YS, Pierce R: **Recreational exposure to aerosolized brevetoxins during Florida red tide events.** *Harmful Algae* 2003, **2**:19-28.

65. Emmett MR, Caprioli RM: **Micro-Electrospray Mass Spectrometry: Ultra-High-Sensitivity Analysis of Peptides and Proteins.** *J Am Soc Mass Spectrom* **1994**, **5**:605-613.

66. Karas M, Bahr U, Dulcks T: **Nano-electrospray ionization mass spectrometry: addressing analytical problems beyond routine.** *Fresenius' Journal of Analytical Chemistry* 2000, **366**(6-7):669-676.

67. Juraschek R, Dulcks T, Karas M: **Nanoelectrospray—more than just a minimized-flow electrospray ionization source**. *J Am Soc Mass Spectrom* 1999, **10**(4):300-308.

68. Risk M, Lin YY, MacFarlane RD, Ramanujam VMS, Smith LL, Trieff NM: **Purification and chemical studies on a major toxin from *Gymnodinium breve.*** In: *Toxic Dinoflagellate Blooms : Proceedings of second International Conference on Toxic*

Dinoflagellate Blooms. Edited by Taylor DL, Seliger HH. New York: Elsevier/North Holland; 1979: 335-344.

69. Washburn BS, Rein KS, Baden DG, Walsh PJ, Hinton DE: **Brevetoxin-6 (pbTx-6), a Nonaromatic Marine Neurotoxin Is a Ligand of the Aryl Hydrocarbon Receptor.** *Arch Biochem Biophy* **1997**, **343**:149-156.

70. Baden DG: **Brevetoxins: Unique polyether dinoflagellate toxins.** *FASEB J* 1989, **3**:1807-1817.

71. Whitney P, Baden DG: **Complex Association and Dissociation Kinetics of Brevetoxin Binding to Voltage-Sensitive Tate Brain Sodium Channels.** *Natural Toxin* **1996**, **4**:261-270.

72. Poli M: **Laboratory Procedures for Detoxification of Equipment and Waste Contaminated with Brevetoxins PbTx-2 and PbTx-3.** *J Assoc Off Anal Chem* **1988**, **71**:1000-1002.

73. Riley RJ, Grime K: **Metabolic screening in vitro: metabolic stability, CYP inhibition and induction**. *Drug Discovery Today:Technology* 2004, **1**(4):365-372.

74. Lin JH, Lu AY: **Role of pharmacokinetics and metabolism in drug discovery and development**. *Pharmacological Reviews* 1997, **49**(4):403-449.

75. Powis G: **The use of human liver for foreigh compound metabolism and toxicity studies**. *Drug Metabolism Reviews* 1989, **20**:379-394.

76. Penman BW, Reece J, Smith T, Yang CS, Gelboin HV, Gonzalez FJ, Crespi CL: *Pharmocogenetics* 1993, **3**:28-39.

77. Li AP: **Screening for human ADME/Tox drug properties in drug discovery**. *Drug Discovery Today* 2001, **6**(7):357-366.

78. Yan Z, Caldwell GW: **Metabolism profiling, and cytochrome P450 inhibition & induction in drug discovery**. *Curent Topics in Medicinal Chemistry* 2001, **1**(5):403-425.

79. Gunaratna C: **Drug metabolism &pharmacokinetics in drug discovery: a primer for bioanalytical chemists**. *Current Separations* 2000, **19**(1):17-23.

Chapter I

Characterization of Rat Liver Microsomal and Hepatocytal Metabolites of Brevetoxins by Liquid Chromatography-Electrospray Tandem Mass Spectrometry

Abstract

Brevetoxins are natural neurotoxins that are produced by "red tide" algae. This class of compounds can cause neurotoxic shellfish poisoning and other health problems. Brevetoxin-2 is the most abundant among the nine brevetoxins that have been characterized, whereas brevetoxin-1 is the most toxic. In this study, brevetoxin-1 and brevetoxin-2 were incubated with rat liver hepatocytes and rat liver microsomes, respectively. After clean-up steps were taken to remove the proteins, samples were analyzed by liquid chromatography (LC) coupled with electrospray mass spectrometry (LC-MS). After incubation of brevetoxin-1, two metabolites were found: brevetoxin-1-M1 (molecular weight = 900 Da), and brevetoxin-1-M2 (molecular weight = 884 Da). The increase in molecular weight combined with evidence from tandem mass spectrometry showing an increased tendency for loss of water molecules; along with considerations of established precedents for chemical transformations led to the conclusion that brevetoxin-1-M1 was formed by converting one double bond in the E or F ring of brevetoxin-1 into a diol. The second metabolite (brevetoxin-1-M2) is proposed to be a hydrolysis product of brevetoxin-1 involving opening of the lactone ring with the addition of a water molecule. The incubation study

of the other starting compound, i.e. brevetoxin-2 found two metabolites in the LC-ES-MS selected ion chromatogram. Brevetoxin-2-M1 (molecular weight = 912 Da) gave a large $[M-H]^-$ peak at m/z 911, and its product ion mass spectrum allowed the deduction that this metabolite was the hydrolysis product of brevetoxin-2 involving conversion of the lactone to a carboxylic acid and an alcohol. The second metabolite (brevetoxin-2-M2, molecular weight = 896 Da) was deduced to have the same structure as that of brevetoxin-3 based on identical chromatographic retention times and similar mass spectra as those obtained for a brevetoxin-3 standard.

Keywords: brevetoxins, red tide, metabolite, electrospray, LC-MS, mass spectrometry

1.1 Introduction

Brevetoxins are natural toxins that are produced from a single cell dinoflagellate *Karenia brevis* (formerly known as *Ptychodiscus brevis and Gymnodinium breve*) that is responsible for blooms of "red tide" algae [1, 2]. This algae can grow rapidly under appropriate conditions of nitrate concentration, salinity, water depth and other factors [3]. Outbreaks of "red tide" have been a recurring problem in the Gulf of Mexico in recent years. In fact, it is reported that since the 1970s, the rate of reoccurrence of this harmful algal bloom in the US has increased. For example, the *Karenia brevis* outbreak off the western coast of Florida occurs every 3-5 years [4]. The

toxins produced from such algae are lipid soluble polyether neutrotoxins that can cause massive fish kills. They also can cause human health hazards such as food (shellfish) poisoning [5], respiratory problems, eye irritation and skin irritation[6-8]. Such harmful blooms usually impair the fishery industries (e.g. causing closing of shellfish beds), as well as the tourism industry. For example, in October of 1996, a *Karenia brevis* bloom occurred in the shellfish harvesting waters (Gulf of Mexico) off of Louisiana, Mississippi and Alabama. Brevetoxin-2 dominated the *Karenia brevis* toxin profile in the bloom, and shellfish toxicity exceeded the guidance level for 75 days even after the bloom had dissipated [9]. Also in the spring of that same year, a bloom of *Karenia brevis* appeared along the southwest coast of Florida, and at least two hundred manatees were found dead or dying in the coastal waters, or on beaches, in an ecological disaster[10]. The physiological effects of brevetoxins are mainly neurotoxic symptoms in animals and humans. This type of toxin can induce central depression of respiratory and cardiac functions, spontaneous muscle contractions, spasms, rhinorrhea, and the symptoms sometimes led to death[11].

The structures of brevetoxins are complicated and their molecular weights are nearly 1000 Da, so the structural elucidation of these compounds is quite challenging. In 1981, Lin et al. [12] first reported the structural identification of brevetoxin-2, the most naturally abundant brevetoxin species. Since then, there are a total of nine brevetoxins that have been structurally elucidated[5, 13, 14]. Based on their backbone structures, they can be divided into two categories (Figure 1.1): type A, which has 10 polyether rings; and type B, which has 11 polyether rings.

Currently, there are only a few reports on metabolite studies of brevetoxins, and these mainly pertain to metabolites found in shellfish. A case study of shellfish poisoning in Florida found four major metabolites by HPLC-MS and radioimmunoassy[15]. One is identified as brevetoxin-3, which was likely produced by reduction of the dominant parent toxin brevetoxin-2. When detected in the form of protonated molecules, $[M+H]^+$, the remaining three metabolites appeared at m/z 1018, 1034 and 1006. Two of these metabolites were recently identified as a cysteine conjugate (m/z 1018) and its sulfoxide form (m/z 1034) of brevetoxin-2 [16]. In addition, that same recent study assigned m/z 990 and m/z 1006 as a cysteine-brevetoxin-1 conjugate and its sulfoxide, respectively. In 1993, more than 280 people suffered from shellfish poisoning in New Zealand in a single incident[17, 18] related to consumption of "Greenshell Mussels". Two major metabolites were separated and identified: One appeared at m/z 1135.7 in negative mode FAB-MS. Combined with information obtained from NMR studies, the structure was determined to be a D-ring opening of brevetoxin-2 with esterification of the resulting alcohol and oxidation of the terminal aldehyde to the acid form[17, 19]. The other metabolite appeared at m/z 1034.5 in its protonated form. It can be described as a 1,4-addition of L-cysteine to the terminal side chain group of brevetoxin-2 followed by oxidation of the sulfide to sulfoxide and reduction of the aldehyde to an alcohol. However, studies on the metabolic pathways of brevetoxins in mammalian species are still rare. An early study in 1989 reported the observation of two metabolic products in rat liver hepatocytes using a radiolabeled compound. However, the structures of these two metabolites were not elucidated[20].

In the current study, rat liver microsomes were applied to the *in vitro* metabolism study of brevetoxin-2, the dominant species of brevetoxins, and high performance liquid chromatography

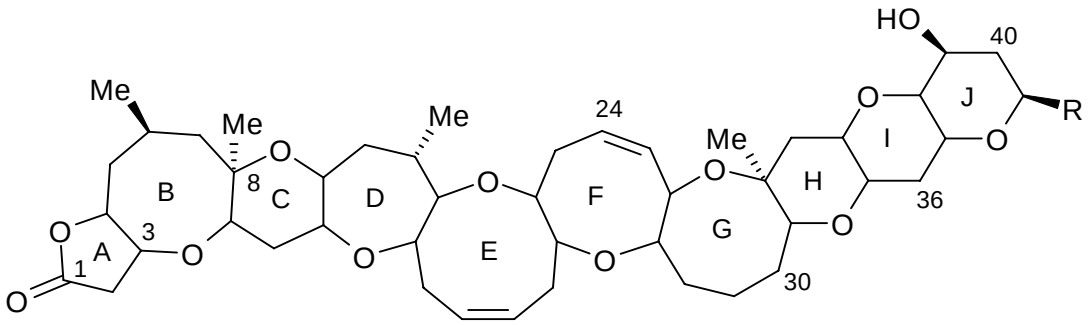

(monoisotopic mass, M_r)

Type-A Brevetoxins:	Brevetoxin-1, R=$CH_2C(=CH_2)CHO$	(866.5)
	Brevetoxin-7, R=$CH_2C(=CH_2)CH_2OH$	(868.5)
	Brevetoxin-10, R=$CH_2CH(CH_3)CH_2OH$	(870.5)

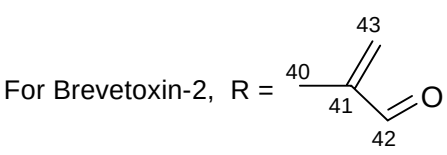

(monoisotopic mass, M_r)

Type-B Brevetoxins:	Brevetoxin-2, R=$CH_2C(=CH_2)CHO$	(894.6)
	Brevetoxin-3, R=$CH_2C(=CH_2)CH_2OH$	(896.6)
	Brevetoxin-8, R=CH_2COCH_2Cl	(916.4)
	Brevetoxin-9, R=$CH_2CH(CH_3)CH_2OH$	(898.6)
	Brevetoxin-5, the K-fing acetate of brevetoxin-2	(936.6)
	Brevetoxin-6, the H-ring epoxide of brevetoxin-2	(910.6)

Figure 1.1. General structures of the two main types of brevetoxins

coupled with tandem mass spectrometry was used for separation and identification of metabolic products. In addition, brevetoxin-1 was incubated with rat hepatocytes and analyzed by similar LC-MS/MS approaches.

2.2 Experimental Section

Materials: Brevetoxin-1 was purchased from Chiral Corp. (Miami, FL), Brevetoxin-2 and brevetoxin-3 were purchased from CalBiochem (La Jolla, CA), HPLC-grade methanol and water were purchased from EM Sciences (Gibbstown, NJ). Rat hepatocyte wells were purchased from CEDRA Corp. (Austin, TX); rat liver microsomes and NADPH regenerated system were purchased from Genetest Corp. (Woburn, MA).

Microsomal incubation: According to the basic approach of Degawa et al. [21] and Zhang et al. [22, 23], 2 μL of 5 mM brevetoxin-2 in ethanol was added to the incubation system as the substrate, the incubation mixture also included rat liver microsomes (at 1.5 mg/mL protein concentration), 16.5 mM glucose-6-phosphate, 16.5 mM magnesium chloride, and 70 mM potassium phosphate buffer (pH 7.4) to make 0.1 mL aliquots each containing 0.1 mM brevetoxin-2[22]. The incubation was conducted in a VWR 1225 (Cornelius, OR) water bath at 37 °C for 12-24 hours. Blank and control incubations were also conducted, including incubation in the absence of microsomes, incubation in the absence of brevetoxin-2, and incubation in the absence of NADPH regenerating system. The incubation was stopped by adding an equal volume of ice cold methanol; the mixture was then vortexed and centrifuged, and the supernatant was passed through a Microcon YM-3 filter (Pittsburgh, PA) to further remove protein.

Rat hepatocyte incubation: The procedure was based on the method of Ekwall et al. [24]. Substrate solution (10 μg brevetoxin in 1 mL William E medium) was added into a rat hepatocyte well containing about 1 million cells. After 24 hours incubation at 37 ^{0}C in a 5% CO_2 incubator, the incubation was stopped by adding 2 mL CH_3CN. The solution was filtered (0.2 μm) and evaporated to 0.8 mL to eliminate virtually all organic solvent[25]. Blank (hepatocyte incubation performed with no added brevetoxin) and control tests (brevetoxin-1 added after a blank incubation was quenched to check for the possibility of solution hydrolysis) were also performed. These controls insured that observed peaks actually corresponded to brevetoxin metabolites . The solution containing substrate and metabolites was cleaned up by solid phase extraction and concentrated to 100 μL prior to LC/MS analysis.

LC-MS and LC-MS-MS Analyses: After incubation and protein clean-up, the brevetoxin-2 incubation sample was separated by liquid chromatography (LC) equipped with parallel LC-10 ADVP pumps and a UV-Vis SPD-10ADVP detector (Shimadzu Instruments Co. Columbia, MD). A 2.1 x 100 mm, 3.5 μm C-18 Agilent (Wilmington, DE) LC column, coupled with 2.1 x 12.5 mm Agilent (Wilmington, DE) C-18 guard column was employed to separate the mixture. The mobile phase was 80:20 methanol:water for the first 2.5 minutes, then linearly changed to 90:10 methanol:water in one minute. The flow rate was set at 0.2 mL/min. The brevetoxin-1 sample was separated on a 1 x 100 mm, 3 μm C-18 Spherisorb column (ISCO, Lincoln, NE), with an isocratic mobile phase (85:15 methanol/water at 20 μL/min). After exiting the column, the LC eluents were directly infused into the Quatro II triple-quadrupole mass spectrometer,

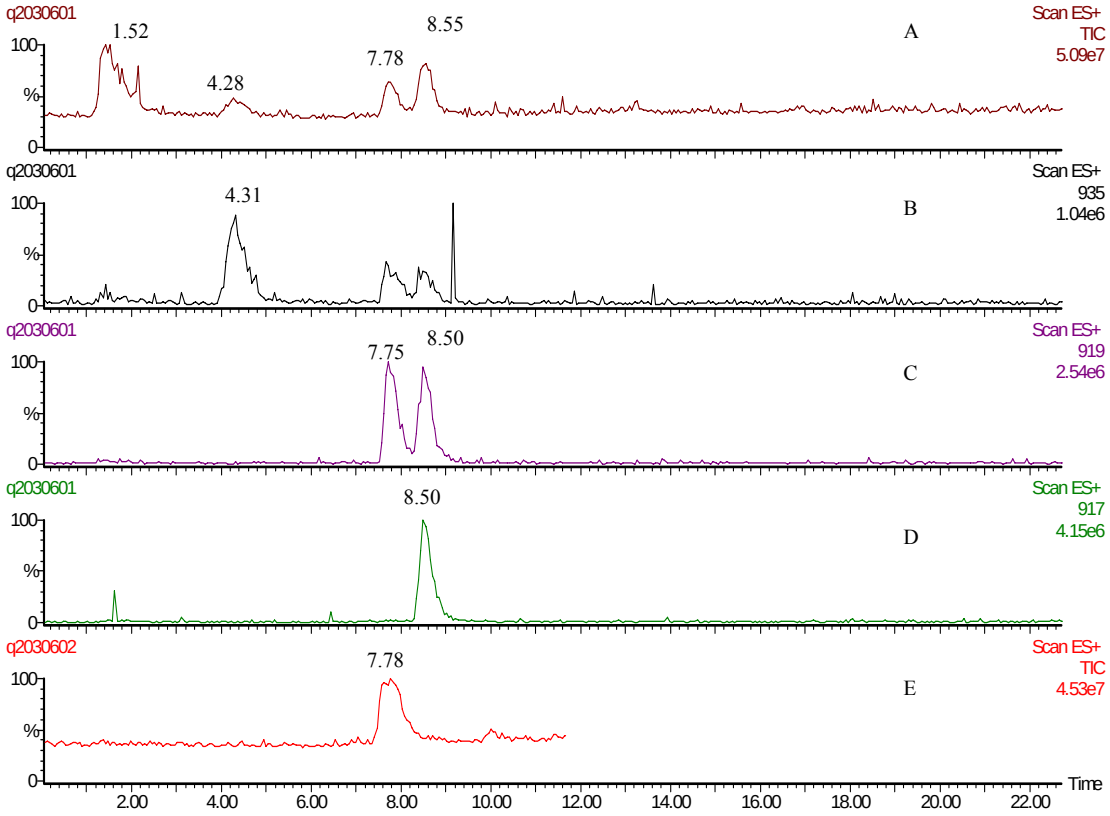

Figure 1.2. LC-MS chromatograms for brevetoxin-2 rat microsomes incubation sample and a brevetoxin-3 standard. a) TIC for incubation sample. b) SIC of m/z 935 from the incubation sample. The peak at 4.31 min represents metabolite brevetoxin-2-M1. c) SIC of m/z 919 from the incubation sample. In this chromatogram, the peak at 7.75 min represents a metabolite brevetoxin-2-M2, whereas the peak at 8.50 min is the M+2 peak of the sodium adduct of unreacted brevetoxin-2. d) SIC of m/z 917, $[\text{Brevetoxin-2} + \text{Na}]^+$, unreacted substrate from the incubation sample. e) TIC for brevetoxin-3 standard. The retention time of brevetoxin-3 overlaps that of brevetoxin-2-M2.

equipped with an electrospray ionization source (Micromass Inc. Manchester, UK). Nitrogen gas was employed as both drying gas and nebulizing gas. The ES "needle" voltage was set at 3.7 kV, and the cone voltage was set at 40 V, for both positive and negative modes. Collision-induced decomposition (CID) tandem mass spectra were acquired at 70-75 eV collision energy, using argon as collision gas at a pressure of 2.1 x 10^{-2} Pa (gauge external to cell). All mass spectra represent the average of 10 to 20 scans. M/z values were rounded down (truncated) to the nearest integer values, that is, the nominal mass of the fragment ions are reported in the spectra.

1.3 Results and Discussion

Brevetoxin-2 metabolism: The LC-MS traces of the brevetoixn-2 sample incubated with rat microsomes are shown in Figure 1.2. Two main metabolite peaks were observed in addition to the peak representing unreacted brevetoxin-2. The averaged mass spectrum for the first chromatographic peak at 4.3 min (Figure 1.2b), representing the metabolite that we are calling brevetoxin-2-M1, showed mass spectral signals at both m/z 935 and 951 (Figure 1.3a), which suggested that these could be the sodium and potassium adducts, respectively, of a neutral molecule of 912 Da. The averaged mass spectrum for the second chromatographic peak at 7.8 min (Figure 1.2c), which represents the second metabolite that we are calling brevetoxin-2-M2, showed m/z 919 as the base peak and also m/z 935 (Figure 1.3b). The third peak on the chromatogram at 8.5 min (Figure 1.2d) also showed two peaks, i.e., m/z 917 as base peak and m/z 933 (Figure 1.3c), which represent the sodium and potassium adducts of unreacted brevetoxin-2 in the incubation solution. Selected ion chromatograms of m/z 917 (Figure 1.2d) and 919 (Figure 1.2c), clearly show the peaks for sodium adducts of brevetoxin-2 and its

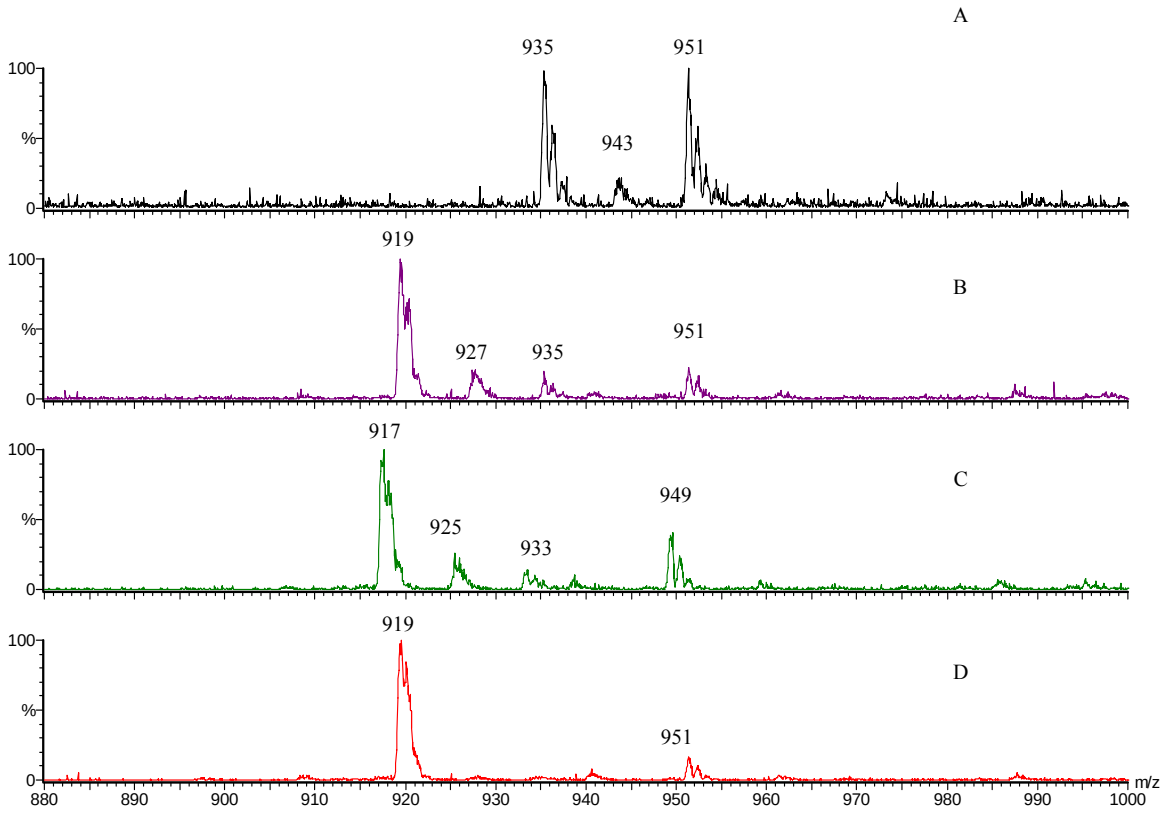

Figure 1.3. Mass spectra corresponding to major peaks observed in Figure 2. a) The peak at 4.3 min is assigned as Brevetoxin-2-M1 (912 Da), the hydrolysis product of brevetoxin-2. m/z 935 and 951 correspond to sodium and potassium adducts, respectively; m/z 943 represents [2brevetoxin-2-M1 + Na + K]$^{2+}$. b) The peak at 7.8 min is assigned as Brevetoxin-2-M2 (896 Da), a reduced form of brevetoxin-2, i.e., brevetoxin-3: m/z 919 represents [brevetoxin-2-M2 + Na]$^{+}$, m/z 935 is [brevetoxin-2-M2 + K]$^{+}$, m/z 927 is the doubly charged dimer of the above two species, and m/z 951 is [2brevetoxin-2-M2 + Na + MeOH]$^{+}$. c) The peak at 8.5 min corresponds to unreacted brevetoxin-2: m/z 917 represents [brevetoxin-2 + Na]$^{+}$, m/z 933 is [brevetoxin-2 + K]$^{+}$, m/z 925 is the doubly charged dimer of the above two species, and m/z 949 is [brevetoxin-2 + Na + MeOH]$^{+}$. Note that each peak is shifted toward lower m/z by two units as compared to 3b. d) Brevetoxin-3 standard. m/z 919 is the sodium adduct of brevetoxin-3, and m/z 951 is the sodium-plus-methanol adduct of brevetoxin-3.

metabolite, respectively. No other significant peak was found by searching selected ion chromatograms of other m/z values, nor by extending the chromatographic running time. Based on this information, we postulate that the second chromatographic peak at 7.8 min corresponds to the sodium and potassium adducts of the metabolite brevetoxin-2-M2 of mass 896 Da, which has the same molecular weight as brevetoxin-3 (see Figure 1.1).

We postulate that brevetxin-2-M2 is formed by metabolic reduction of the tail (addition of two hydrogen atoms to become the aldehyde), thereby forming brevetoxin-3. To confirm the postulation that the peak at 7.8 min (brevetoxin-2-M2, Figure 1.2) has the same structure as brevetoxin-3, LC-MS of a brevetoxin-3 standard in methanol (0.05 mM) was conducted, and its retention time (7.78 min figure 1.2e was found to be the same as that of brevetoxin-2-M2 under the same chromatographic conditions. The averaged mass spectrum of this standard (Figure 1.3d) also gave a signal at m/z 919, but did not give a strong signal at m/z 935 (no potassium adduct). This could be rationalized by considering that the brevetoxin-3 standard (with ubiquitous sodium contamination) was dissolved in pure methanol, whereas the incubation sample is actually in a solution of potassium phosphate buffer (pH 7.4). Brevetoxins have very strong binding affinities for sodium ion, and even trace levels of sodium in the system are already enough for brevetoxins to form sodium adducts[26]. Notably, peaks corresponding to noncovalent methanol addition to sodium adducts of brevetoxins were observed at m/z 951 in figure 1.3d, and at m/z 949 in figure 1.3c. Of course, these peaks appeared with the same retention times as the corresponding sodiated brevetoxin species. Lastly, doubly charged mixed adducts of brevetoxins containing Na^+ and K^+ were observed at m/z 943 in figure 1.3a, m/z 927 in figure 1.3b, and at m/z 925 in figure 1.3c [27].

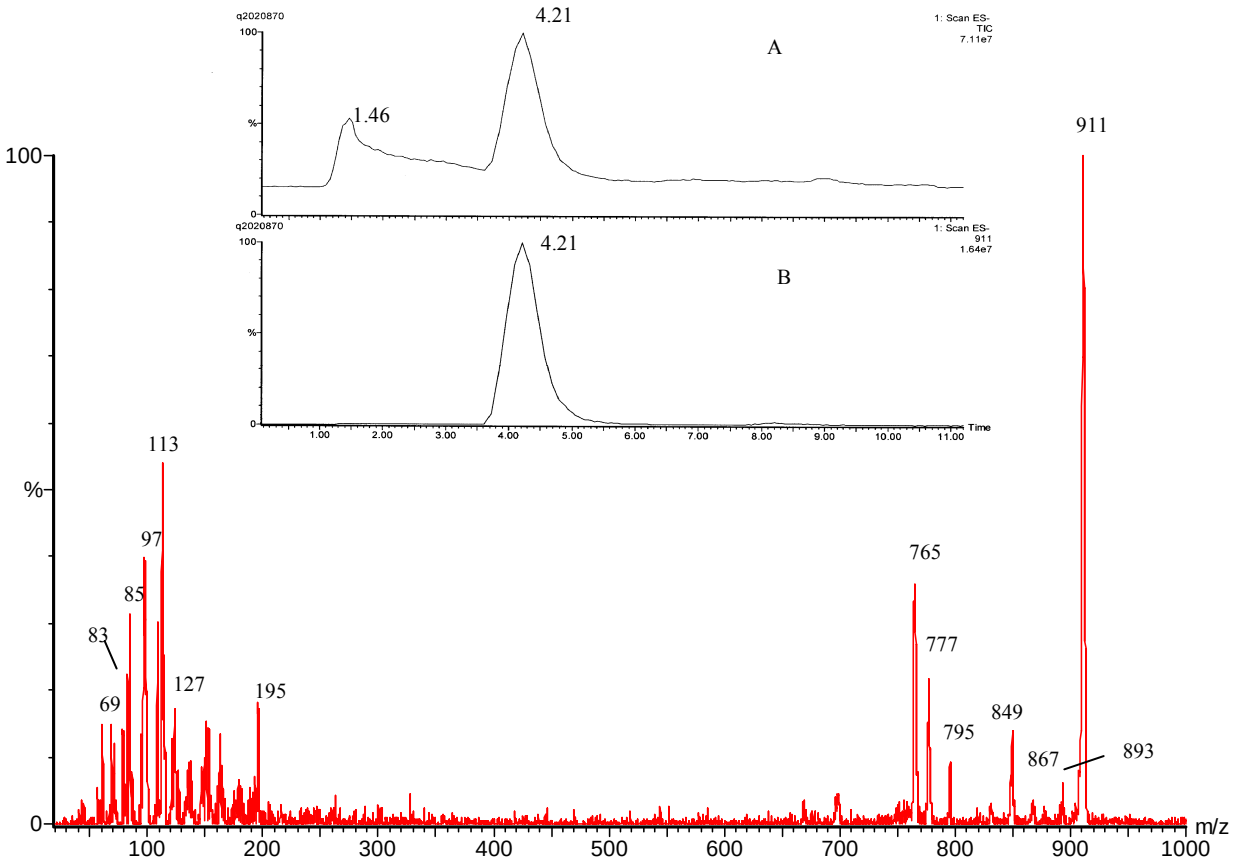

Figure 1.4: LC-MS/MS negative mode product ion mass spectrum of m/z 911, [brevetoxin-2-M1 - H]$^-$. (inset figure, LC-MS negative ion mode chromatograms for brevetoxin-2 incubation sample. a) TIC; b) SIC for m/z 911, the deprotonated form of the metabolite Brevetoxin-2-M1.

To further confirm the postulation that the second metabolite peak was brevetoxin-3, tandem mass spectrometry was performed. However, CID of the sodium adduct of brevetoxins only yields Na^+, and no informative fragments[26]. In order to obtain a more useful tandem mass spectrum, protonated brevetoxin is a preferable precursor ion. In our study, both passing incubation mixture through the ionic exchange resin (Dowex 50WX8) and direct acidification with 0.4 M TFA were attempted to promote formation of protonated molecules; direct acidification yielded stronger signals, but the signal-to-noise ratios for protonated precursor molecules eluting during LC-MS were still not strong enough to obtain adequate product ion mass spectra. During the separation, apparently traces of sodium on the LC column and elsewhere converted protonated molecules back to sodium adducts. The approach of acidifying the mobile phase (by adding TFA) was also tried, but satisfactory $[M + H]^+$ signals that would allow LC-MS/MS were still not obtained.

The first metabolite peak (represented as brevetoxin-2-M1) has a deduced molecular weight of 912 Da, 18 Da higher than the mass of brevetoxin-2. We propose that this metabolite is a hydrolyzed form of brevetoxin-2. In negative mode LC-ES-MS operation, the incubation sample showed a large chromatographic peak at 4.2 min (Figure 1.4 inset). The negative ion mass spectrum corresponding to this peak, shown in figure 1.4, reveals the $[M-H]^-$ counterpart, at m/z 911, to the $[M+Na]^+$ ion (m/z 935) already seen in figure 1.2b and 1.3a. The fact that the intensity of m/z 911 was so much higher than any of the brevetoxins and brevetoxin metabolites in the negative ion mode suggests that this metabolite is likely to be a carboxylic acid. In fact, neither brevetoxin-2 nor brevetoxin-3 in pure solvent gives a significant signal in negative mode

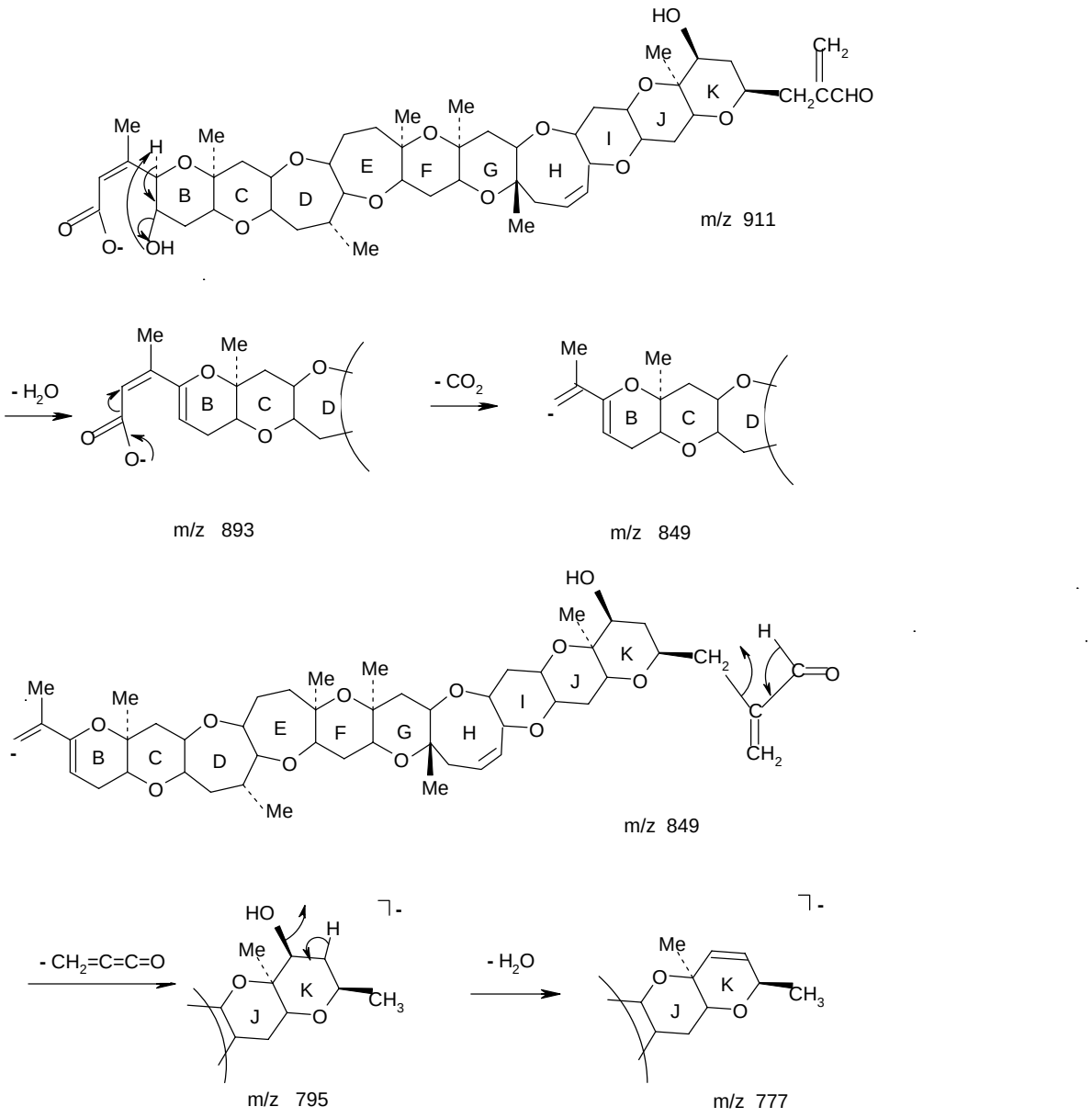

Figure 1.5. Proposed fragmentation of [brevetoxin-2-M1 - H]$^-$ (m/z 911), leading to formation of m/z 893, 849, 795 and 777.

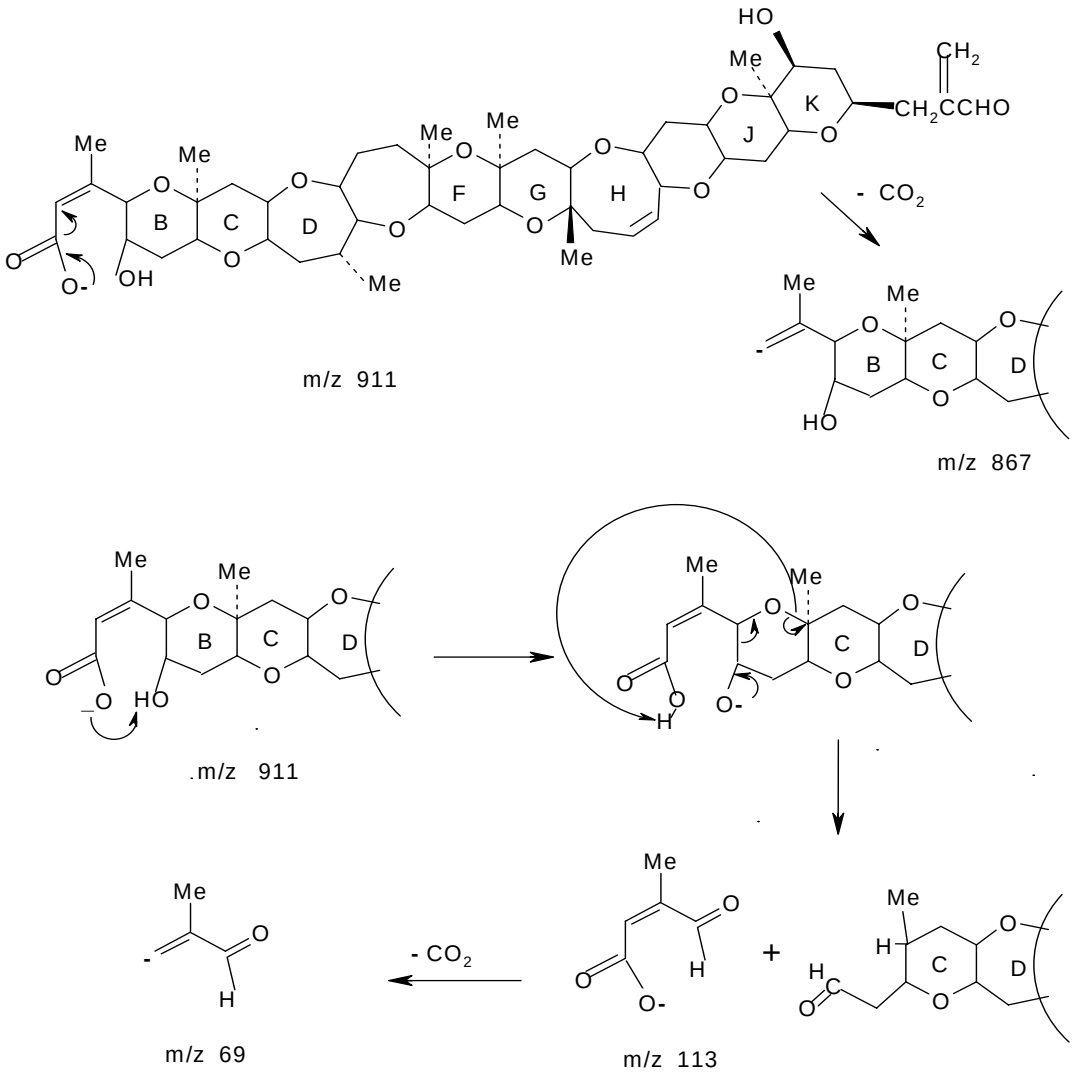

Figure 1.6. Proposed fragmentation mechanisms of [brevetoxin-2-M1 - H]$^-$ (m/z 911), leading to formation of m/z 867, 113 and 69.

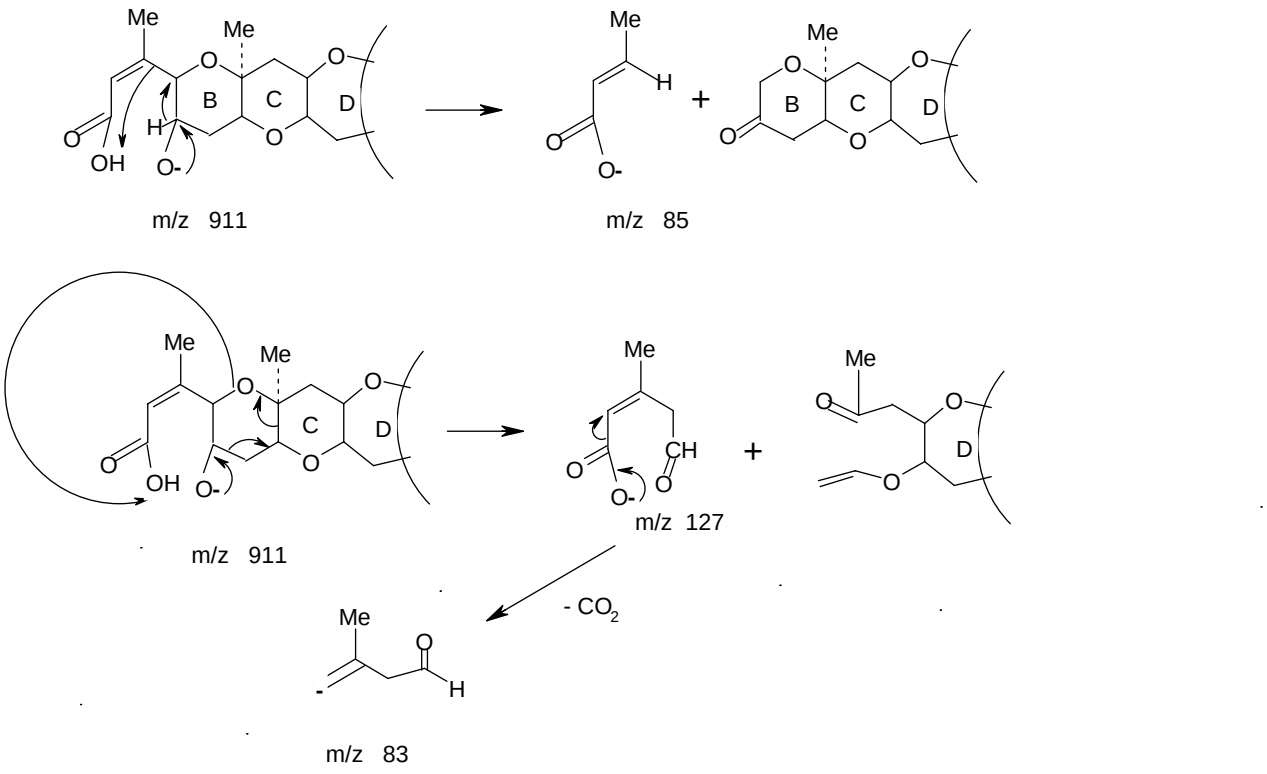

Figure 1.7. Proposed fragmentation mechanisms of [brevetoxin-2-M1 - H]$^-$ (m/z 911), leading to formation of m/z 85, 127 and 83.

ES-MS. The problem is largely that the most acidic hydrogen atoms on brevetoxin-2 and brevetoxin-3 are the hydroxyl hydrogen atoms that are apparently not readily deprotonated under the employed negative ion electrospray conditions. Tandem mass spectrometry of m/z 911 (figure 1.4) provided further evidence to support our proposed structure.

Figure 1.4 shows the LC-ES-MS/MS product ion spectrum of the m/z 911 precursor ion representing the deprotonated metabolite brevetoxin-2-M1. A charge remote fragmentation mechanism (Figure 1.5) can explain the formation of m/z 893 (by water loss), and subsequent charge induced CO_2 loss leads to m/z 849. Alternatively, CO_2 loss may occur first (yielding m/z 867, figure 1.6) with water loss occurring afterwards to form m/z 849. The latter m/z 849 ion can undergo charge remote loss of a 54 Da neutral to form m/z 795 (Figure 1.5), with subsequent water loss to produce m/z 777 (Figure 1.5). At a CID energy of 75eV (E_{LAB}), the hydrogen of the hydroxyl group on the B-ring may be transferred to the nearby carboxylic group (Figure 1.6 middle panel), thereby initiating two possible fragmentation pathways leading to fragments at m/z 113, the largest fragment peak in the figure 1.4 product ion spectrum, and m/z 69 (Figure 1.6). This same initial higher energy alkoxide form of m/z 911 is proposed to be responsible for the formation of m/z 85 (Figure 1.7), and m/z 127 (Figure 1.7). The latter can undergo CO_2 loss to form m/z 83 (Figure 1.7). The brevetoxin-2-M1 metabolite is apparently formed by opening of the head lactone ring with concomitant addition of a water molecule. This type of reaction can be accelerated by enzymes such as esterase or lactonase in the microsomes[28, 29].

Brevetoxin-1 metabolism: After incubation of brevetoxin-1 with rat hepatocytes and clean-up, similar LC/MS approaches as above were applied to the analysis of the incubation samples. By

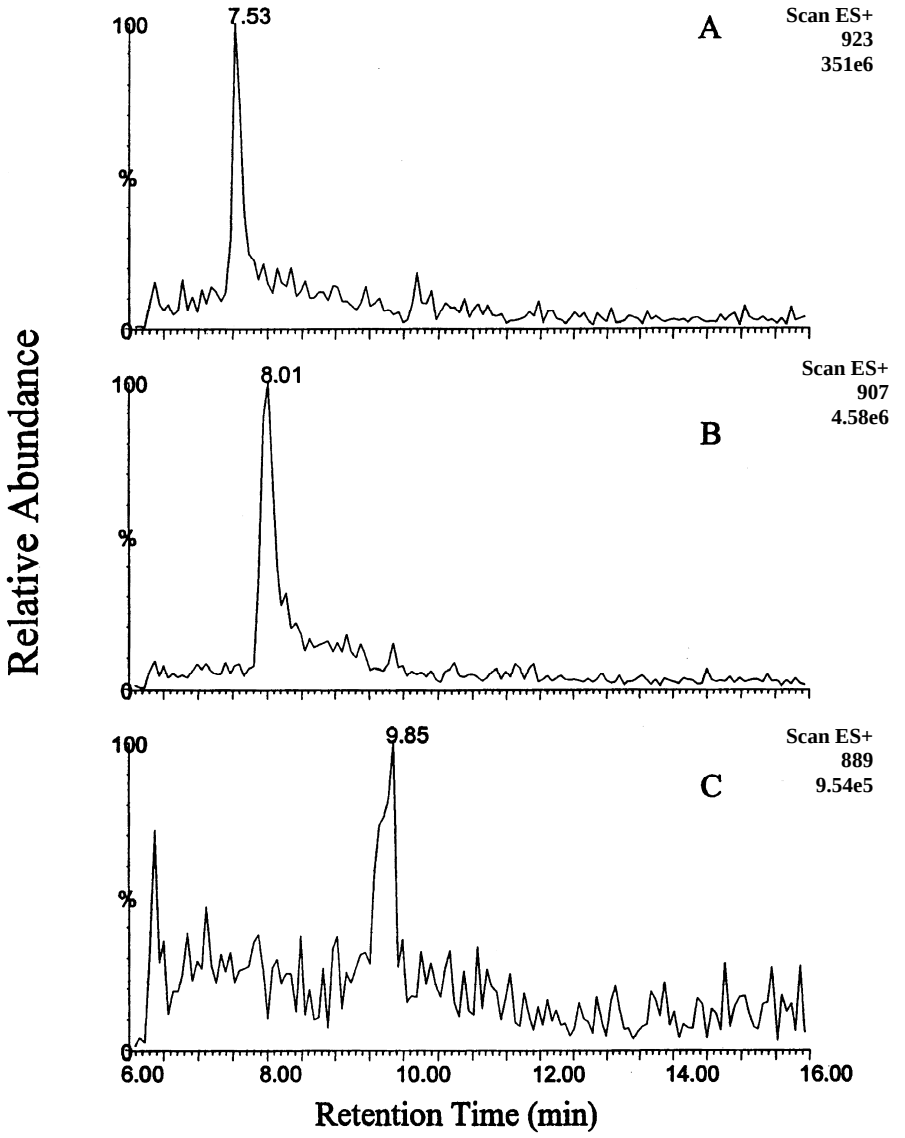

Figure 1.8. LC/MS selected ion chromatograms of brevetoxin-1 rat hepatocytes incubation sample. a) SIC of m/z 923, $[\text{Brevetoxin-1-M1} + \text{Na}]^+$. b) SIC of m/z 907, $[\text{Brevetoxin-1-M2} + \text{Na}]^+$. c) SIC of m/z 889, $[\text{Brevetoxin-1} + \text{Na}]^+$.

searching the entire range of masses contained in the total ion chromatogram, three ion peaks were revealed, and their single ion chromatograms are shown in figure 1.8 with peak retention times of 7.5 min, 8.0 min and 9.8 min in figure 1.8a, 1.8b, 1.8c, respectively. The peak retention time of 9.8 min in figure 1.8c and corresponding m/z value (889) are the same as those of the brevetoxin-1 standard starting material. This peak is clearly the sodium adduct [brevetoxin-1 + $Na]^+$ of the remaining substrate. The peaks in figure 1.8a (assigned as [brevetoxin-1-M1+$Na]^+$) and in figure 1.8b (assigned as [brevetoxin-1-M2 + $Na]^+$) are proposed to be the sodiated forms of two brevetoxin-1 metabolites. To verify the mass assignment of the sodium adducts, the same solution was acidified by HCl addition (1:1 ratio of sample:0.33 M HCl), and the resultant solution was injected into the LC/MS system. The obtained selected ion chromatograms did show peaks corresponding to the mass of protonated species that appeared at the same time as the sodiated ions. The peak in figure 1.9b was assigned as [brevetoxin-1-M1 + $H]^+$, and the peak in Figure 1.9d was assigned as [brevetoxin-1-M2 + $H]^+$. The polarity of these two brevetoxin metabolites appears to be greater than that of precursor brevetoxin-1, as the latter eluted later from the reversed phase C-18 column.

To gain more insight into the structure of brevetoxin-1-M1, the product ion tandem mass spectrum of the [brevetoxin-1-M1 + $H]^+$ precursor was acquired and is shown in figure 1.10a. For comparison purposes, the product ion spectrum of the standard precursor [brevetoxin-1+$H]^+$ obtained under identical instrumental conditions is given in figure 1.10b. While at least three consecutive water losses are detectable from [brevetoxin-1-M1 + $H]^+$ (giving product ions at m/z 849, 831 and 813 in figure 1.10b), the water losses are much more prominent relative to other fragmentations for [brevetoxin-1-M1 + $H]^+$. In fact, the peak corresponding to loss of two water

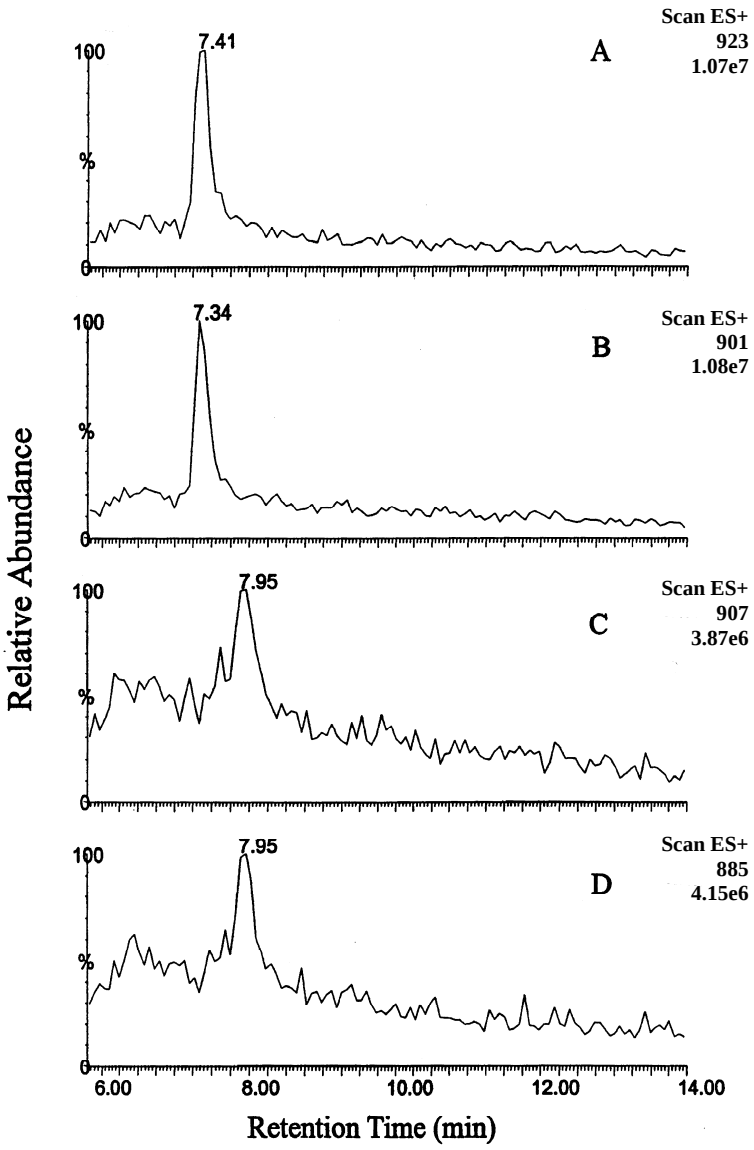

Figure 1.9. To examine the structures of metabolites, sample was acidified by 0.33 N HCl in a 1:1 ratio. The resultant solution showed peaks corresponding to protonated species that coexist with the sodiated ions in LC-MS. a). SIC for m/z 923, the peak of $[Brevetoxin\text{-}1\text{-}M1 + Na]^+$. b) SIC for m/z 901, the peak of $[Brevetoxin\text{-}1\text{-}M1 + H]^+$. c) SIC peak of $[Brevetoxin\text{-}1\text{-}M2 + Na]^+$, m/z 907. d) SIC for m/z 885, $[Brevetoxin\text{-}1\text{-}M2 + H]^+$.

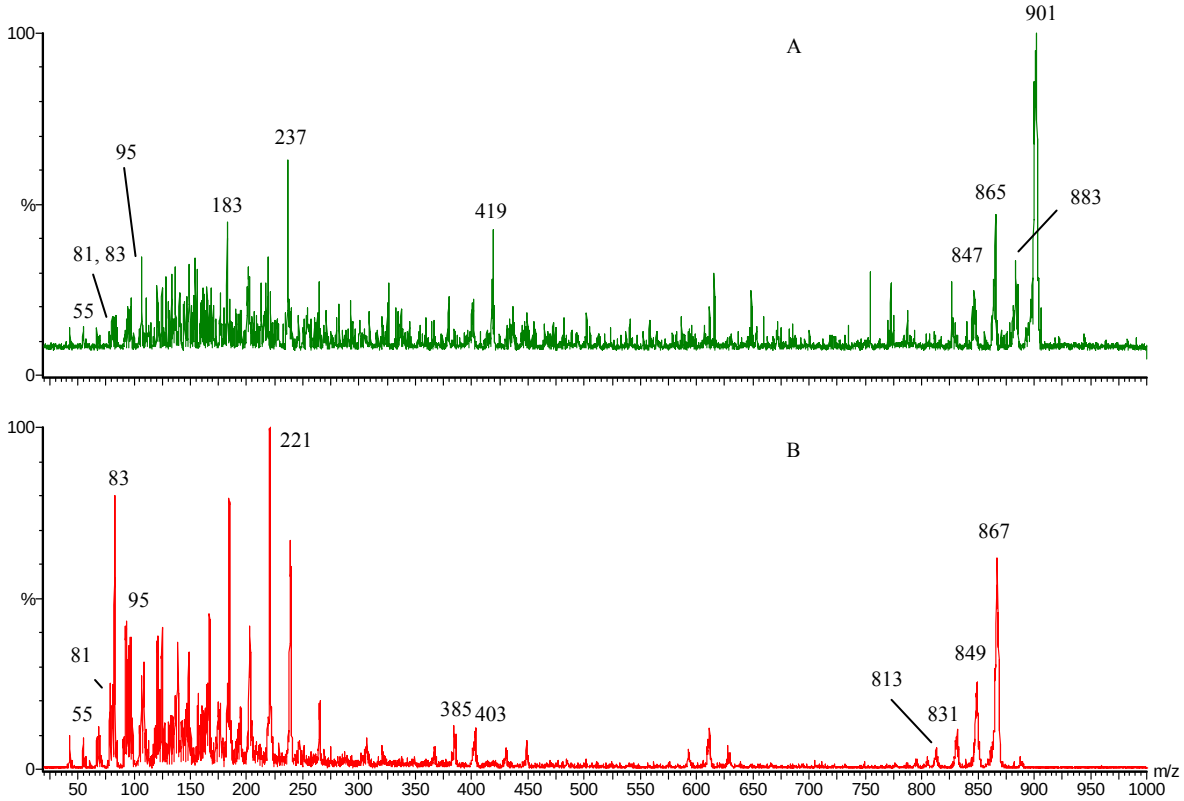

Figure 1.10. LC-MS/MS product ion mass spectra. a) m/z 901, protonated brevetoxin-1-M1 from incubation sample. b) m/z 867, $[\text{brevetoxin-1} + H]^+$ standard.

molecules (m/z 865) is even larger than the peak corresponding to a single water loss (m/z 883). Moreover, loss of a third water molecule (yielding m/z 847) gives a moderate signal relative to other product ions. The increased prominence of the second and third consecutive water losses for $[\text{brevetoxin-1-M1+H}]^+$ combined with its higher mass (34 Da) relative to brevetoxin-1 leads us to propose that brevetoxin-1-M1 is an oxidation product resulting from the metabolic conversion of a double bond on brevetoxin-1 into a diol. The question becomes: which of the three double bonds is converted to the diol?

In the lower ends of the product ion mass spectra, both figure 1.10a and 1.10b show peaks at m/z 55, 81 and 95, these peaks are proposed to be characteristic of the brevetoxin-1 side chain (Figure 1.11). Because these same three peaks appear for decompositions of brevetoxin-1 and brevetoxin-1-M1, with no new peaks found for brevetoxin-1-M1 at m/z 89, 115 or 129, i.e., 34 Da higher than the proposed "tail" fragments for brevetoxin-1, it seems unlikely that the "tail" side chain unsaturation on brevetoxin-1-M1 is the site of diol conversion. Rather, we propose that diol formation is occurring on one of the two double bonds on the E or F ring (structures shown in Figure 1.12). The mechanism could be described as a two-step reaction wherein the double bond is oxidized to form an epoxide structure catalyzed by enzyme P-450, followed by hydrolysis to form two hydroxyl groups. The structure of the second metabolite, i.e., brevetoxin-1-M2, is proposed and shown in Figure 1.12. This metabolite is formed by opening of the lactone ring and by the addition of a water molecule. This kind of reaction can proceed spontaneously in aqueous solution and can be accelerated by enzymes such as esterases in the hepatocytes[30]. The reaction is very much analogous to that involved in brevetoxin-2-M1 formation from brevetoxin-2 except that there, an unsaturated six-membered ring lactone was involved; whereas

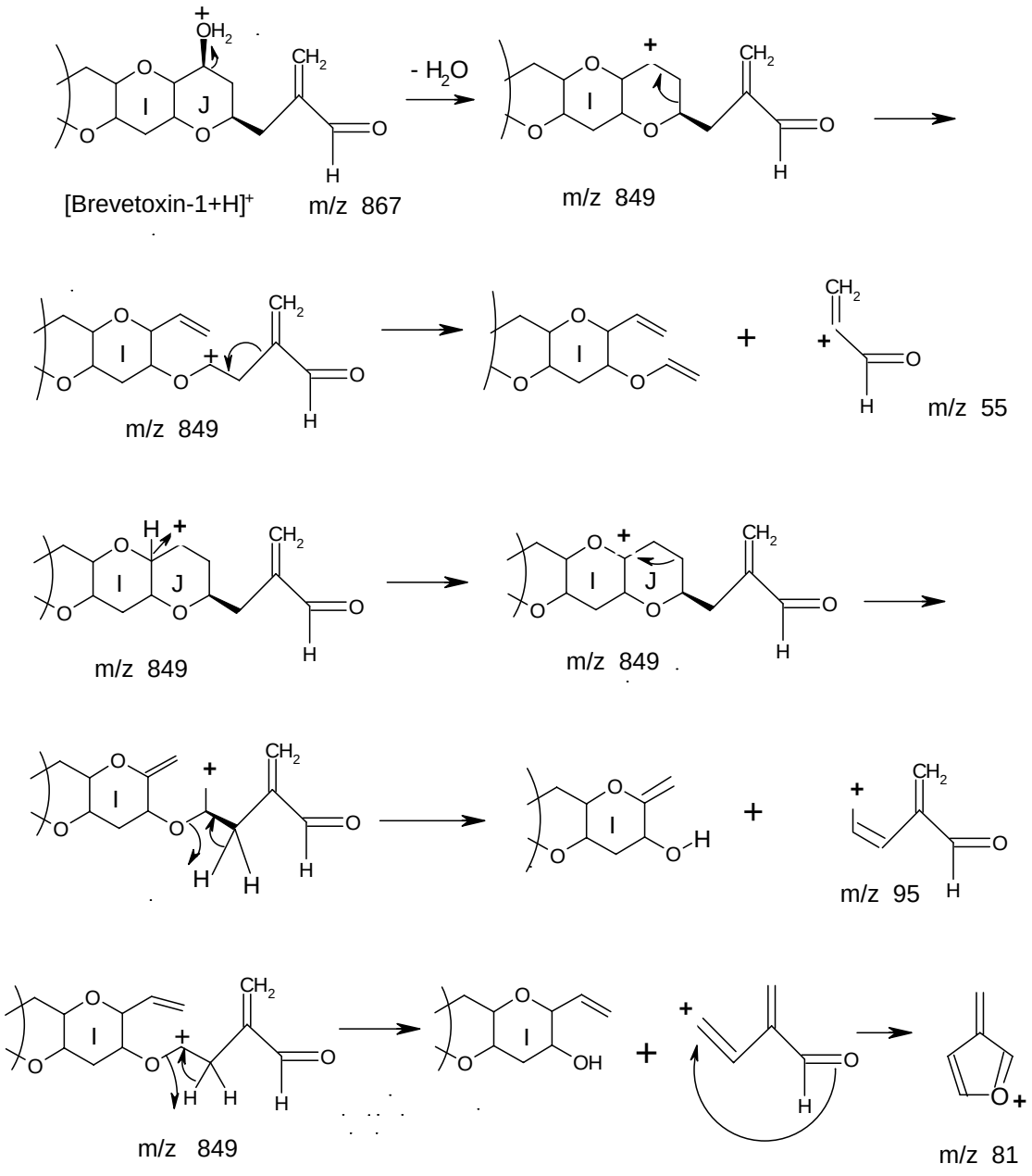

Figure 1.11. Proposed fragmentation mechanisms for "tail" portion side chain of $[\text{brevetoxin-1} + H]^+$ (m/z 867) leading to formation of m/z 55, 81 and 95. These three fragment ions also appear during CID of $[\text{brevetoxin-1-M1} + H]^+$ indicating that the side chain "tail" of the latter is the same as that of brevetoxin-1.

for brevetoxin-1, a saturated five-membered ring undergoes hydrolysis (see figure 1.1). While not reported for brevetoxin-1 and brevetoxin-2, similar hydrolytic opening of the A-ring was observed previously for brevetoxin metabolites isolated from oyster [16] such as the cysteine conjugate of brevetoxin-1 and brevetoxin-2, with molecular weights of 1008 and 1036 Da, respectively.

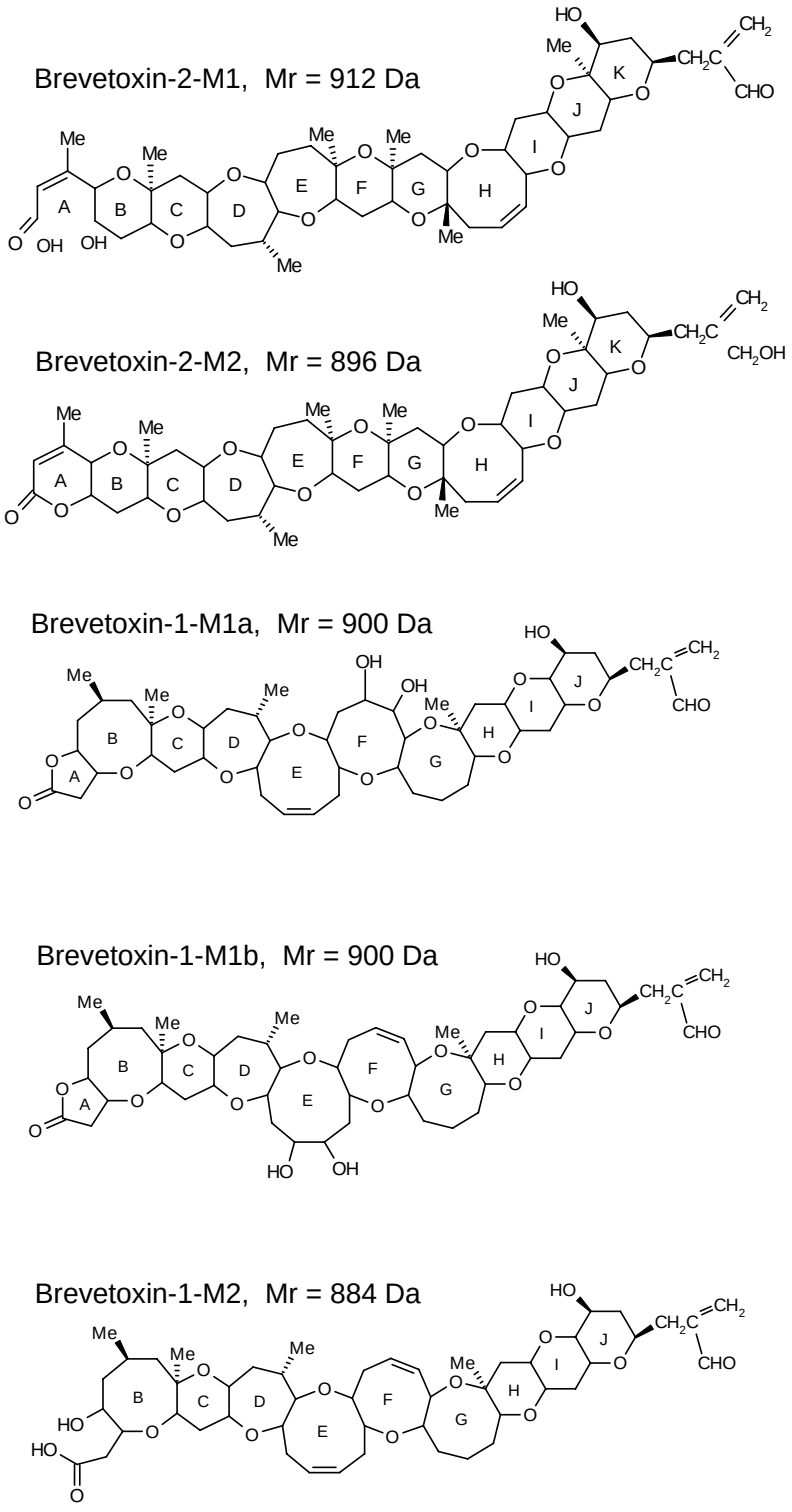

Figure1.12. Proposed structures for the metabolites of brevetoxin-2 and brevetoxin-1.

Conclusion

LC/ES-MS and LC/ES-MS/MS have been shown to be useful tools for the characterization of brevetoxin metabolites. Brevetoxin-2 was shown to undergo *in vitro* metabolism by rat liver microsomes to yield two metabolites. One is assigned as the hydrolysis product of the head portion six-membered lactone ring of the substrate; the other is proposed to be brevetoxin-3, the metabolically reduced product of brevetoxin-2 (figure 1.12). Brevetoxin-1 was shown to be metabolized by rat liver hepatocytes, also producing two metabolites. One is postulated to be formed by transforming a double bond on the E or F ring into a diol, while the other is proposed to be a hydrolysis product of brevetoxin-1 involving opening of the head group five-membered lactone ring (figure 1.12).

References:

1. Risk M, Lin YY, MacFarlane RD, Ramanujam VMS, Smith LL, Trieff NM: **Purification and chemical studies on a major toxin from *Gymnodinium breve.*** In: *Toxic Dinoflagellate Blooms : Proceedings of second International Conference on Toxic Dinoflagellate Blooms.* Edited by Taylor DL, Seliger HH. New York: Elsevier/North Holland; 1979: 335-344.
2. Daugbjerg N, Hansen G, Larsen J, Moestrup O: **Phylogeny of some of the major genera of dinoflagellates based on ultrastructure and partial LSU rDNA sequesnce data**. *Phycologia* 2000, **39**(4):302-317.
3. Margalef R, Estrada M, Blasco D. In: *Toxic Dinoflagellate Bloom : Proceedings of second International Conference on Toxic Dinoflagellate Blooms.* Edited by Taylor DL, Seliger HH. New York: Elsevier/North Holland; 1979: 89-94.
4. Derby ML, Galliano M, Martin DF, Krzanowski JJ: **Allelopathic interatcion of *Nannochloris spp.* with the red tide organism *Gymnodinium breve.*** In: *222nd ACS National Meeting, Division of Environmental Chemistry: 2001; Chicago, IL, USA*: American Chemical Society; 2001: 243-248.
5. Baden DG: **Brevetoxins: Unique polyether dinoflagellate toxins.** *FASEB J* 1989, **3**:1807-1817.
6. Pierce RH, Henry MS, Proffitt LS, Hasbrouck PA: **Red Tide Toxin (Brevetoxin) Enrichment in Marine Aerosol.** In: *Toxic Marine Phytoplankton.* Edited by Graneli E, Sundstrom B, Edler L, Anderson D. New York: Elsevier Publishing Co.; **1990**: 397-402.

7. Steidinger KA: **A Re-Evaluation of Toxic Dinoflagellate Biology and Ecology.** *Prog Phycol Res* **1983**, **2**:147-188.

8. Pierce RH: **Red Tide (Ptychodiscus Brevis) Toxin Aerosols: A Review.** *Toxicon* **1986**, **24**:955-965.

9. Dickey R, Jester E, Granade R, Mowdy D, Moncreiff C, Rebarchik D, Robl M, Musser S, Poli M: **Monitoring brevetoxins during a *Gymnodinium breve* red tide: comparison of sodium channel specific cytotoxicity assay and mouse bioassay for determination of neutoxic shellfish toxins in shellfish extracts.** *Natural Toxins* 1999, **7**(4):157-165.

10. Trainer VLB, Daniel G.: **High affinity binding of red tide neurotoxins to marine mammal brain.** *Aquatic Toxicology* 1999, **46**(2):139-148.

11. Washburn BS, Rein KS, Baden DG, Walsh PJ, Hinton DE: **Brevetoxin-6 (pbTx-6), a Nonaromatic Marine Neurotoxin Is a Ligand of the Aryl Hydrocarbon Receptor.** *Arch Biochem Biophy* **1997**, **343**:149-156.

12. Lin YY, Risk M, Ray SM, Van Engen D, Clardy J, Golik J, James JC, Nakanishi K: **Isolation and Structure of Brevetoxin B from the "Red Tide" Dinoflagellate Ptychodiscus brevis (Gymnodinium breve).** *J Am Chem Soc* **1981**, **103**:6773-6775.

13. Rakotoniaina CA, Miller DM: **Assays for Ciguatera-Type Toxins.** . In: *Ciguatera Seafood Toxins'.* Edited by Miller DM. Boca Raton, FL: CRC Press; 1991: 73-86.

14. Rein KS, Lynn B, Gawley RE, Baden DG: **Brevetoxin B: Chemical modifications, synaptosome binding, toxicity, and an unexpected conformational effect.** *J Org Chem* 1994, **59**:2107-2113.

15. Poli MA, Musser SM, Dickey RW, Wilers PP, S. H: **Neurotoxinc shellfish poisoning and brevetoxin metabolites: a case study from Florida.** *Toxicon* 2000, **38**(7):981-993.

16. Wang Z, Plakas SM, El Said KR, Jester EL, Granade HR, Dickey RW: **LC/MS analysis of brevetoxin metabolites in the Eastern oyster (Crassostrea virginica)**. *Toxicon* 2004, **43**(4):455-465.

17. Ishida H, Nozawa A, Totoribe K, Muramatsu N, Nukaya H, Tsuji K, Yamaguchi K, Yasumoto T, Kaspar H, Berkett N *et al*: **Brevetoxin B1, a New Polyether Marine Toxin from the New Zealand Shellfish.** *Tetrahedron Letters* **1995**, **36**:725-728.

18. Murata K, Satake M, Naoki H, Kaspar HF, Yasumoto T: **Isolation and Structure of a New Brevetoxin Analog, Brevetoxin B2, from Greenshell Mussels from New Zealand.** *Tetrahedron Letters* **1998**, **54**:735-742.

19. Morohashi A, Satake M, Murata K, Naoki H, Kaspar HF, Yasumoto T: **Brevetoxin B3, a New Brevetoxin Analog Isolated from the Greenshell Mussel *Perna canaliculus* Involved in Neurotoxic Shellfish Poisoning in New Zealand.** *Tetrahedron Letters* **1995**, **36**:8995-8998.

20. Poli MA, Templeton CB, Pace JG, Hines GB: **Detection, Metabolism, and Pathophysiology of Brevetoxins.** In: *Marine Toxins; (ACS Symposium Series 418): **1990***: American Chemical Society; **1990**: 176-191.

21. Degawa M, Kanazawa C, Hashimoto Y: **In vitro metabolism of o-aminoazotoluene and mutagensis of Salmonella by the metabolites**. *Carcinogensis* 1982, **3**(10):1113-1117.

22. Zhang Q, Ma P, Iszard M, Cole RB, Wang W, Wang G: ***In Vitro* metabolism of R(+)-[2,3-dihydro-5-methyl-3-[(morpholinyl)methyl]pyrrolo [1,2,3-de]1,4-benzoxazinyl)]-(1-naphthalenyl)methanone mesylate, a cannabiniod receptor agonist**. *Drug Metabolism and Disposition* 2002, **30**(10):1077-1086.

23. Zhang Q, Ma P, Wang W, Cole RB, Wang G: **Characterization of Rat Liver Microsomal Metabolites of AM-630, a Potent Cannabinoid Receptor Antagonist, by High-Performance Liquid Chromatography/Electrospray Ionization Tandem Mass Spectrometry.** *J of Mass Spectr* 2004, **39**(672-81).

24. Ekwall B, Acosta D: **In Vitro comparative toxicity of selected drugs and chemicals in HeLa cells, Chang liver cells, and rat hepatocytes**. *Drug and Chemical Toxicology* 1982, **5**(3):219-231.

25. Pierce RH, Henry MS, Proffitt LS, deRosset AJ: **Evaluation of Solid Sorbent for the Recovery Plyehter Toxins(Brevetoxins) in Seawater**. *Bull Environ Contam Toxicol* 1992, **49**:479-484.

26. Hua Y, Cole RB: **Electrospray ionization tandem mass spectrometry for structural elucidation of protonated brevetoxins in red tide algae.** *Anal Chem* 2000, **72**(2):376-383.

27. Hua Y, Lu W, Henry MS, Pierce RH, Cole RB: **On-line high performance liquid chromatography-electrospray ionization mass spectrometry for the determination of brevetoxins in "red tide" algae.** *Anal Chem* 1995, **67**:1815-1823.

28. Kawada M, Takiguchi H, Kagawa Y, Szuki K, Shimazono N: **Comparative studies on soluble lactonases.** *J Biochem (Tokyo)* 1962, **51**:405-415.

29. Sun G, Alexson SE, Harrison EH: **Purification and charcterization of a neutral , bile salt- independent retinyl ester hydrolase from rat liver microsomes: relations to rat carboxylesterase ES-2.** *Journal of Biological Chemistry* 1997, **272**(39):24488-24493.

30. Williams FM, Mutch E, Blain PG: *Biochemical Pharmacology* 1991, **41**(4):527-531.

Chapter II

Improved Collision Induced Decomposition Efficiency and Structural Assessment for "Red Tide" Brevetoxins employing Nano-electrospray Mass Spectrometry

Abstract

Brevetoxins are a group of natural neurotoxins found in blooms of red tide algae. Previous electrospray mass spectrometry (ES-MS) studies show that all brevetoxins have high affinities for sodium ions, and they form abundant sodium adduct ions, $[M + Na]^+$, in ES-MS, even when trace contamination is the only source of sodium ion. Attempts to obtain informative product ions from the collision induced decomposition (CID) of $[M + Na]^+$ brevetoxin precursor ions only resulted in uninformative sodium ion signals, even under elevated collision energies. In this study, a nano-ES-MS approach was developed wherein ammonium fluoride was used to form cationic $[M + NH_4]^+$ adducts of brevetoxin-2 and brevetoxin-3; a significant increase in the abundance of protonated brevetoxin molecules $[M + H]^+$ also resulted, whereas the abundance of sodium adducts of brevetoxins $[M + Na]^+$ was observed to decrease. Under CID, both $[M + NH_4]^+$ and $[M + H]^+$ gave similar, abundant product ions and thus underwent the same types of fragmentation. This indicates that ammonium ions initially attached to brevetoxins forming $[M + NH_4]^+$ readily lose neutral ammonia in a first step in the gas phase, leaving protonated brevetoxin $[M + H]^+$ to readily undergo further fragmentation under CID.

Key Words: nano-electrospray; ammonium adduct; brevtoxins; structure; fragmentation; mechanism

2.1 Introduction

Brevetoxins are a class of natural marine toxins that are produced from the single cell dinoflagellate *Karenia brevis*.[1, 2] Under suitable conditions, the algae reproduce rapidly, causing the appearance of a "red tide" bloom [3]. Such outbreaks are responsible for large scale, periodic fish kills in the Gulf of Mexico and other salt water locations. The brevetoxins produced by a bloom of red tide can also lead to human health problems, such as neurotoxic shellfish poisoning (NSP) [4].

Structurally, brevetoxins are classified as type A or Type B [5]. The compounds in the first category have 10 connected polyether rings, while the compounds in the second category have 11 rings (Figure 1.1) [5, 6]. The molecular weights of brevetoxins are close to 1000 Da. A liquid chromatography-electrospray-mass spectrometry (LC-ES-MS) method was developed in our lab to analyze the various types of brevetoxins in "red tide" algae extracts [7, 8]. This circumvented the use of derivatizing agents that were employed during a previous HPLC-FAB-MS study of brevetoxin-3 [9].

LC-MS methods have also been employed to analyze metabolites of brevetoxins, in a NSP case study from Florida, Poli et al. [10] reported using LC-MS to identify brevetoxin-3, which was likely a metabolite of brevetoxin-2, in the extracts of contaminated shellfish samples. Plakas et al. [11] confirmed LC-MS fractions containing m/z 1018 and 1034 as protonated molecules of cysteine-brevetoxin and cysteine-brevetoxin sulfoxide conjugates, respectively, in the Eastern oyster (*Crassostrea virginica*) exposed to pure brevetoxin-2 and to a *Karenia brevis* culture. In a follow-up study, Wang et al. [12] identified a cysteine-brevetoxin conjugate and its sulfoxide with an A-type brevetoxin backbone as probable derivatives of brevetoxin-1 in *Crassostrea virginica*, as well as other metabolites such as glycine-cysteine-brevetoxin; γ-glutamyl-cysteine-brevetoxin and glutathione-brevetoxin conjugates. In our lab, we performed *in vitro* incubations of brevetoxin-1 with rat liver hepatocytes, and brevetoxin-2 with rat liver microsomes, that resulted in hydrolytic lactone-ring opening products for both brevetoxins; brevetoxin-3 as metabolite of brevetoxin-2, and a metabolite of brevetoxin-1 postulated to have undergone a double bond transformation in the E or F ring, forming a diol [13].

Brevetoxins exhibit high affinities for sodium ions, and thus readily form sodium adducts $[M + Na]^+$ that dominate the electrospray mass spectra, even when only traces of sodium are present. Consequently, without further treatment, excellent sodium adduct signals may be obtained for all types of brevetoxins by electrospray mass spectrometry (ES-MS). The sodium adducts, however, did not yield structurally informative product ions by collision induced decomposition (CID), and only sodium ions were produced at high collision energies [14]. To promote the formation of

protonated molecules instead of sodiated ones, we added strong acid (HCl) to solutions containing brevetoxin [15].

This method succeeded in producing high levels of $[M + H]^+$ ions that were quite susceptible to CID, thus providing structural information. A potential drawback, however, was that the acidic conditions required to sufficiently displace sodium cations by protons (i.e., pH ≈ 3) may be potentially deleterious to the sample and/or the instrument. Therefore, we searched for other means to enhance the yields of structurally informative fragments. In later work, Nozawa, Ishida and coworkers [16, 17] reported a LC-MS/MS method using an acidified acetonitrile mobile phase to identify and quantitatively determine brevetoxins found in shellfish following an outbreak of NSP in New Zealand. Optimum signal-to-noise ratios of $[M + H]^+$ ions promoted by formic acid addition to either methanol or acetonitrile appeared quite comparable to one another [16].

Besides addition of acid, an alternative approach to reducing the abundance of sodium ion adducts and increasing the number of protonated molecules was proposed by Stark et al [18]. They found that adding ruthenium chloride to certain complex natural products could suppress the formation of sodium adducts and concomitantly increase the abundance of protonated molecules. However, the detailed mechanism underlying this phenomenon has not been fully elucidated. In our hands, the limited solubility of ruthenium chloride necessitated filtering of sample solutions prior to electrospray, and created a higher risk of source fouling (usually at the orifice of the sampling cone).

The strategy of adding ammonium ions to the electrospray solvent, to create a yield of ammonium adducts of certain analytes has also been documented. Fleet et al. [19] using direct infusion positive ES-MS, reported that chrysanthemic acid ester pyrethroid insecticides yielded $[M + H]^+$ and $[M + NH_4]^+$ ions in an isopropanol water/formic acid/ammonium acetate environment, and found $[M + NH_4]^+$ underwent source-derived CID at high "cone" voltages and yielded $[M + H]^+$ and diagnostic fragment ions. Yin et al. [20] studied a series of peroxides by ES-MS that were found to form ammonium adducts from a methanol/water (50:50) solution with 10 mM ammonium acetate; CID experiments on $[M + NH_4]^+$ precursor ions were shown to give informative fragments.

In the current study, ammonium fluoride was used as an additive to study solutions containing brevetoxins. Low flow ES, also known as "nanoelectrospray" was employed to generate mass spectra, including CID experiments. Since Wilm and Mann [21] developed the idea of solvent pump-free nanoelectrospray in 1996, the approach has been widely used in both direct infusion MS analyses and on-line LC-MS applications. Different from conventional electrospray that runs at a flow rate of about 5 uL/min and forms 1-2 um diameter liquid droplets, nanoelectrospray can run at flow rates as low as 20 nL/min and creates droplets of less than 200 nm diameter, which improves the ionization efficiency because of the greater surface-volume ratio. This low flow rate dramatically reduces sample consumption and greatly prolongs the available analysis time for scarce and/or valuable samples [22]. Because of the prohibitively expensive cost of commercially-available brevetoxins, the use of nanoelectrospray turned out to be particularly advantageous.

2.2 Experimental

Brevetoxins were purchased from CalBiochem (La Jolla, CA), and ammonium fluoride, ammonium acetate, ammonium chloride were purchased from Aldrich (Milwaukee, WI). Nanospray tips were purchased from New Objective (Woburn, MA); the diameter of the employed tip orifice was 4 μm. All mass spectrometry experiments were performed on a Quattro II triple quadrupole mass spectrometer (Micromass, Inc., Manchester, UK) equipped with a direct infusion nanospray assembly. The "needle" voltage was set at 1.6-1.8 kV, and the source temperature was set at 30 ºC. All mass spectra represent the average of 20 scans or more; the *m/z* values were rounded down (truncated) to the nearest integer values, i.e., the nominal masses of the detected ions are reported in the spectra.

2.3 Results and Discussion

In conventional ES-MS analyses, aqueous/organic mixtures, sometimes with weak acid additives, are the most frequently used solvents for positive mode analysis. However, due to their high affinities for sodium ions, it is very difficult for brevetoxins to yield highly abundant protonated molecules under such conditions (Figure 2.1a). In previous studies in our lab, strong acid addition (i.e. trifluoroacetic acid or hydrochloric acid) was used to suppress the appearance of sodium adducts by favoring production of protonated molecules [15] In this paper, we present an alternative approach, i.e., that of adding ammonium ions to compete with the formation of brevetoxin-sodium adducts.

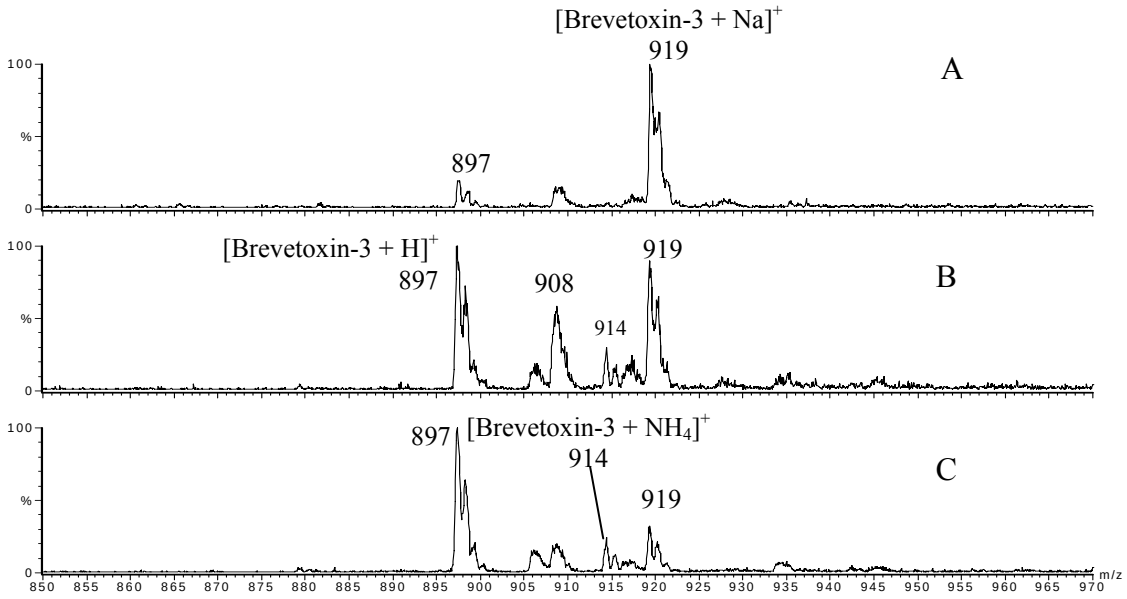

Figure 2.1. Electrospray mass spectra of brevetoxin-3 as a function of ammonium fluoride addition. The concentration of brevetoxin-3 was set at 5 x 10^{-5} M in a 1:1 water/methanol solution, and the concentration of ammonium fluoride was at (A) 0, (B) 2 x 10^{-4} M, and (C) 5 x 10^{-4} M. The peak at *m/z* 908 is assigned as $[2\text{brevetoxin-3} + \text{Na} + \text{H}]^{2+}$. The abundance of protonated brevetoxin-3 (m/z 897) increased, and that of $[\text{brevetoxin-3} + \text{Na}]^{+}$ (*m/z* 919) decreased, as the concentration of ammonium ions, introduced as NH_4F, was raised.

Figure 2.1a displays the mass spectrum of brevetoxin-3 (a neutral molecule of 896 Da) dissolved in 1:1 (water:methanol), showing a low abundance of [brevetoxin-3 + H]$^+$ at *m/z* 897, and a high abundance of the sodium adduct [brevetoxin-3 + Na]$^+$ at *m/z* 919. The source of sodium ions is the ubiquitous trace level contamination of sodium in the solvent and elsewhere. As ammonium fluoride is added to the system, and the molar ratio of ammonium ion vs brevetoxin-3 reaches 4:1 (Figure 2.1b), the abundance of [brevetoxin-3 + H]$^+$ in the spectrum rises to a level comparable to that of [brevetoxin-3 + Na]$^+$, with the ammonium adduct [brevetoxin-3 + NH_4]$^+$ at *m/z* 914 now appearing in a moderate abundance. As addition of ammonium fluoride continues to 10:1, [brevetoxin-3 + H]$^+$ at *m/z* 897 becomes the base peak (Figure 2.1c), while the relative abundance of [brevetoxin-3 + Na]$^+$ (m/z 919) continues to descend. A similar result (not shown) was achieved for ammonium fluoride addition to brevetoxin-2, a compound having a similar structure to brevetoxin-3, except that the former contains an aldehyde functionality in place of an alcohol group in the "tail" portion (see Figure 1). Notably, ammonium acetate and ammonium chloride were also tried in place of ammonium fluoride, and similar adducts were observed in positive ion ES mass spectra.

An important parameter to influence relative signal intensities in ES-MS is the "cone" voltage (nozzle-skimmer differential). Detailed studies showing the abundances of the three adducts of interest vs cone voltage appear in Figure 2.2a and 2.2b. In a water/methanol environment, with a ten-fold excess of ammonium fluoride relative to brevetoxin-2 (894 Da neutral) the [brevetoxin-2 + NH_4]$^+$ adduct (*m/z* 912) is readily formed, and at low cone voltage (5 V) it dominates as the base peak (Figure 2.2a). As the cone voltage is increased, the abundance of the ammonium adduct first climbs rapidly, reaches a maximum at 20 V, then drops off at higher voltage values.

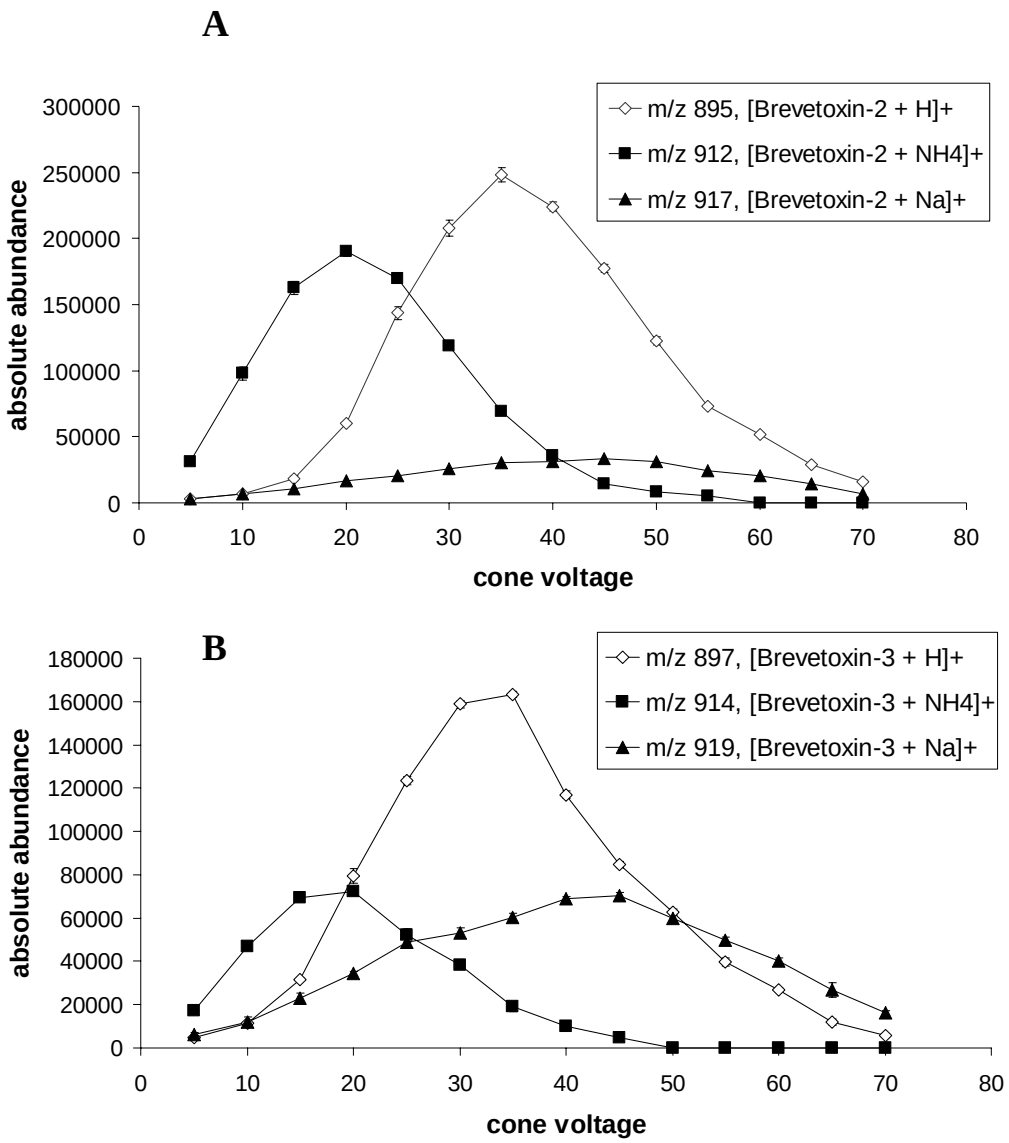

Figure 2.2. Ion abundance vs. cone voltage for brevetoxins molecular ions from a 1:1 water/methanol system containing (a) 5 x 10^{-5} M brevetoxin-2 and 5 x 10^{-4} M NH_4F; (b) 5 x 10^{-5} M brevetoxin-3 and 5 x 10^{-4} M NH_4F. The abundances of $[\text{brevetoxin-2} + NH_4]^+$ and $[\text{brevetoxin-3} + NH_4]^+$ reached their maxima at 20 V, whereas those of $[\text{brevetoxin-2} + H]^+$ and $[\text{brevetoxin-3} + H]^+$ reached their maxima at 35 V.

On the other hand, protonated brevetoxin-2, [brevetoxin-2 + H]$^+$ at *m/z* 895, is barely visible at 5 V; as the cone voltage rises, the abundance of *m/z* 895 increases slowly at first, then more quickly, reaching its maximum at 35 V. The decrease of the ammonium adduct (*m/z* 912) and concurrent increase in [brevetoxin-2 + H]$^+$ (*m/z* 895) between 20 and 35 V is attributed to a decomposition of the former via loss of ammonia, thereby forming the latter. Above 35V, the increasing nozzle-skimmer differential results in fragmentation of protonated brevetoxin-2, leading to an abundance drop for [brevetoxin-2 + H]$^+$. On the other hand, the sodium adduct of brevetoxin-2 is a much more robust adduct than [brevetoxin-2 + NH_4]$^+$ or [brevetoxin-2 + H]$^+$, and the abundance of [brevetoxin-2 + Na]$^+$ (*m/z* 917) shows a much slower decrease with the rising cone voltage beyond its maximum at 45 V.

An analogous experiment conducted using brevetoxin-3 in place of bevetoxin-2 showed a similar result (Figure 2.2b), where the abundance of the ammonium adduct [brevetoxin-3 + NH_4]$^+$ (*m/z* 914) reaches its peak at a cone voltage of 20 V, and production of protonated brevetoxin-3 [brevetoxin-3 + H]$^+$ (*m/z* 897) reaches an optimum at 35 V; the higher stability sodium adduct [brevetoxin-3 + Na]$^+$ (*m/z* 919) exhibits its maximum at 45 V.

In order to optimize the addition of ammonium ions, a detailed study of adduct abundances as a function of initial ammonium concentration was conducted. Employing a fixed cone voltage of 20 V, i.e., Figure 2.2b's optimum value for the [brevetoxin-3 + NH_4]$^+$ (ammonium-brevetoxin-3 adduct), the absolute intensities of the same three ions of interest were monitored using increasing concentrations of ammonium fluoride and a fixed concentration of brevetoxin-3 (5 x 10^{-5} M); a single nanospray tip was used throughout the entire experiment. Figure 2.3a shows

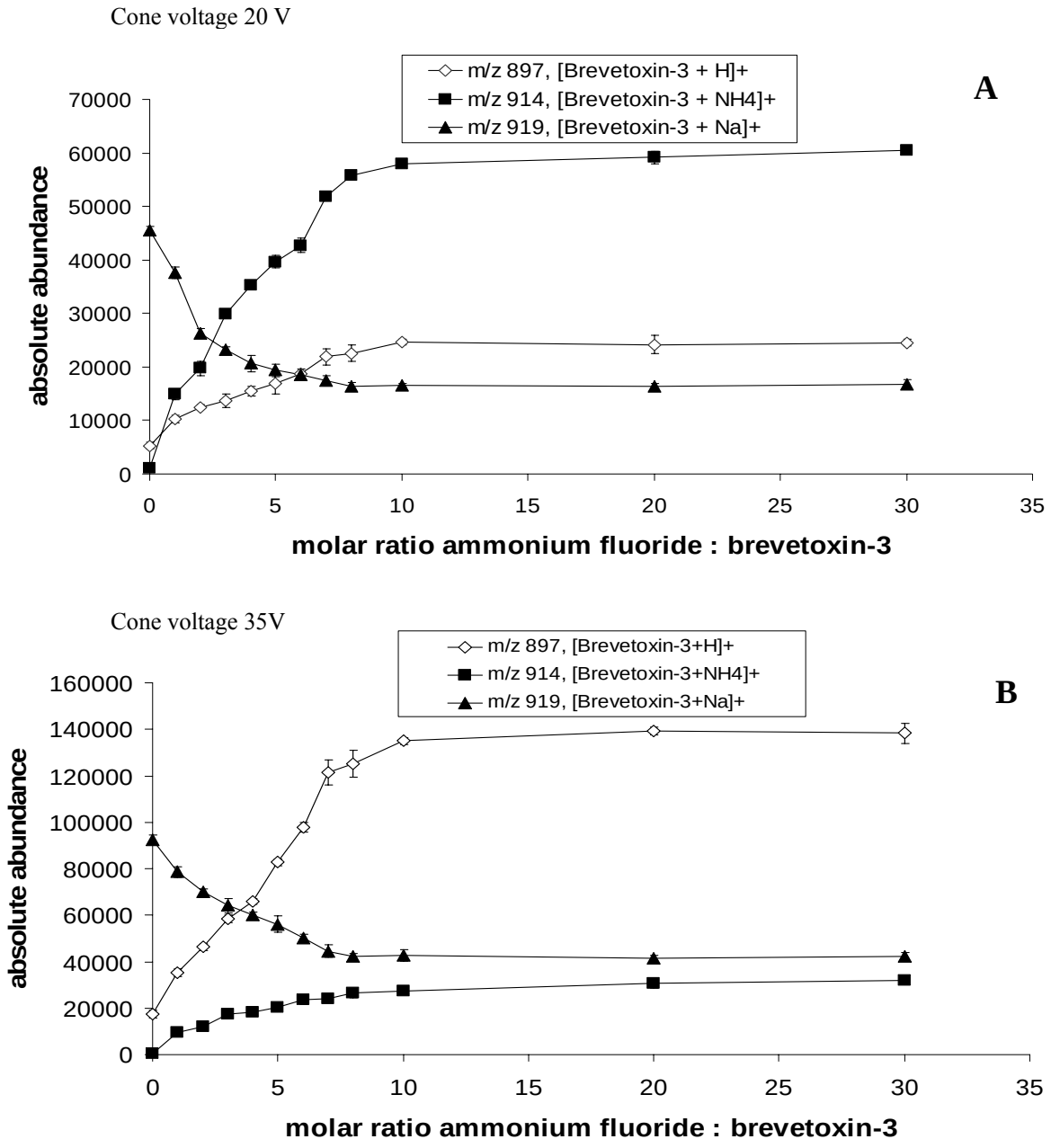

Figure 2.3. Absolute abundances of molecular ions of brevetoxin-3 vs molar ratio ammonium fluoride : brevetoxin-3. The concentration of brevetoxin-3 was set at 5 x 10^{-5} M, while the concentration of NH_4F was varied from 0 to 1.5 x 10^{-3} M; cone voltage was set at (a) 20 V and (b) 35 V.

that when brevetoxin-3 is dissolved in 1:1 methanol:water (no added ammonium fluoride), the *m/z* 919 sodium adduct $[\text{brevetoxin-3} + \text{Na}]^+$ (sodium from the environment) dominates the mass spectrum, while protonated brevetoxin-3 appears in very low abundance. However, as ammonium fluoride addition starts, the abundance of $[\text{brevetoxin-3} + \text{Na}]^+$ begins to drop significantly while $[\text{brevetoxin-3} + \text{NH}_4]^+$ at *m/z* 914 climbs dramatically. When the molar ratio of ammonium:brevetoxin-3 goes beyond 3:1, the abundance of $[\text{brevetoxin-3} + \text{NH}_4]^+$ surpasses that of $[\text{brevetoxin-3} + \text{Na}]^+$, and ammonium adducts become the base peak in the spectrum. The abundance of $[\text{brevetoxin-3} + \text{NH}_4]^+$ keeps increasing until the molar ratio reaches 10:1, where leveling off occurs. Meanwhile, the abundance of $[\text{brevetoxin-3} + \text{Na}]^+$ steadily declines until the 10:1 ratio is reached; beyond this point its signal levels off. This experiment indicates that, in order to observe the maximum $[\text{brevetoxin-3} + \text{NH}_4]^+$ signal, the optimum ammonium:brevetoxin-3 molar ratio should be about 10:1. Beyond this value, the ionic strength of the solution is needlessly increased.

An analogous experiment was conducted at a higher cone voltage, 35 V, the optimum value for observation of protonated brevetoxin-3 $[\text{brevetoxin-3} + \text{H}]^+$ (see Figure 2.2b). Figure 2.3b shows that at 35 V, when brevetoxin-3 is dissolved in 1:1 methanol:water (no added NH_4F), $[\text{brevetoxin-3} + \text{H}]^+$ at *m/z* 897 appears in only minor abundance while $[\text{brevetoxin-3} + \text{Na}]^+$ at *m/z* 919 dominates as the base peak (also seen in Figure 2.1a). As the addition of ammonium fluoride starts, the abundance of protonated molecules $[\text{M} + \text{H}]^+$ increases almost linearly with molar ratio (ammonium:brevetoxin-3) in the range of 1 to 8. A further molar ratio increase beyond 10 does not result in a significant change of the abundance. The ammonium adduct $[\text{brevetoxin-3} + \text{NH}_4]^+$ at *m/z* 914 follows a similar trend, except that it appears in lower

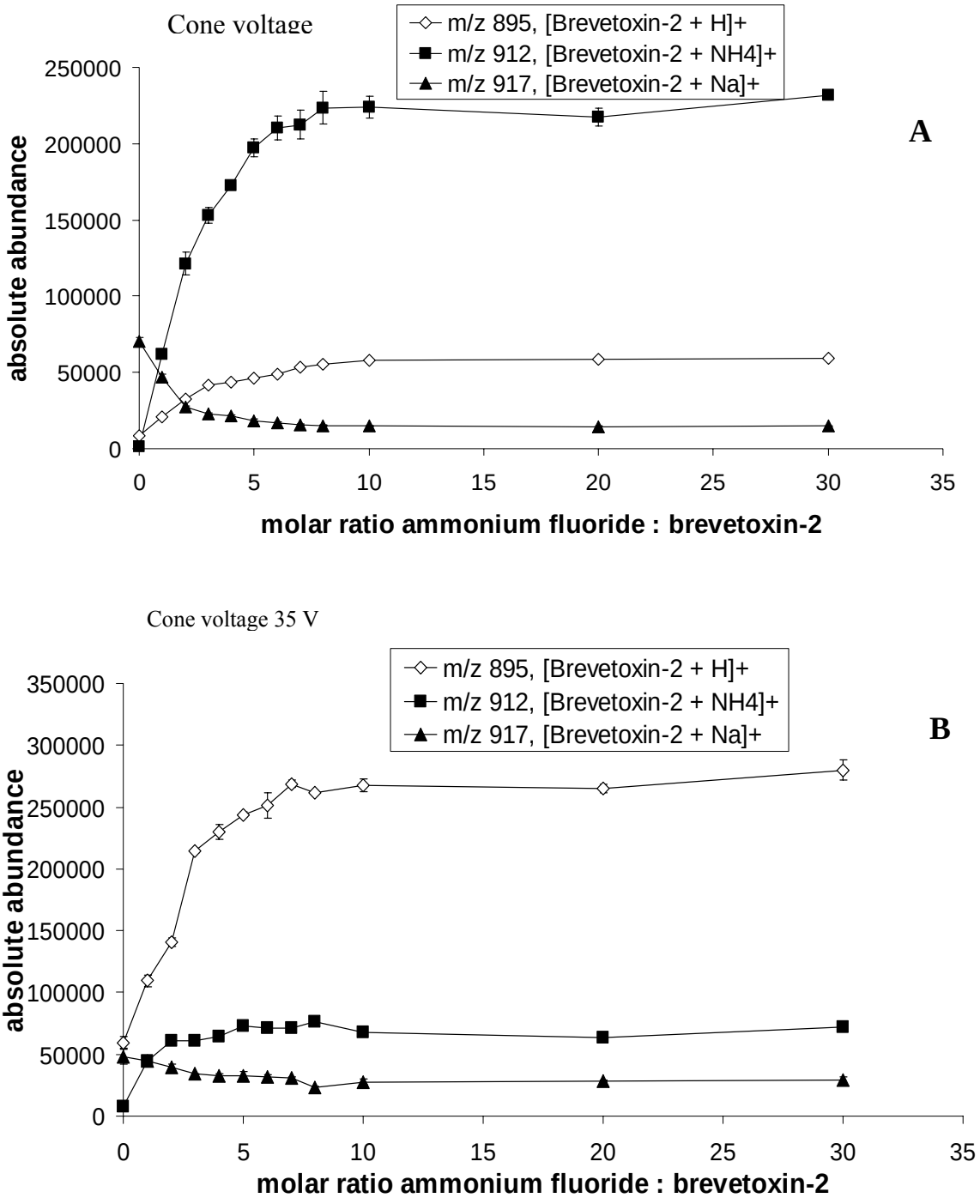

Figure 2.4. Absolute abundances of molecular ions of brevetoxin-2 vs ammonium fluoride : brevetoxin-2 molar ratio. The concentration of brevetoxin-2 was set at 5 x 10^{-5} M, while the concentration of NH_4F was varied from 0 to 1.5 x 10^{-3} M; cone voltage was set at (a) 20 V; and (b) 35 V.

abundance at each molar ratio (the cone voltage is not set at the optimal value for preservation of the ammonium adduct). The sodium adduct [brevetoxin-3 + Na]$^+$ at *m/z* 919 displays an opposite trend: it shows high abundance before ammonium addition, and its abundance decreases rapidly upon addition; it levels off when the molar ratio goes beyond 8:1. Figure 2.3b shows that the optimum molar ratio to observe protonated brevetoxin-3 is 10:1 (ammonium fluoride:brevetoxin-3). Analogous experiments monitoring adduct signals as a function of ammonium fluoride addition were conducted for brevetoxin-2. Figures 2.4a and 2.4b show that the optimum molar ratio is again approximately 10:1 (ammonium fluoride:brevetoxin-2) for appearance of either [brevetoxin-2 + NH_4]$^+$ or [brevetoxin-2 + H]$^+$ at cone voltages of 20 V or 35 V, respectively.

Yin et al. [20] reported that under appropriate CID conditions, ammonium adducts of peroxides could undergo fragmentation to yield fragment ions that incorporate the ammonium ion. In the current study, the product ion scan of the [brevetoxin-3 + NH_4]$^+$ precursor is shown in Figure 2.5a. When compared to Figure 2.5b, the analogous product ion spectrum of protonated brevetoxin-3 [brevetoxin-3 + H]$^+$, the similarities in fragment ions formed via CID are obvious. In addition, the spectra are devoid of even mass ions, which indicates that the ammonium ion is not incorporated in any of the Figure 2.5a fragments. These observations indicate that the first decomposition step for the [brevetoxin-3 + NH_4]$^+$ precursor is loss of a neutral ammonia molecule. Afterwards, consecutive decompositions take place from the remaining protonated brevetoxin-3, hence, the similarity in the products formed.

Figures 2.6a and 2.6b, the product ion mass spectra generated from the ammonium-brevetoxin-2 adduct and protonated brevetoxin-2, respectively, also share similar fragment ions with one

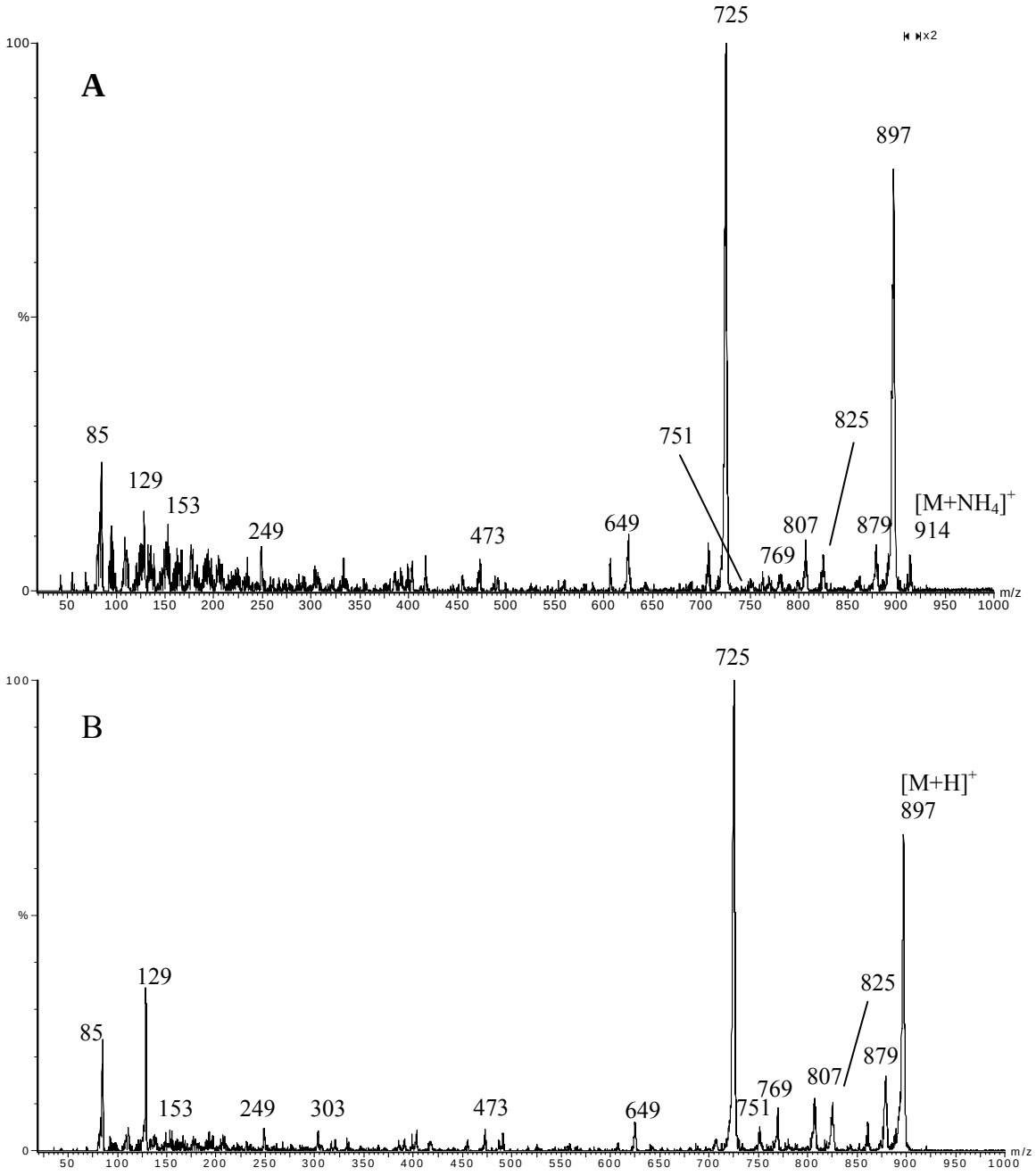

Figure2.5. Product ion spectra showing CID of (a) *m/z* 914 precursor, the ammonium adduct of brevetoxin-3, [brevetoxin-3 + NH_4]$^+$; and (b) *m/z* 897 precursor, protonated brevetoxin-3, [brevetoxin-3 + H]$^+$. The similarity of these two spectra indicates that the ammonium adduct loses NH_3 rapidly, then other (consecutive) decompositions occur from the remaining protonated species.

another. Similar to the above findings, no ammonium-containing fragments are observed in Figure 2.6a. These findings indicate that the first step for CID of [brevetoxin-2 + NH_4]$^+$ is ammonia loss, leaving the protonated molecule to undergo consecutive decompositions.

Detailed mechanisms to rationalize fragmentations of the two studied brevetoxins are illustrated in Figures 2.7 and 2.8. Upon collisional activation of the m/z 914 [brevetoxin-3 + NH_4]$^+$ precursor where ammonium ion has attached to the hydroxyl group (Figure 2.7), an ammonia molecule leaves the adduct to yield [brevetoxin-3 + H]$^+$ at *m/z* 897. Subsequent water loss produces a fragment at *m/z* 879, and ensuing fragmentation results in *m/z* 751 or *m/z* 769 (Figure 2.7). The latter two ions may also be formed during direct compositions of the [brevetoxin-3 + H]$^+$ precursor. Analogous mechanisms apply to the brevetoxin-2 ammonium adduct at *m/z* 912 and protonated brevetoxin-2 at *m/z* 895, to yield in both cases, analogous fragments at *m/z* 877, *m/z* 769 and *m/z* 751 (Figure 2.6).

Originating either directly from the protonated precursor [brevetoxin-3 + H]$^+$, or in the case where ammonia is lost from the initial [brevetoxin-3 + NH_4]$^+$ adduct and the excess proton becomes localized on the oxygen atom at ring H, the protonated ether oxygen will initiate subsequent fragmentation to yield *m/z* 473, as illustrated in Figure 2.8. Ammonium ion may also attach to the electron-rich double bond at the "tail" portion, and upon ammonia loss, can undergo fragmentation to yield *m/z* 825; subsequent water loss produces *m/z* 807 (Figure 2.8). These latter two fragment ions may also be produced from direct decompositions of the protonated brevetoxin-3 precursor (see figure 2.5b). Because the same sites of ammonium ion (or proton) attachment shown in Figure 2.8 are also available on brevetoxin-2, in principle, the analogous

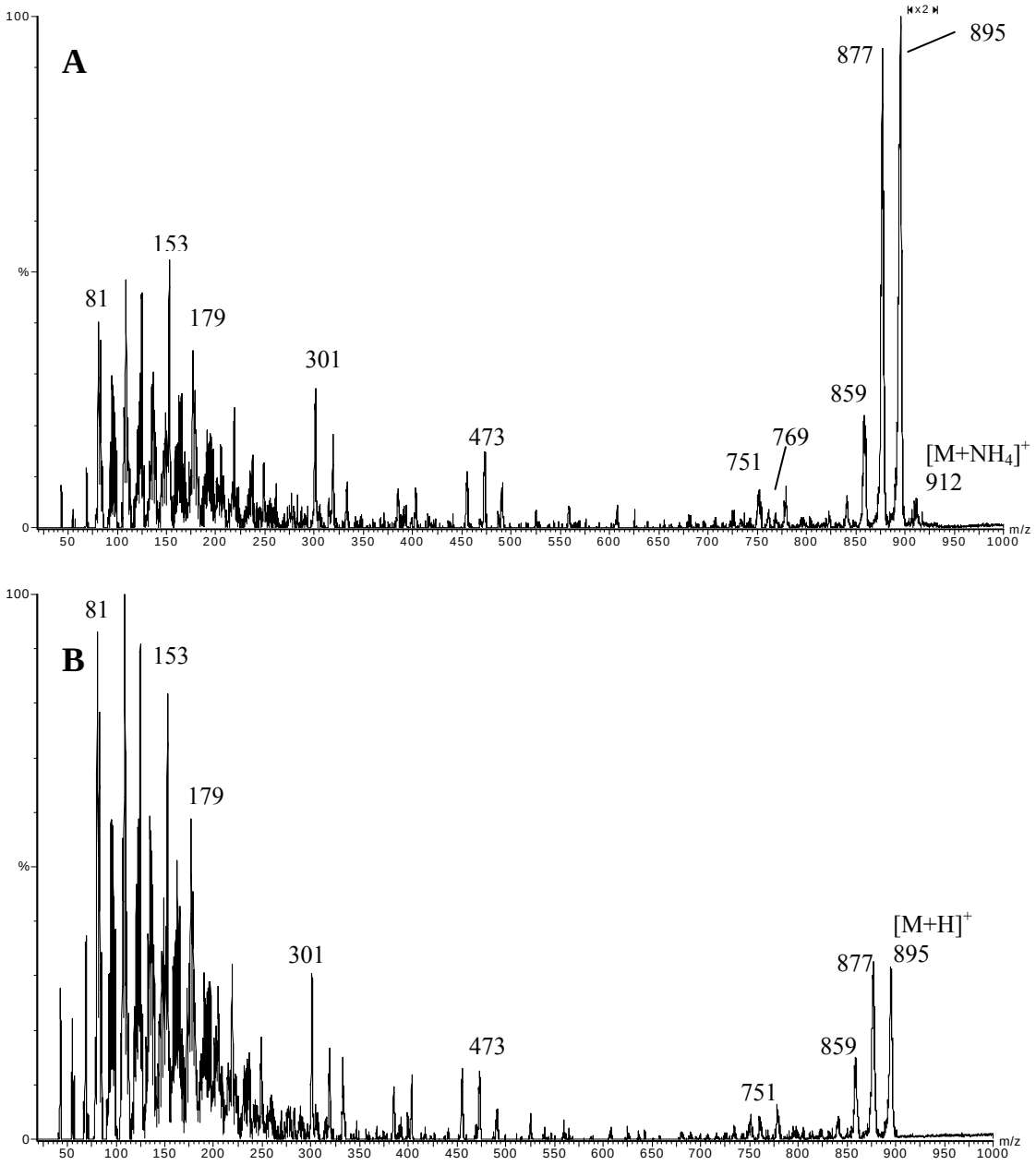

Figure 2.6. Product ion spectra of (a) *m/z* 912 precursor, the ammonium adduct of brevetoxin-2, [brevetoxin-2 + NH_4]$^+$; and (b) *m/z* 895 precursor, protonated brevetoxin-2. The similarity of these two spectra indicates that the ammonium adduct first loses NH_3, and then consecutive decompositions occur.

three decomposition pathways leading to m/z 473, 807 and 825 could apply to the latter neurotoxin; in practice, only the m/z 473 peak appeared in high abundance (see Figure 2.6).

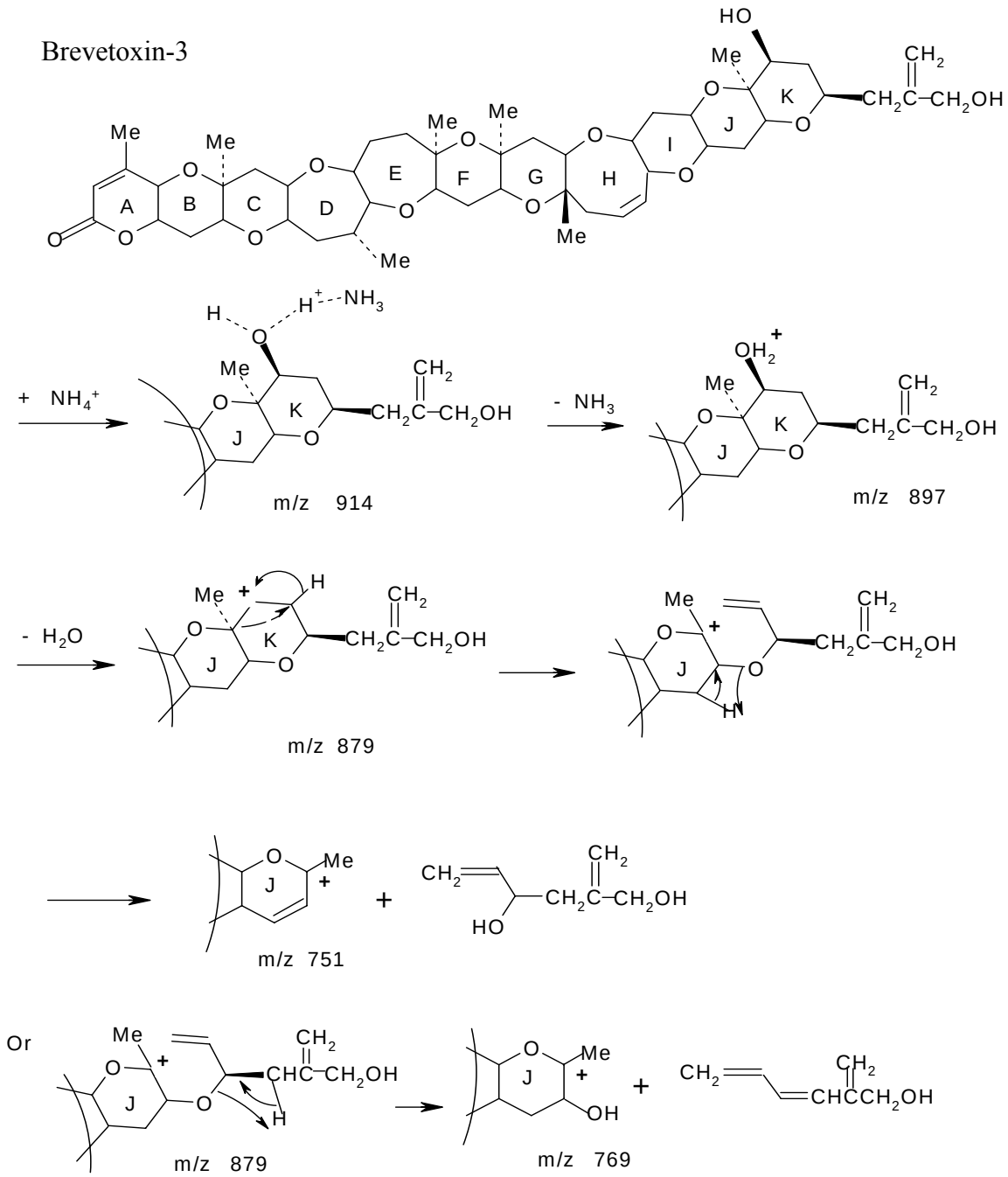

Figure 2.7. Proposed fragmentation of $[\text{brevetoxin-3} + NH_4]^+$ leading to *m/z* 751 and 769. Similar routes also apply to $[\text{brevetoxin-3} + H]^+$, $[\text{brevetoxin-2} + NH_4]^+$, and $[\text{brevetoxin-2} + H]^+$.

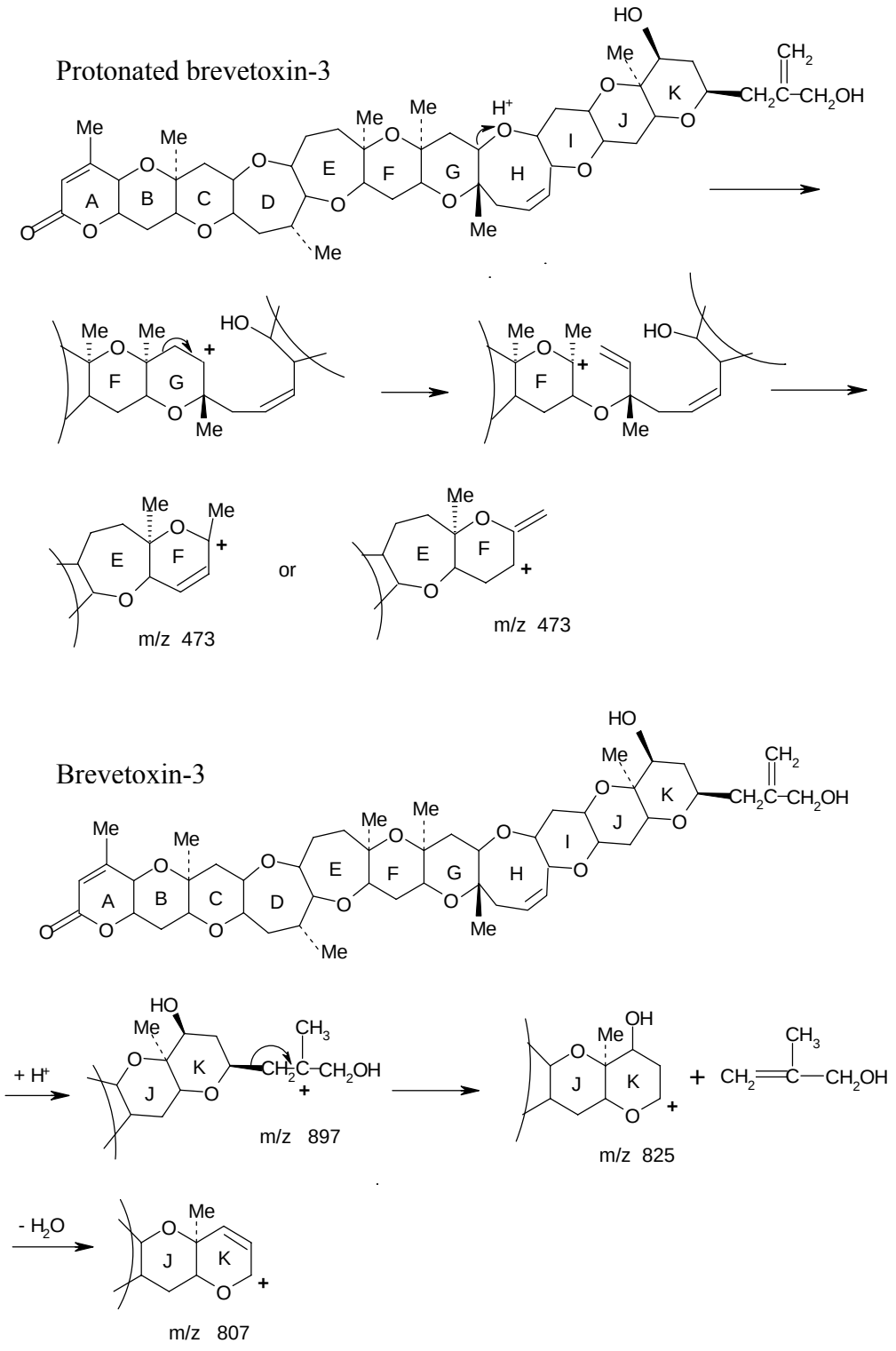

Figure 2.8. Proposed mechanisms for *m/z* 473, 807 and 825 formation from decompositions of [brevetoxin-3 + H]$^+$. Protonated brevetoxin-2 may also undergo analogous fragmentation pathways.

Conclusions

In this study, a sample-conserving nanoelectrospray method was developed to improve CID efficiency and the ability to deduce structural information from brevetoxins. The abundant sodium adducts typically observed during ES of brevetoxins do not efficiently yield product ions upon CID. Via addition of ammonium fluoride, ammonium ions were found to form cationic adducts with brevetoxins at very low cone voltages, reaching a maximum abundance at 20 V. When the cone voltage was further raised, the abundance of ammonium adducts decreased, while the abundance of protonated brevetoxin increased to become the base peak. The method thus allows the production of protonated brevetoxins under mild solution conditions (near neutral pH). These protonated brevetoxins readily underwent CID fragmentation, and they yielded similar product ions as compared to their ammonium adduct counterparts. This latter result indicates that the first step in ammonium adduct decomposition is loss of ammonia to form protonated brevetoxin which can undergo consecutive fragmentations. The addition of ammonium fluoride combined with the use of moderate cone voltages can markedly improve the ability to obtain structural information by ES-MS/MS from brevetoxins and other sodium-scavenging, robust compounds.

References

1. Risk M, Lin YY, MacFarlane RD, Ramanujam VMS, Smith LL, Trieff NM: **Purification and chemical studies on a major toxin from *Gymnodinium breve.*** In: *Toxic Dinoflagellate Blooms : Proceedings of second International Conference on Toxic Dinoflagellate Blooms.* Edited by Taylor DL, Seliger HH. New York: Elsevier/North Holland; 1979: 335-344.
2. Daugbjerg N, Hansen G, Larsen J, Moestrup O: **Phylogeny of some of the major genera of dinoflagellates based on ultrastructure and partial LSU rDNA sequesnce data**. *Phycologia* 2000, **39**(4):302-317.
3. Margalef R, Estrada M, Blasco D. In: *Toxic Dinoflagellate Bloom : Proceedings of second International Conference on Toxic Dinoflagellate Blooms.* Edited by Taylor DL, Seliger HH. New York: Elsevier/North Holland; 1979: 89-94.
4. Baden DG: **Brevetoxins: Unique polyether dinoflagellate toxins.** *FASEB J* 1989, **3**:1807-1817.
5. Rein KS, Lynn B, Gawley RE, Baden DG: **Brevetoxin B: Chemical modifications, synaptosome binding, toxicity, and an unexpected conformational effect.** *J Org Chem* 1994, **59**:2107-2113.
6. Rakotoniaina CA, Miller DM: **Assays for Ciguatera-Type Toxins.** . In: *Ciguatera Seafood Toxins'.* Edited by Miller DM. Boca Raton, FL: CRC Press; 1991: 73-86.
7. Hua Y, Lu W, Henry MS, Pierce RH, Cole RB: **On-line high performance liquid chromatography-electrospray ionization mass spectrometry for the determination of brevetoxins in "red tide" algae.** . *Anal Chem* 1995, **67**:1815-1823.

8. Hua Y, Lu W, Henry MS, Pierce RH, Cole RB: **On-line liquid chromatography-electrospray ionization mass spectrometry for determination of the brevetoxin profile in natural "red tide" algae blooms.** *J Chromatography A* 1996, **750**:115-125.

9. Dickey RW, Bencsath FA, Granade HR, Lewis RJ: **Liquid chromatograhic mass spectrometric methods for the determination of marine polyether toxins.** *Bull Soc Pathol Exot* 1992, **85**(5 Pt 2):514-515.

10. Poli M: **Laboratory Procedures for Detoxification of Equipment and Waste Contaminated with Brevetoxins PbTx-2 and PbTx-3.** *J Assoc Off Anal Chem* **1988**, **71**:1000-1002.

11. Plakas SM, El Said KR, Jester EL, H. RG, Musser SM, Dickey RW: **Confirmation of brevetoxin metabolism in the Eastern oyster (*Crassostrea virginica*) by controlled exposures to pure toxins and to *Karenia brevis* cultures**. *Toxicon* 2002, **40**(6):721-729.

12. Wang Z, Plakas SM, El Said KR, Jester EL, Granade HR, Dickey RW: **LC/MS analysis of brevetoxin metabolites in the Eastern oyster (Crassostrea virginica)**. *Toxicon* 2004, **43**(4):455-465.

13. Wang W, Hua Y, Wang G, Cole RB: **Characterization of rat liver microsomal and hepatocytal metabolites of brevetoxins by liquid chromatography-electrospray tandem mass spectrometry.** . *Anal and Bioanal Chem* 2005, **383**(1):67-75.

14. Hua Y, Cole RB: **Solution reactivity of brevetoxins as monitored by electrospray ionization mass spectrometry and implications for detoxification**. *Chem Res Toxicol* 1999, **12(12)**:1268-1277.

15. Hua Y, Cole RB: **Electrospray ionization tandem mass spectrometry for structural elucidation of protonated brevetoxins in red tide algae.** *Anal Chem* 2000, **72**(2):376-383.

16. Nozawa A, Tsuji K, Ishida H: **Implication of brevetoxin B1 and PbTx-3 in neurotoxic shellfish poisoning in New Zealand by isolation and quantitative determination with liquid chromatography-tandem mass spectrometry** *Toxicon* 2003, **42**(1):91-103.

17. Ishida H, Nozawa A, Nukaya H, Tsuji K: **Comparative concentrations of brevetoxins PbTx-2, PbTx-3, BTX-B1 and BTX-B5 in cockle, Austrovenus stutchburyi, greenshell mussel, Perna canaliculus, and Pacific oyster, Crassostrea gigas, involved neurotoxic shellfish poisoning in New Zealand**. *Toxicon* 2004, **43**(7):779-789.

18. Stark CBW, Lopes NP, Fonseca T, Gates PJ: **The effect of ruthenium (III) chloride on the formation of protonated parent ions in electrospray mass spectrometry.** *Chem Commun* 2003(21):2732-2733.

19. Fleet IA, Monaghan JJ: **Comparison of electrospray mass spectrometry of chrysanthemic acid ester pyrethroid insecticides with electron ionization and positive-ion ammonia chemical ionization methods.** *Rapid Commun in Mass Spectrom* 1997, **11**(7):796-802.

20. Yin H, Hachey DL, Porter NA: **Structural analysis of diacyl peroxides by electrospay tandem mass spectrometry with ammonium acetate**. *Rapid Commun Mass Spectrom* 2000, **14**(14):1248-1254.

21. Wilm M, Mann M: **Analytical Properties of the Nanoelectrospray Ion Source.** *Anal Chem* 1996, **68**:1-8.

22. Cech NB, Enke CG: **Practical implications of some recent studies in electrospray ionization fundamentals**. *Mass Spectrom Rev* 2001, **20**:362-387.

Chapter III

Enhanced CID Efficiency and Unraveling of Novel Fragmentation Pathways of Brevetoxins in Negative Ion Electrospray Mass Spectrometry

Abstract

Brevetoxins are a group of natural neurotoxins characterized by polyether ring systems that are found in the blooms of red tide algae. In a conventional water/organic solvent system, without any other additives, deprotonated molecules of brevetoxins do not appear in high abundance in negative mode electrospray-mass spectrometry (ES-MS) due to lack of acidic functional groups, thus they are not well-suited for collision induced dissociation (CID) experiments in negative mode electropsray. In this study, several anions were tested for their abilities to form anionic adducts by mixing ammonium salts of these anions with brevetoxin-2 and brevetoxin-3. Under CID, $[M + Br]^-$, $[M + OAc]^-$, $[M + HCOO]^-$, and $[M + NO_3]^-$ adducts all produced only the respective anions in CID experiments, and thus provided no structural information. In contrast, upon CID, both $[M + F]^-$ and $[M + HCO_3]^-$ precursor adducts gave structurally-informative fragment peaks that exhibited similarities to those of $[M - H]^-$ ions, which indicated that the first step in gas phase decomposition of these anionic adducts was loss of neutral HF or H_2CO_3 molecules, respectively, leaving deprotonated brevetoxin $[M - H]^-$ to undergo consecutive fragmentations. Compared to bicarbonate adducts, fluoride adducts provided more fragment peaks, thus more structural information. It is therefore the anion of choice to study brevetoxins in

negative mode electrospray mass spectrometry using the anionic adduct approach. The detailed fragmentation mechanisms are discussed; optimum values of cone voltage and anion concentration were determined. To test the developed methodology, a sample of brevetoxin-2 subjected to *in vitro* microsomal incubation was analyzed and identified as brevetoxin-3, a reduction product of the substrate.

Key words: mass spectrometry, negative ion electrospray, brevetoxins, anionic adducts, LC-MS/MS.

3.1 Introduction

Brevetoxins are a family of lipid-soluble, polycylic ether marine neurotoxins that are produced from the single cell dinoflagellate *Karenia brevis* (formerly known as *Ptychodiscus brevis* and *Gymnodinium breve*)[1] [2]. Under suitable conditions of temperature and salinity, the algae may reproduce rapidly, causing a "red-tide" bloom, a phenomenon that was documented by Spanish explorers along the Florida Gulf coast as far back as the 1530s [3]; reports of red-tide induced marine mammal toxicity can be dated back to 1844 [4] [5]. Such harmful algal blooms can cause periodic massive fish kills along the Gulf of Mexico coast and other salt water locations [6] [7], in fact, blooms containing 0.2 million cells/Liter of *Karenia brevis* effectively kill fish [8]. Consumption of shellfish contaminated by brevetoxins leads to neurotoxic shellfish poisoning in

humans [9] [10] . In addition, due to the fragile nature of dinoflagellates, *Karenia brevis* cells can be broken during more violent wave motions, thereby releasing brevetoxins into open water [11], as well as creating a toxin-containing aerosol [12]. Humans living in coastal areas will experience respiratory irritation and other symptoms when inhaling such an aerosol [13] [14].

At least 9 brevetoxins have been found and their structures fully elucidated, their structures can been seen in our previous publication [15]. Among them, brevetoxin-1 is the most toxic one and brevetoxin-2 is the most abundant in the red tide bloom [16]. Based on two different backbone structures, brevetoxins can be classified as either type A, which has a 10-ring polyether system, and type B, which has 11 polyether rings [17].

A variety of analytical methods have been developed to measure brevetoxins, from functional assays such as the mouse bioassay that has been used to monitor the level of brevetoxin in shellfish [18], to immunoassays such as radio-immunoassay [19] and ELISA [20] that have been used to detect brevetoxins in sea water, shellfish and mammalian body fluid. However, direct chemical analysis of brevetoxins, especially mass spectrometry-based methods that have inherently high specificities certainly are advantageous, and have become the major analytical method of choice.

Dickey et al. [21] developed a method of HPLC-FAB-MS to study brevetoxin-3 by employing derivatizing agents in the early 1990s. Later, a liquid chromatography–electrospray-mass spectrometry (LC-ES-MS) was developed in our lab to directly analyze the various types of brevetoxins in red-tide extracts [22, 23]. Poli et al. [19] reported using LC-MS to identify

brevetoxin-3 in shellfish, a likely metabolite of brevetoxin-2. Plakas et al. [24, 25] exposed Eastern oysters (*Crassostrea virginica*) to brevetoxin-2, where the toxin was extensively metabolized. LC-MS fractions contained m/z 1018 and 1034 representing protonated molecules of cysteine-brevetoxin and cysteine-brevetoxin sulfoxide conjugates, respectively. In a follow up paper, Wang et al. [26] identified several amino acid conjugates of brevetoxins, as well as other metabolites such as glutathione and related peptide conjugates. To date, most accounts of mass spectrometry-based brevetoxin analyses are focused on positive mode electrospray. In our lab, brevetoxin-1 and brevetoxin-2 were found to form metabolites via rat liver hepatocytes and rat liver microsomal incubations, respectively [27]. They were first studied in the positive ion mode. We also elucidated certain acidic products resulting from hydrolytic lactone-ring (A-ring) opening by negative mode tandem mass spectrometry [27]. Abraham et al. [28] later reported the existence of open A-ring brevetoxin analogues in *Karenia brevis* cultures and in natural blooms by using solid phase extraction (SPE) and LC-MS/MS. Such fractions are rather polar and were poorly extractable by conventional non-polar solvents like chloroform.

Due to the unique molecular architecture of brevetoxins, including multiple ether linkages, they exhibit a high affinity toward sodium ions and readily form sodium adducts $[M + Na]^+$. Without sample pre-treatment, even just trace levels of ubiquitous sodium, will result in $[M + Na]^+$ ions dominating the positive mode electrospray mass spectrum. Sodium adducts of brvetoxins, however, are quite resistant to decomposition, even under higher energy collision induced dissociation (CID); Under harsh collision conditions, they tend to produce mostly sodium ions, without significant yields of structurally-informative fragments [29].

To promote the signals of protonated brevetoxins over sodium adducts, various approaches have been employed. In our lab, we treated brevetoxins with strong acid to favor production of $[M + H]^+$ ions that were shown to readily fragment under moderate (50-70 eV) CID conditions [30]. After our report, Nozawa and coworkers [31] and Ishida and coworkers [32] promoted $[brevetoxins + H]^+$ ions by adding formic acid to the LC-MS/MS mobile phase, while Radwan et al. [33] used a mobile phase containing acetic acid to perform LC-MS/MS multiple reaction monitoring (MRM). In later work, we developed an alternative method employing nanoelectrospray where ammonium salts of selected anions were added to the solvent to promote the formation of protonated brevetoxin molecules and ammonium adducts [15]. Ammonium adducts of brevetoxins produced fragmentation patterns similar to those of the protonated brevetoxins. The latter procedure avoided the drawbacks of analyzing strongly acidic solvents and reduced the level of sample consumption.

An alternative way to study brevetoxins by electrospray mass spectrometry is to use the negative ion mode of operation, however, such studies are still rare. Because brevetoxins do not have acidic functional groups, e.g. carboxylic acid moieties, without further treatment, deprotonated brevetoxins are not formed in high enough yields for CID study. Although adding base to the system is a common technique to enhance deprotonation, it increases the risk of hydrolysis reactions. On the other hand, for compounds that lack acidic sites, anion attachment can be a practical approach to negative mode ES mass spectrometric analysis [34]. Although evidence of anion attachment in negative mode electrospray can be traced back to Yamshita and Fenn's work in 1984 [35], this area, as well as negative mode electrospray in general, has received far less attention than positive mode endeavors, partially due to the lower stability of negative mode

electrospray signals, caused by an added tendency toward electrical (corona) discharge. Nevertheless, negative ion electrospray may provide a totally different view to improve understanding of the analyte. In this study, several types of anions were employed to undergo attachment with brevetoxin molecules. We report on the success of various anionic adducts in providing useful structural information concerning brevetoxins in negative mode electrospray tandem mass spectrometry.

3.2 Experiment

Brevetoxins were purchased from CalBiochem (La Jolla, CA), and ammonium fluoride, ammonium acetate, ammonium bicarbonate, ammonium chloride, ammonium bromide, ammonium formate, ammonium nitrate and ammonium hydroxide were all purchased from Aldrich (Milwaukee, WI). All mass spectrometry experiments were performed on a Quattro II and Quattro micro "triple quadrupole" (quadrupole-hexapole-quadrupole) mass spectrometer equipped with an electrospray ionization source (Micromass/Waters Inc. Manchester, UK). The flow rate for direct infusion was set at 1 μL/min. Nitrogen gas was employed as both drying gas and nebulizing gas; the ES "needle" voltage was set at 2.7 kV. Collision-induced decomposition (CID) tandem mass spectra were acquired using argon as collision gas at a pressure of 2.1×10^{-2} Pa on Quattro II instrument and 0.25 Pa on Quattro micro instrument (gauge external to hexapole collision cell). All mass spectra represent the average of 10 to 20 scans. M/z values were rounded down (truncated) to the nearest integer values, that is, the nominal masses of the fragment ions are reported in the spectra.

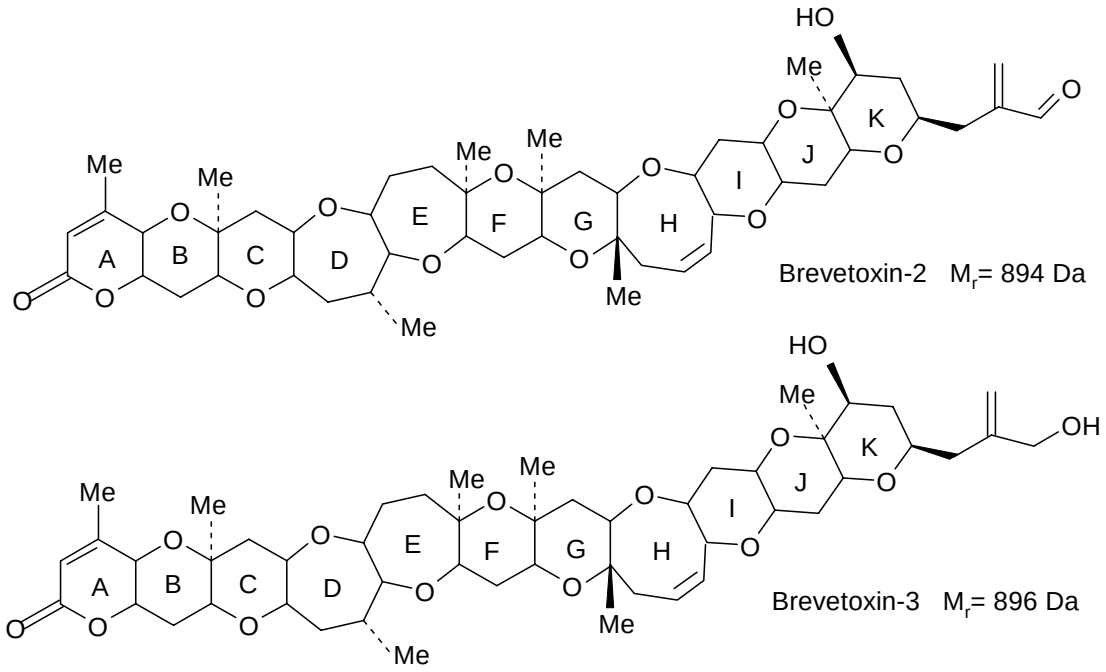

Figure 3.1. Structures of brevetoxin-2 and brevetoxin-3

To test the developed method on a real sample of biological significance, brevetoxin metabolites were generated by conducting *in vitro* incubations of brevetoxin-2, using rat liver microsomes purchased from Gentest Corp. (Woburn, MA). After incubation, the samples containing substrate and metabolites were cleaned up by adding ice cold methanol, and then passing the supernatant through a Microcon YM-3 filter (Pittsburgh, PA) to remove proteins in preparation for LC-MS/MS analysis. The details of microsomal incubation of brevetoxin-2 and LC-MS mobile phase conditions can be found elsewhere [27].

3.3 Results and Discussion

The acidity (or basicity) of a compound plays an important role in electrospray mass spectrometry. Generally speaking, positive mode electrospray is suitable for molecules with enough basicity to readily attract an ionizing proton, whereas negative mode electrospray is a good choice for compounds of high acidity. However, for compounds that lack an acidic functional group, for example, neutral oligosaccharides, without the aid of a base to promote deprotonation, their $[M - H]^-$ signals in negative mode electrospray are usually poor. Previous research has shown that anion attachment is a very useful approach to making such analytes "visible" in negative mode electrospray mass spectrometry.

A series of studies [34, 36-40] conducted in our lab has shown that factors such as a matching of the gas phase basicities of the deprotonated analyte and the selected anion, and the propensity to form hydrogen bonds are critical for the formation and stability of anionic adducts. Follow-up computational studies also helped to understand such analyte-anion adducts [34, 39]. We have

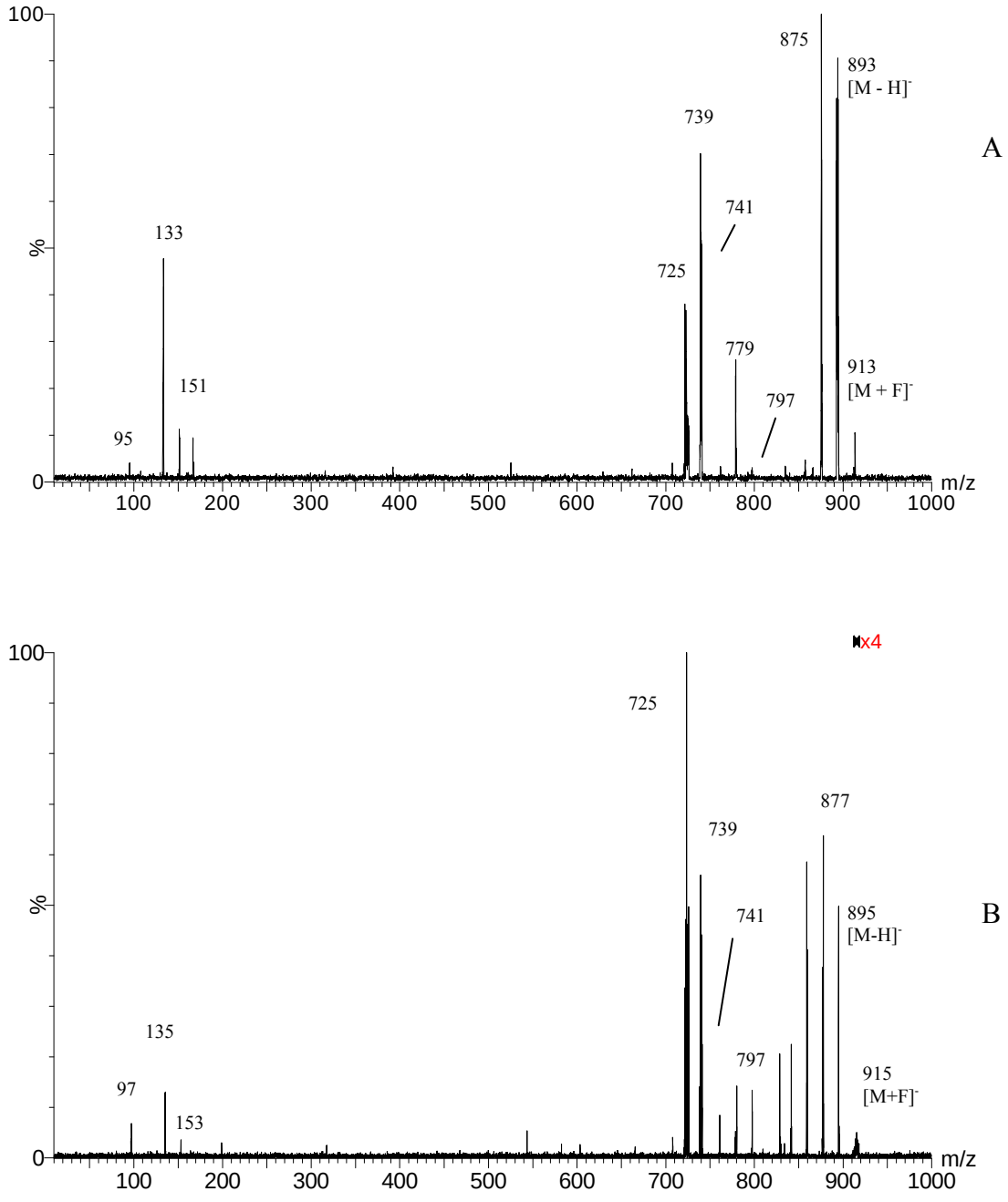

Figure 3.2 A) Negative mode product ion spectrum of m/z 913 precursor, the fluoride adduct of brevetoxin-2 standard [brevetoxin-2 + F]$^-$. B) product ion spectrum of m/z 915 precursor, the fluoride adduct of brevetoxin-3 standard. [brevetoxin-3 + F]$^-$.

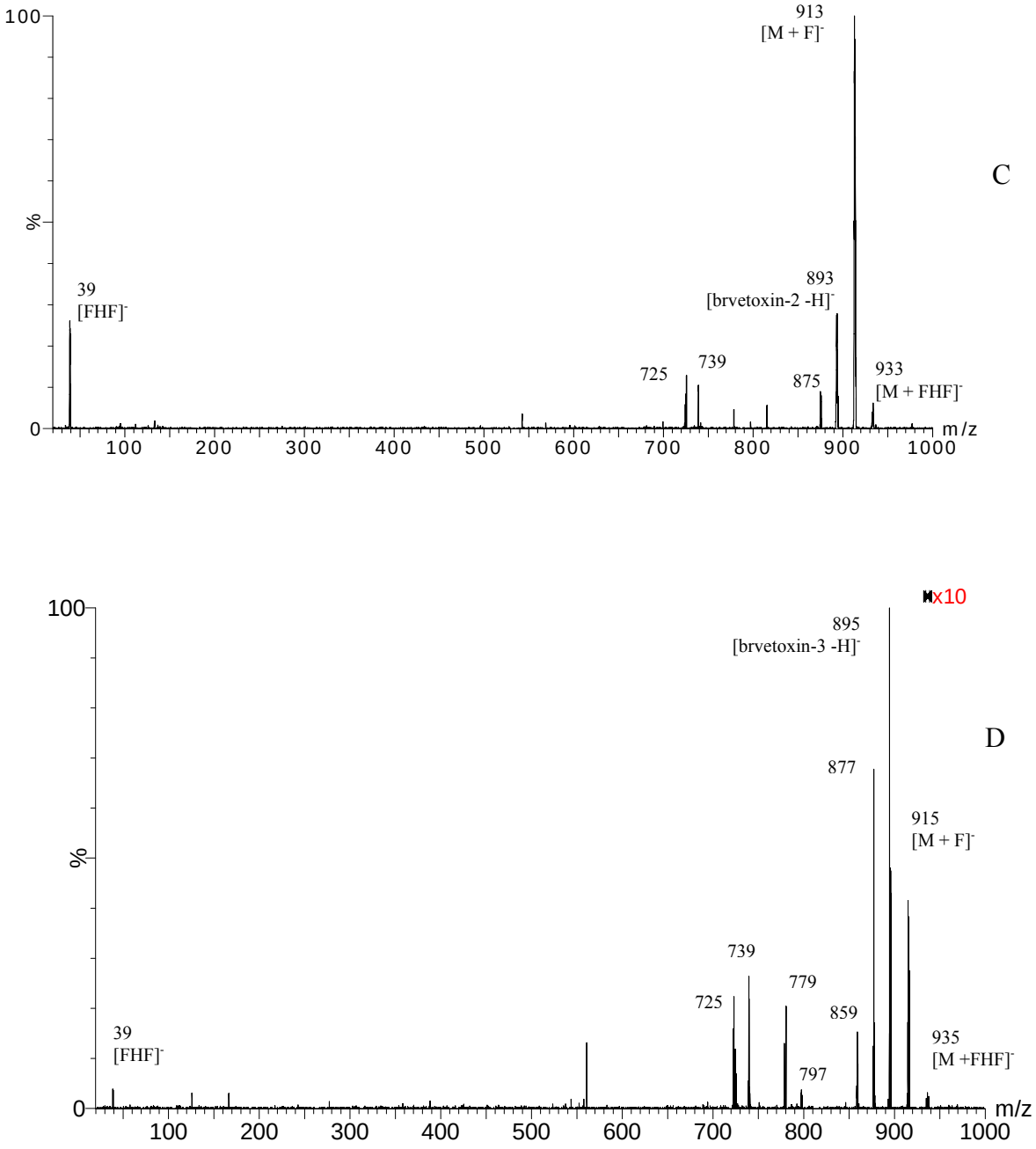

Figure 3.2 contd. C) Negative mode product ion spectrum of m/z 933 precursor, [brevetoxin-2 + FHF]$^-$. D) product ion spectrum of m/z 935 precursor, [brevetoxin-3 + FHF]$^-$.

employed chloride ions for attachment to disaccharides, and decompositions of disaccharide-chloride adducts gave diagnostic glycosidic bond linkage information[38, 41] including anomeric configuration [42]. Murae et al. [43] reported using both chloride and bromide to characterize tetraether lipids in archaea membrane. Harvey [44] tried different anions to study N-linked glycans and found that nitrate adducts gave satisfactory signals in negative ion electrospray, i.e., 10-fold stronger signals than from the corresponding $[M - H]^-$ ions formed with the assistance of added ammonium hydroxide. Sheen and Her [45] analyzed several neutral drugs in plasma by liquid chromatography-negative ion electrospray-tandem mass spectrometry, with the approach of adding fluoride to promote $[M + F]^-$ adducts; good detection limits and linearity were observed.

Anion of Choice

Building upon our previous experience with anion attachment in negative ion ES-MS [34, 36-42], including specific experience with fluoride attachment [40], for the brevetoxin samples under investigation, the first system that we examined was brevetoxin - NH_4F. In addition to producing abundant $[M + F]^-$ adducts, further CID experiments showed that both [brevetoxin-2 + $F]^-$ and [brevetoxin-3 + $F]^-$ precursors gave structurally-informative fragments (as demonstrated in figures 3.2a and 3.2b). The fragmentation patterns were very similar to those of the corresponding $[M - H]^-$ precursors generated by addition of ammonium hydroxide, shown in Figures 3.3a and 3.3b. The similarities in the two pairs of CID spectra indicate that the first step of the decomposition of $[M + F]^-$ adducts in the gas phase was to lose hydrogen fluoride and

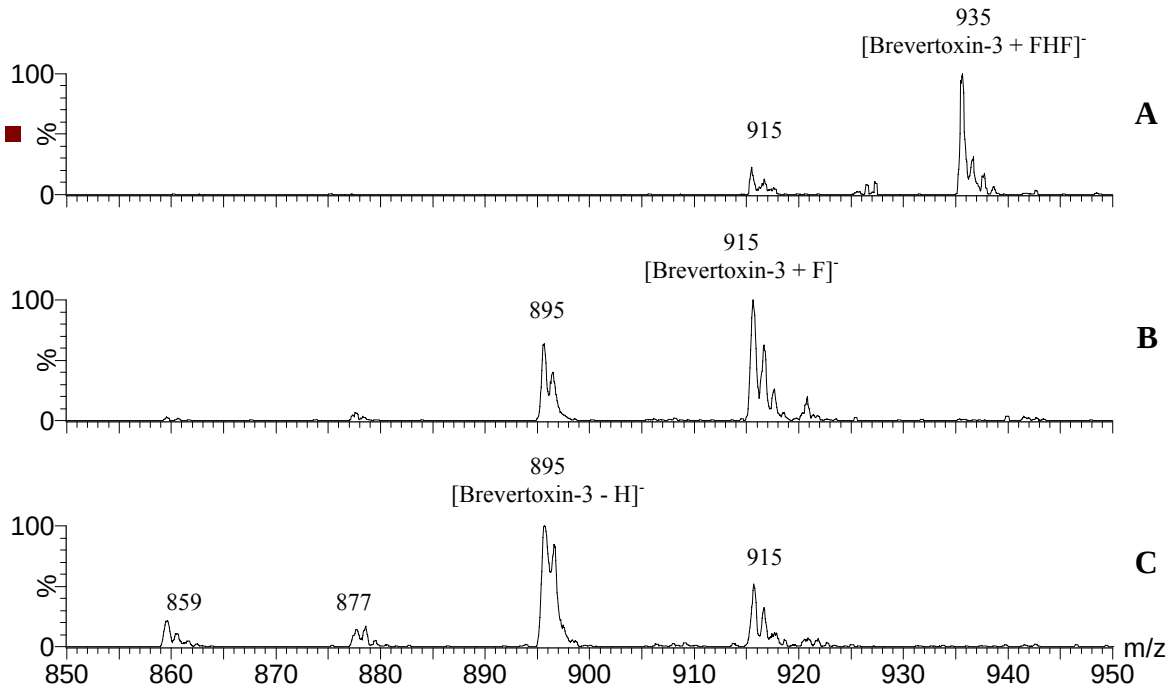

Graph 1. Electrospray mass spectra of (brevetoxin-3 - NH_4F) system as a function of cone voltage. The concentration of brevetoxin-3 was set at 5 x 10^{-5} M in a 1:1 water/acetonitrile solution, and the cone voltage was set at (A) 10 V, (B) 40 V, and (C) 60 V. The abundances of deprotonated brevetoxin-3 (m/z 895) and its fragments (m/z 877 and m/z 859) increased, whereas those of $[\text{brevetoxin-3} + \text{FHF}]^-$ (*m/z* 935) and $[\text{brevetoxin-3} + \text{F}]^-$ (*m/z* 915) decreased, as the cone voltage was raised.

thereby form $[M - H]^-$. Afterwards, consecutive fragmentations of these deprotonated molecules yielded products similar to those appearing in figure 3.3a and 3b.

The production of $[brevetoxin - H]^-$, along with the absence of F^- observed in the product ion mass spectra of $[brevetoxin\text{-}2 + F]^-$ (figure 3.2a) and $[brevetoxin\text{-}3 + F]^-$ (figure 3.3b) precursors indicates that the gas-phase basicity of deprotonated brevetoxin-2 and brevetoxin-3 are lower than that of fluoride. The strong basicity of the fluoride anion allows it to easily capture a proton from neutral brevetoxin and depart as HF.

In the same brevetoxin - NH_4F system, in the low cone voltage range (e.g. 10-20 V), the presence of $[M + 39]^-$ adduct ions was also observed (graph 1a). CID of such adduct precursors showed both $[M + F]^-$ and m/z 39 peaks (figure 3.2c, 3.2d), which indicated that this adduct was the $[M + FHF]^-$ ion, and m/z 39 was the FHF^- ion. Such FHF^- clusters were first detected by Larson and McMahon in 1983 [46], Caldwell and Kebarle [47] studied the gas - phase equilibrium of $F^- + HF \leftrightarrow FHF^-$ in the mid 1980's using a high pressure mass spectrometer, and Li et al. [48] have calculated that the bond angle of the FHF^- ion cluster is very close to linear at 179.4°. Clearly, the FHF^- ion has a lower gas-phase basicity than that of fluoride ion, as it is visible in the product ion scans (figures 3.2c and 3.2d). CID of such adducts also provided structurally-informative fragments, although in lower yields, than direct decompositions of the fluoride adducts (figures 3.2a and 3.2b).

In addition to fluoride, we also attempted to find other anions capable of forming brevetoxin-anion adducts, which hopefully would also provide informative fragmentation, and bicarbonate

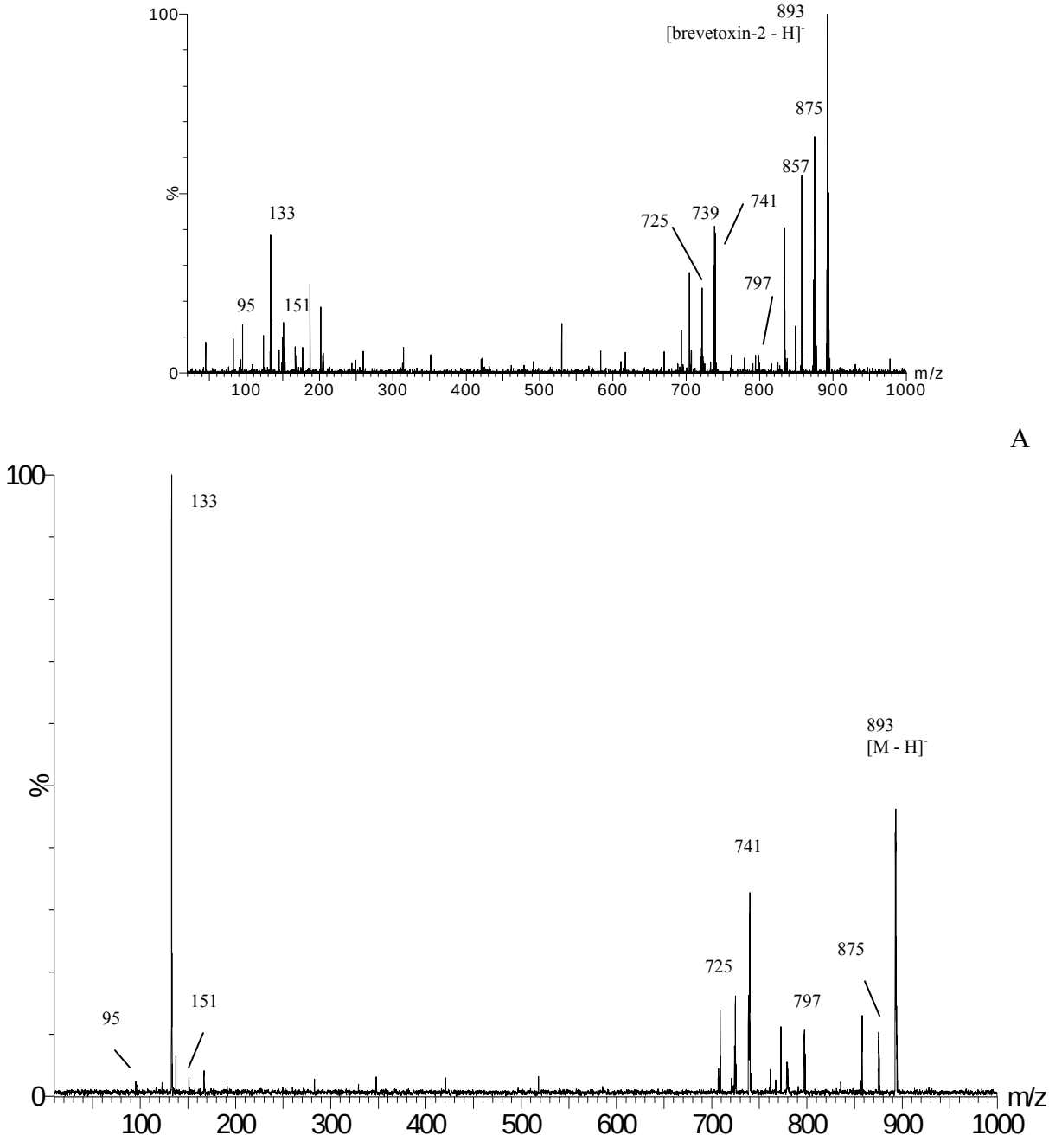

Figure 3.3 A) Negative mode product ion spectrum of m/z 893 precursor, deprotonated brevetoxin-2, promoted by adding ammonium fluoride, inset, product ion spectrum of m/z 893, promoted by adding ammonium hydroxide.

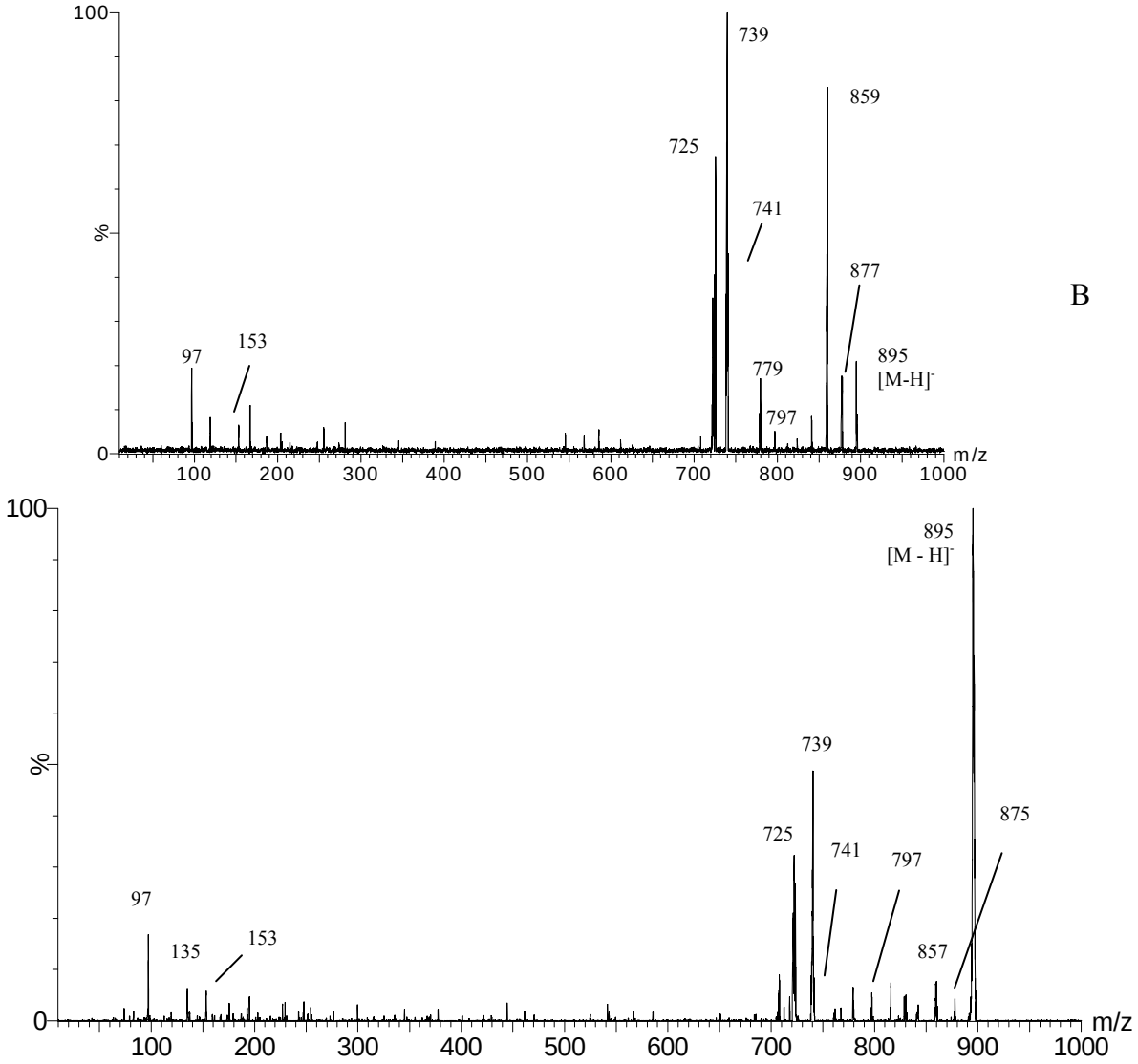

Figure 3.3 continued. B) product ion spectrum of m/z 895 precursor, deprotonated brevetoxin-3 promoted by adding ammonium fluoride; inset, tandem mass spectrum of m/z 895, promoted by ammonium hydroxide addition).

is another anion that was tested for this purpose. In figure 3.4, it is shown that both [brevetoxin-2 + HCO_3]$^-$ at m/z 955 and [brevetoxin-3 + HCO_3]$^-$ at m/z 957 can give structurally-informative brevetoxin fragments upon CID. The patterns of fragmentation are similar to those of the corresponding deprotonated brevetoxins, shown in figure 3.3. This is evidence that, for bicarbonate adducts, losing neutral carbonic acid is the first step of fragmentation (as was also the case for fluoride adducts losing HF). Interestingly, a peak corresponding to water loss from [brevetoxin-2 + HCO_3]$^-$ adducts can be seen at m/z 937 (figure 3.4a), but no such peak is visible for [brevetoxin-3 + HCO_3]$^-$ adducts at m/z 939 (figure 3.4b).

Experiments with other anions showed that brevetoxins would also form anionic adducts with chloride, bromide, formate, acetate and nitrate that were detectable in negative mode electrospray. However, under CID conditions, such precursor adducts only produced the respective anions and could not provide structural information (chloride adducts are shown as examples in figure 3.5). Based on these experiments, we can infer that the gas phase basicities of deprotonated forms of brevetoxin-2 and brevetoxin-3 are higher than those of chloride, bromide, formate, acetate and nitrate anions, but are lower than those of fluoride and bicarbonate, this situates the proton affinity of deprotonated brevetoxin-2 and deprotonated brevetoxin-3 somewhere between 1523 kJ/mol (bicarbonate) and 1427 kJ/mol (acetate); the gas phase bascities of the studied anions are listed in Table 1.

In comparing the product ion spectra of fluoride (Figures 3.2a and 3.2b), and bicarbonate (Figures 3.4a and 3.4b) adduct precursors of brevetoxins, fluoride adducts provide more

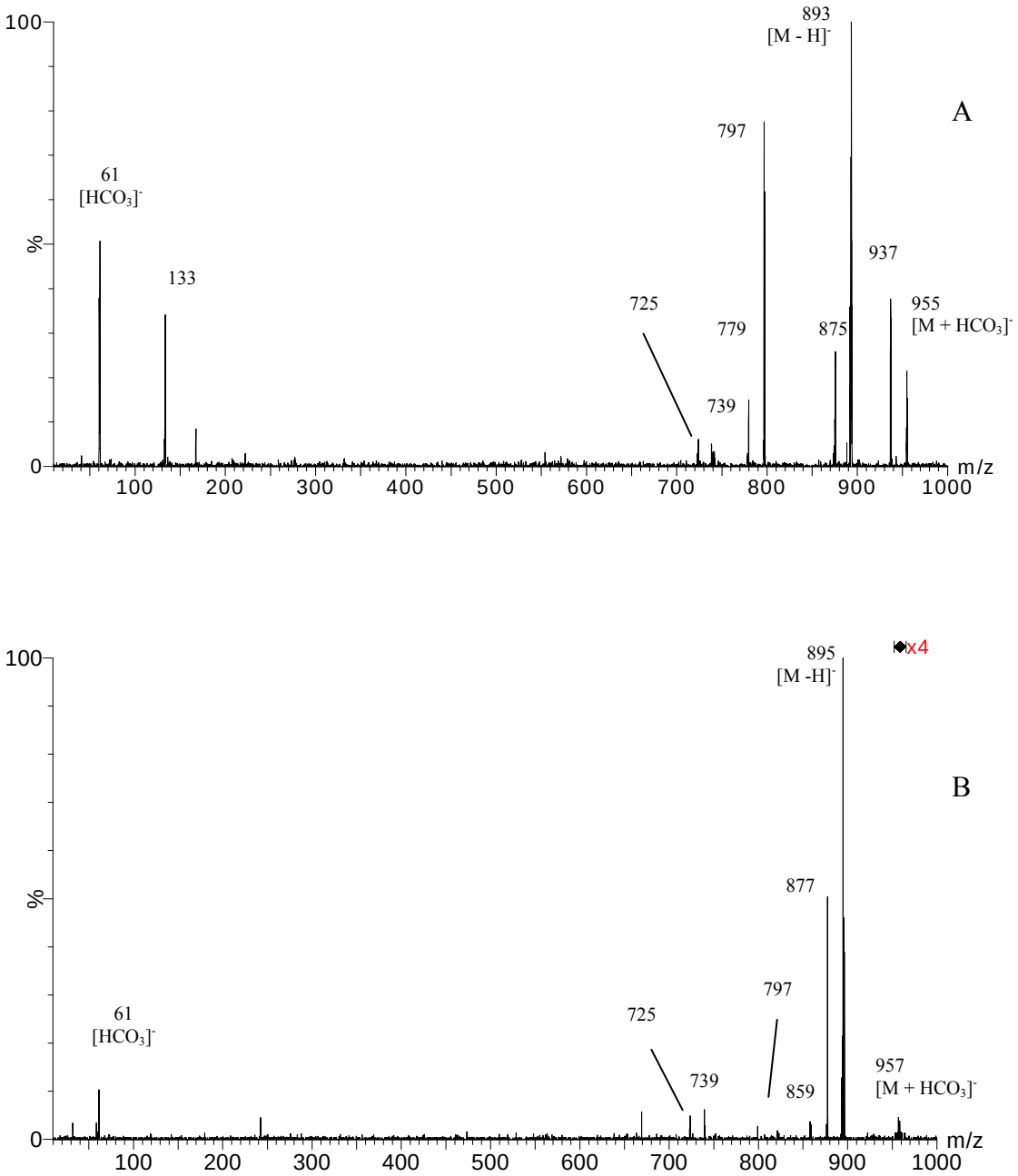

Figure 3.4. Negative mode product ion mass spectrum of m/z 955 precursor, the bicarbonate adduct of brevetoxin-2 standard. Bottom: product ion spectrum of m/z 957 precursor, the bicarbonate adduct of brevetoxin-3 standard.

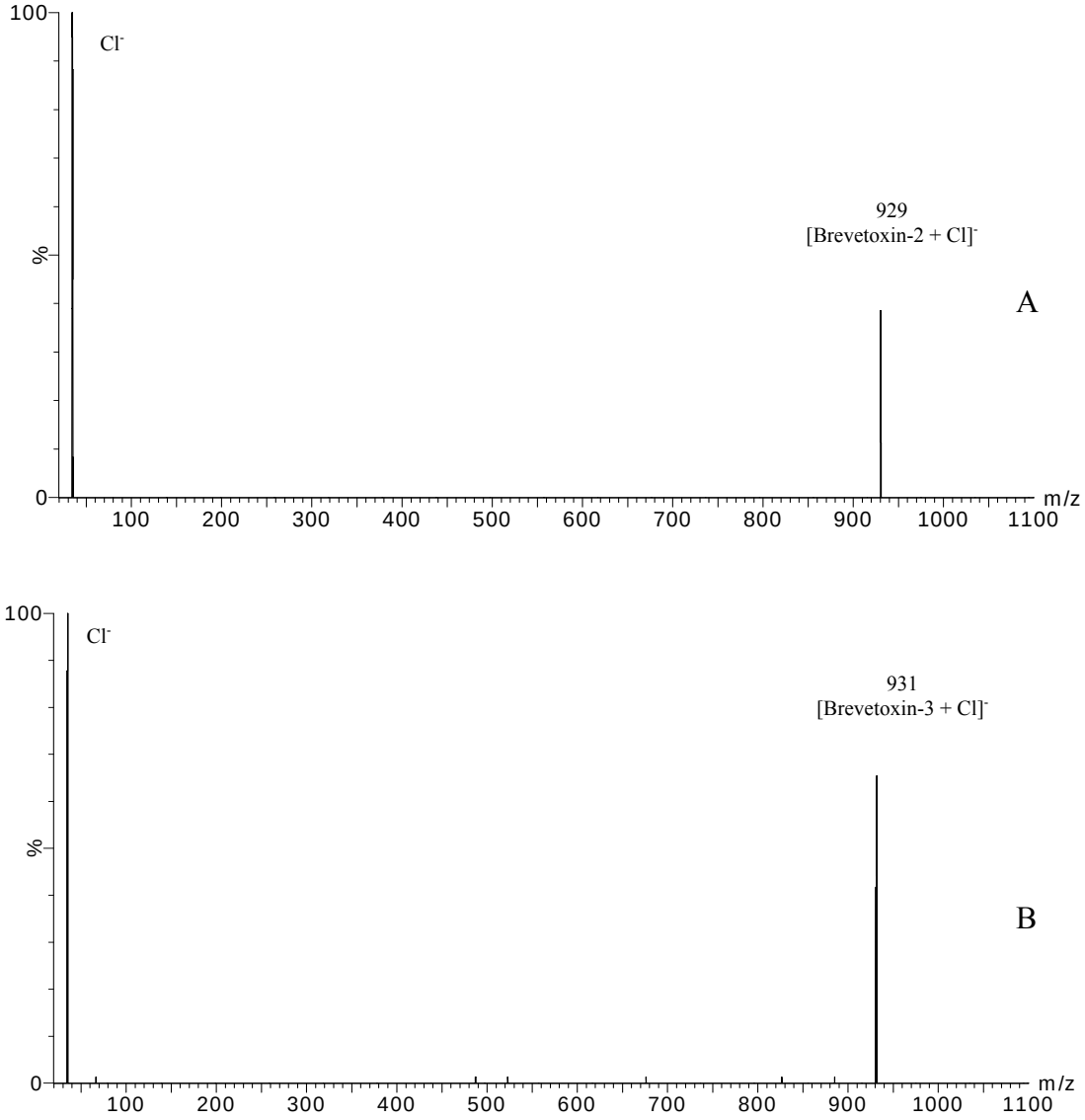

Figure 3.5. Unlike the fluoride adduct, chloride adduct precursors do not give informative fragments in product ion spectra. The sole ion at m/z 35 (Cl^-), and the absence of $[M - H]^-$, are caused by the weaker gas-phase basicity of chloride ion (1370 KJ/mol) versus that of fluoride (1530 KJ/mol). Similar product ion spectra showing only the dissociated anion were obtained for bromide, acetate, formate and nitrate adducts.

Table 1. Gas-Phase Bascities of Some Anions		
Anion	Gas Phase Bascity (KJ/mol)	Fragmentation of anionic adducts
Fluoride	1530.5 ± 1.3	Observed
Bicarbonate	1523 ± 8.4	Observed
Acetate	1427 ± 8.4	Not detected
Formate	1416 ± 8.4	Not detected
Chloride	1372.8 ± 0.84	Not detected
Bromide	1331.8 ± 0.84	Not detected
Nitrate	1329.7 ± 0.84	Not detected

Table 1. Gas-phase basicities of anions employed in this study [49].

fragment peaks and more structural information in CID experiments. It is therefore the anion of choice to analyze brevetoxins in negative mode electrospray by the anionic adduct approach.

Fragmentation pathways

Detailed fragmentation studies of complicated molecules such as the brevetoxins are important to identify or confirm their structures; they are also very useful to deduce the structures of metabolites. When structural modifications occur during metabolism, the MS/MS spectrum of the metabolites can readily reflect the alterations. By comparing MS/MS spectra of the metabolites with the fragmentation patterns of the starting compound, mass shifts of certain peaks can give an indication of the sites at which biotransformations take place. Moreover, the peaks that appear at the same masses for the metabolites and starting material can indicate portions of the molecule that are not altered. Detailed mechanisms to rationalize fragmentations of the two studied brevetoxins are illustrated in Schemes 1, 2 and 3. Upon collisional activation of the m/z 915 [brevetoxin-3 + F]$^-$ precursor where fluoride ion has attached to the hydroxyl group (Scheme 1), a hydrogen fluoride molecule first leaves the adduct to yield [brevetoxin-3 - H]$^-$ at *m/z* 895. The negative charge left on the oxygen then initiates a charge-driven fragmentation, yielding m/z 97 ions. The analogous mechanism also applies to [brevetoxin-2 + F]$^-$ adducts and results in the peak at m/z 95. Another possible site for fluoride attachment is the allylic hydrogen on the "tail" portion of the brevetoxin molecule (scheme 1, Pathway 2). After HF loss and subsequent water loss, the negative charge on the allylic site of m/z 875 ion may

undergo another charge driven-fragmentation. After J-ring opening, the negative charge may have a Michael reaction-like ring formation step (scheme 1), and after a hydrogen transfer, a seven-membered ring with a stable conjugate double bond system is formed (m/z 135 fragment, scheme 1). The analogous route will lead to the m/z 133 for [brevetoxin-2 + $F]^-$ adducts (figure 3.2a) and [brevetoxin-2 + $HCO_3]^-$ (figure 3.4a).

In scheme 2, another mechanism was proposed, fluoride ion first attaches to the allylic hydrogen at the tail part and leaves as a neutral molecule. The remaining negative charge then may take a different route and break the O-C bond in the J-ring, forming an ion-dipole complex. The dissociation of this complex will result in m/z 741 (figures 3.2a and 2b), but if proton transfer occurs, it will yield m/z 151 for [brevetoxin-2 + $F]^-$ adducts (figure 3.2a) or m/z 153 for [brevetoxin-3 + $F]^-$ adducts (figure 3.2b).

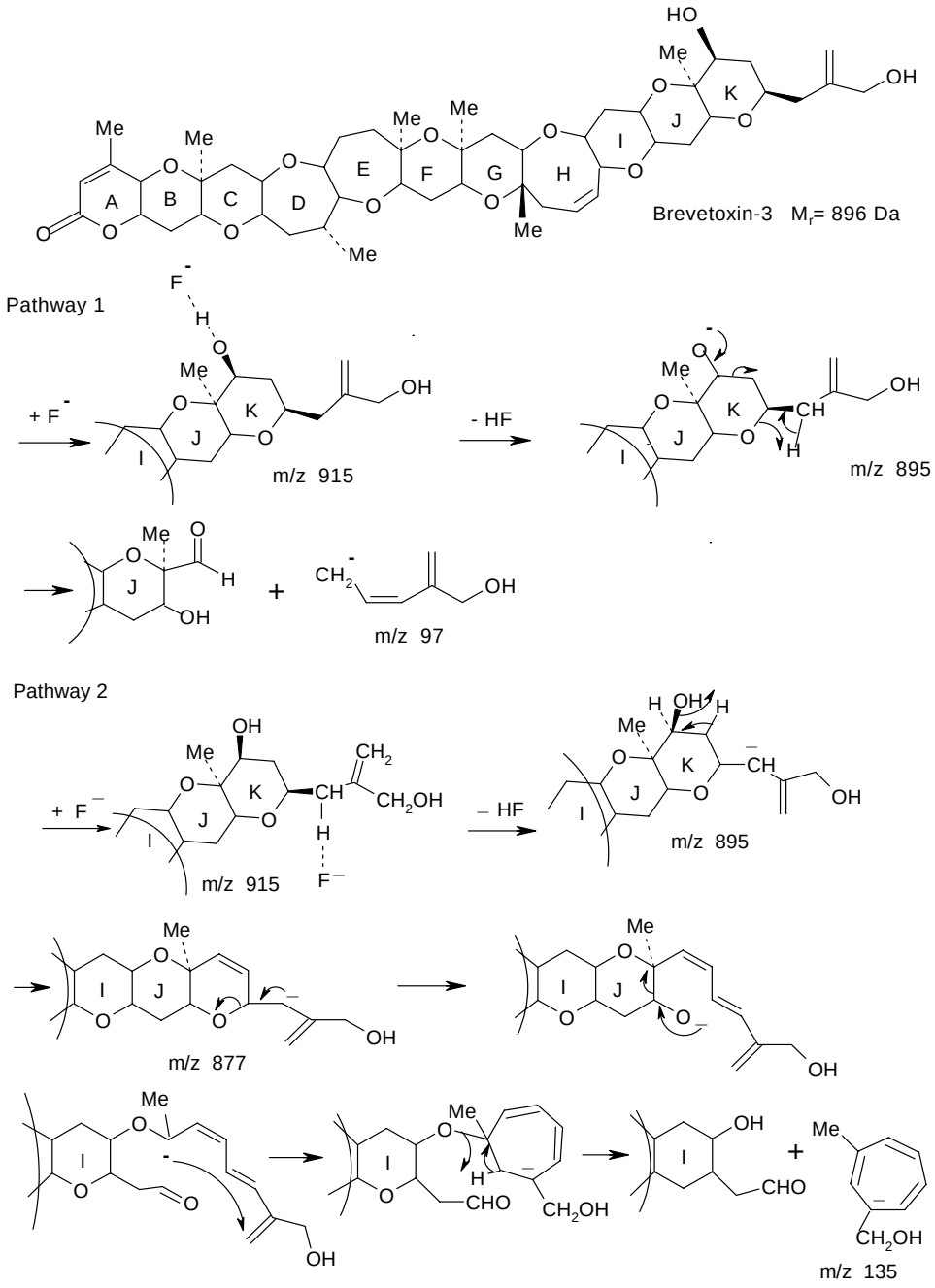

Scheme 1. Proposed fragmentation pathways for [Brevetoxin-3 + F]$^-$, leading to m/z 97 and 135. A similar route also applies to m/z 95 and 133 formation from [Brevetoxin-2 + F]$^-$ and for deprotonated brevetoxins after ammonium hydroxide addition.

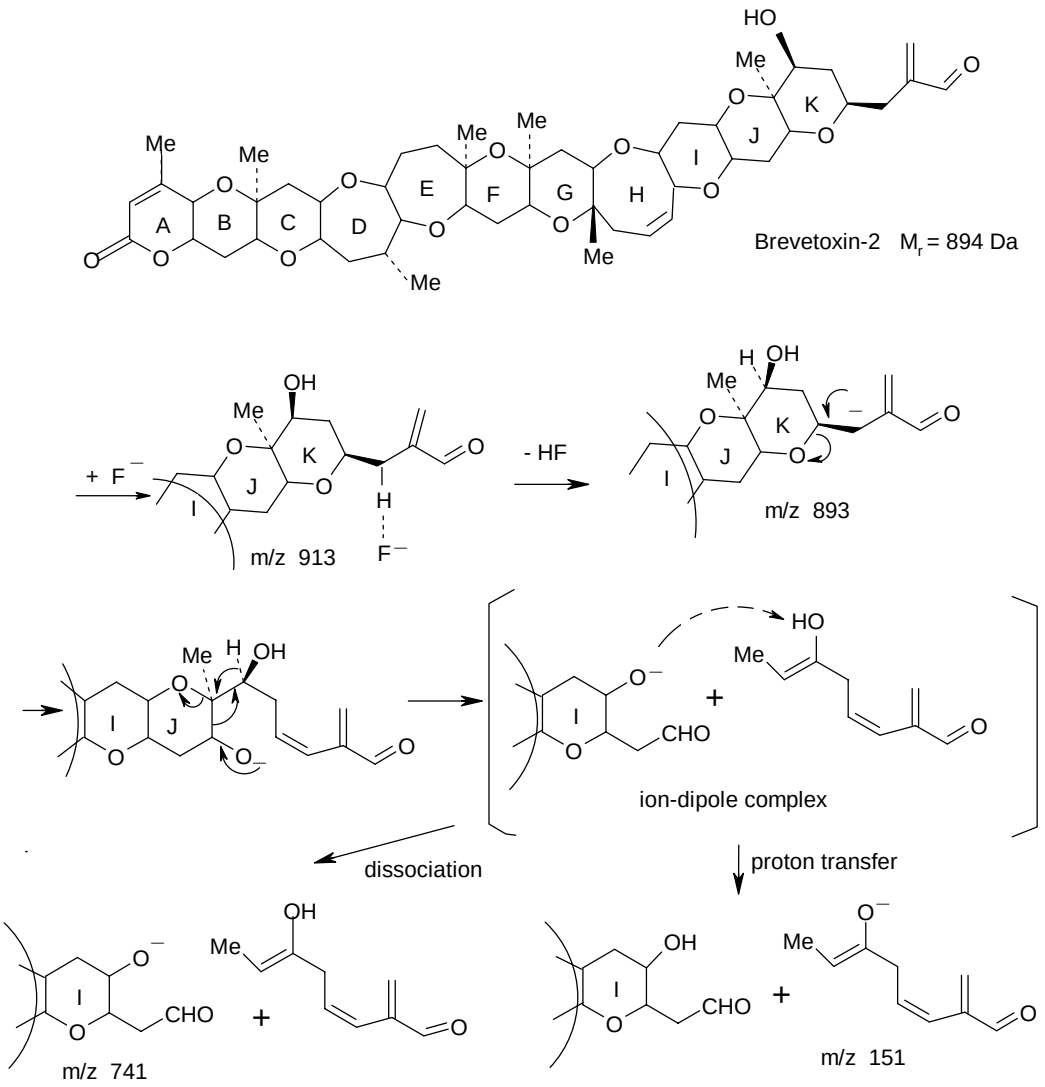

Scheme 2. Proposed fragmentation pathways for [Brevetoxin-2 + F]$^-$, leading to m/z 151 and 741. Similar routes also apply to [Brevetoxin-3 + F]$^-$, yielding m/z 153 and 741 respectively and for deprotonated brevetoxins after ammonium hydroxide addition.

Generated either directly from the deprotonated precursor [brevetoxin-3 - H]$^-$ at *m/z* 895, or as shown in Scheme 3, where carbonic acid is lost from the initial [brevetoxin-3 + HCO_3]$^-$ adduct and the negative charge becomes localized on the oxygen atom attached to the K-ring, the residing charge breaks open the K-ring, causing the loss of its "tail" portion as an alkene. This produces the m/z 797 peak (figures 3.4a and 3.4b) and analogous ions in figures 3.2a, 3.2b, 3.3a and 3.3b. The ensuing charge driven fragmentation may break ring J (scheme 3) and yield m/z 725 peak (scheme 3). Another possible pathway is that after ring J is broken, the charge on the tertiary carbon may initiate two-hydrogen-transfers to produce the peak at m/z 739 (scheme 3). In fact, these two peaks are not only seen in the product ion scans of [M + HCO_3]$^-$ adducts, but also in the MS/MS spectra of [M + F]$^-$, [M + FHF]$^-$, and [M - H]$^-$ ions, and m/z 739 usually appears in higher abundance than m/z 725.

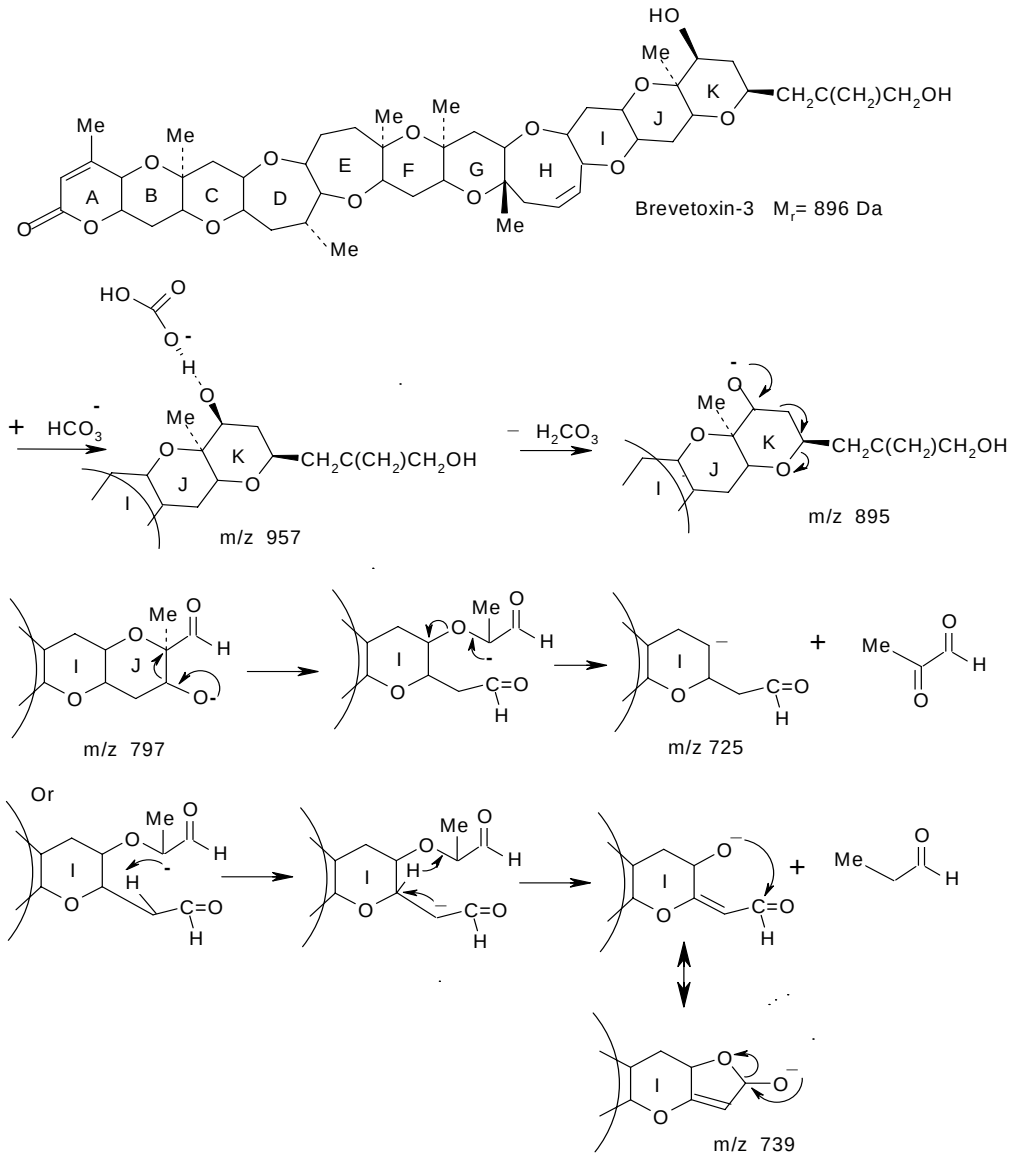

Scheme 3. Proposed fragmentation mechanisms for [Brevetoxin-3 + HCO3]$^-$ yielding m/z 797, 725 and 739. Analogous pathways also can apply to [Brevetoxin-2 + HCO3]$^-$ and fluoride adducts.

Influence of Cone Voltage

The optimization of experimental parameters in negative electrospray mass spectrometry is quite important to obtaining high signal-to-noise ratios. One critical parameter is the potential difference between the sampling cone and skimmer i.e. the so-called "cone voltage" or nozzle-skimmer voltage. A detailed study of the effect of this voltage on observed signals of three relevant ions was conducted using a water/acetonitrile system (1:1 by volume) containing 0.05 mM brevetoxin-3 (896 Da neutral) and a concentration of 0.5 mM ammonium fluoride (figure 3.6A and graph 1). The bifluoride adduct [brevetoxin-3 + FHF]$^-$, at m/z 935, was the first component to reach its maximum abundance at 20 V, and then it dropped off quickly. The abundance of [brevetoxin-3 + F]$^-$, at m/z 915, on the other hand, kept increasing with voltage until it reached its peak at 40 V. This is partially due to the instability of [brevetoxin-3 + FHF]$^-$ which dissociated to yield [brevetoxin-3 + F]$^-$ when the cone voltage was raised above 20 V to help elevate the m/z 915 signal. As the cone voltage increased beyond 40 V, [brevetoxin-3 + F]$^-$ underwent in-source CID, yielding [brevetoxin-3 - H]$^-$, at m/z 895. The resulting [brevetoxin-3 - H]$^-$ exhibited the highest signal at 60 V; after this point, an increasing cone voltage resulted in in-source CID that imparted energy high enough to break covalent bonds, and the abundance of [M - H]$^-$ began to fall. The experiment with brevetoxin-2- NH_4F system showed similar results, with optimal cone voltage for [brevetoxin + FHF]$^-$, [brevetoxin-3 - H]$^-$ and [brevetoxin-3 + F]$^-$ at 20, 40 and 60 V respectively. These respective values were used as the operating cone voltages when MS/MS experiments were conducted on the corresponding precursors.

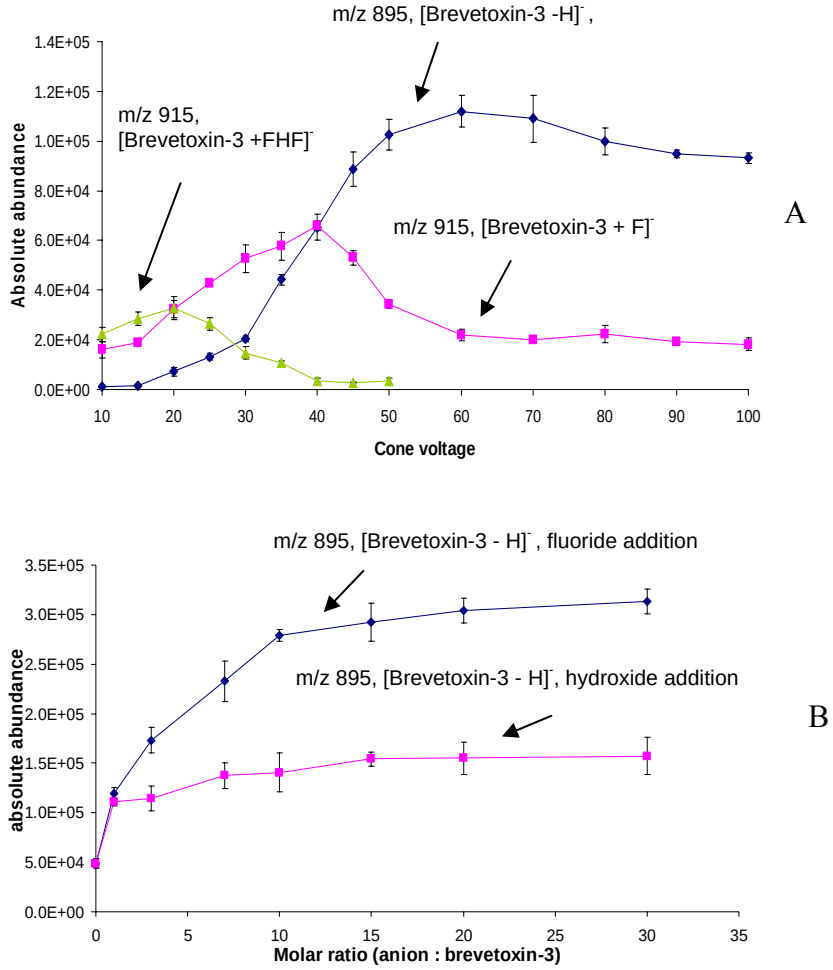

Figure 3.6. A) Ion abundance vs. cone voltage for brevetoxin-3 molecular ions from a 1:1 water/acetonitrile system containing 0.05 mM brevetoxin-3, and 0.5 mM NH4F. The abundance of [brevetoxin-3 + FHF]$^-$ reaches its maximum at 20 V, the abundance of [brevetoxin-3 + F]$^-$ reaches its maximum at 40 V, whereas that of [brevetoxin-3 - H]$^-$ reaches its maximum at 60 V. B) Absolute abundances of molecular ions of brevetoxin-3 vs molar ratio of anion : brevetoxin-3, cone voltage was set at 60V,

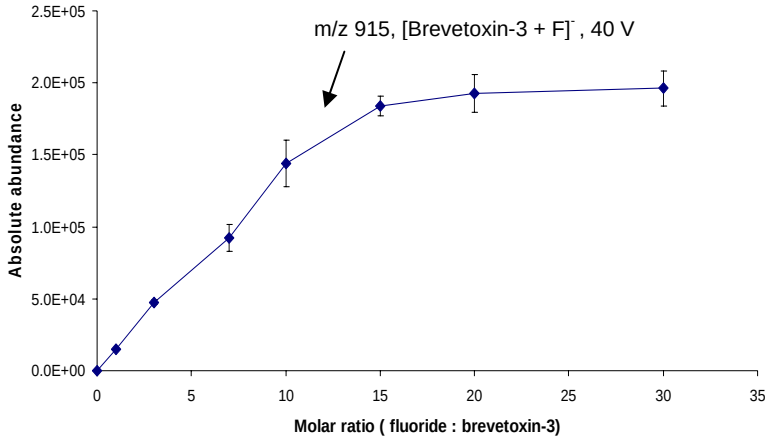

C

Figure 3.6. continued C) Absolute abundances of fluoride adducts of brevetoxin-3 vs molar ratio of fluoride : brevetoxin-3 at 40 V cone voltage. The concentration of brevetoxin-3 was set at 0.05 mM, while the concentration of NH_4F and NH_4OH was varied from 0 to 1.5 x mM. The cone voltage was set at 60 V. The abundance increase of $[M - H]^-$ slows beyond 10:1, and NH_4F serves better than NH_4OH to yield $[M - H]^-$ in high abundance.

Anion ratio study

Because brevetoxins are quite expensive reagents, in another experiment, we tried to optimize the addition of fluoride ions to achieve the highest signal intensity at low level brevetoxin concentrations. One series of mixtures are water/acetonitrile solutions (1:1 by volume) containing a fixed concentration of brevetoxin-3 (0.05 mM) and increasing concentrations of ammonium fluoride. The other series of mixtures are water/acetonitrile solutions (1:1 by volume) containing the same concentration of brevetoxin-3 and increasing concentrations of ammonium hydroxide. Under a fixed cone voltage of 60 V (i.e. the optimum value for $[\text{brevetoxin-3 - H}]^-$ drawn from Figure 3.6a), Figure 3.6b shows that when there was no additive in the system,(i.e. molar ratio on x-axis = 0 for plain organic/water solution), the signal of m/z 895, deprotonated brevetoxin-3 was low. Adding an amount of either ammonium fluoride or ammonium hydroxide equal to the analyte concentration each promoted the production of $[\text{brevetoxin-3 - H}]^-$ and in similar abundance. However, further increasing the concentration of hydroxide didn't increase $[\text{brevetoxin-3 - H}]^-$ significantly. In contrast, further increasing the fluoride concentration kept promoting the formation of $[\text{brevetoxin-3 - H}]^-$. This trend began to level off after a 10:1 molar ratio, but still slowly increased until 30:1. From Figure 3.6b, it can be see that fluoride is a more efficient additive to promote the formation of $[\text{brevetoxin-3 - H}]^-$ compared to the commonly used weak base ammonium hydroxide.

When employing a fixed cone voltage of 40 V, the optimum value for the formation of $[M + F]^-$ (from figure 3.6a), a test similar to the one above showed that the abundance of the $[M + F]^-$ brevetoxin-3 adduct increased rapidly as the fluoride: brevetoxin-3 ratio changed from 0 to 15:1

(Figure 3.6c). At higher molar ratios, a leveling off of $[M+F]^-$ signal was observed, and the extra ammonium fluoride will elevate the conductivity of the solution unnecessarily. Combining the two studies above, it is concluded that the optimal condition to study brevetoxins in negative mode electrospray mass spectrometry is to add a 10-15 fold excess of ammonium fluoride (relative to analyte concentration) to the solution and perform CID on the fluorideadducts at a cone voltage of 40 V, or on the deprotonated molecules at 60 V.

Metabolite sample analysis

Our previous study of microsomal brevetoxin-2 metabolites has elucidated the structure of one metabolite, brevetoxin-2-M1 as a hydrolysis product of brevetoxin-2 with A-ring opening [27]. Based on its retention time and mass, which are the same as those of a brevetoxin-3 standard, the other metabolite, brevetoxin-2-M2 was postulated to have the same structure as brevetoxin-3. By applying the fluoride adduct approach (using 0.1 mM ammonium fluoride in stead of water as mobile phase A), we analyzed an identically prepared microsomal metabolite sample in negative mode ES-MS, and obtained the product ion scan of brevetoxin-2-M2. The LC-MS traces of the brevetoxin-2 incubation sample are shown in Figure 3.7. Two main metabolite peaks were observed in addition to the peak representing unreacted brevetoxin-2. The selected ion chromatogram (SIC) of m/z 911 showed the peak at 4.5 min (figure 3.7b), which represents the metabolite brevetoxin-2-M1. The SIC of m/z 913, revealed the fluoride adduct of brevetoxin-2 at 8.5 min (figure 3.7c), while the SIC of m/z 915, showed the fluoride adduct of the 2nd metabolite brevetoxin-2-M2 at 7.7 min (figure 3.7d), its retention time matches that of brevetoxin-3

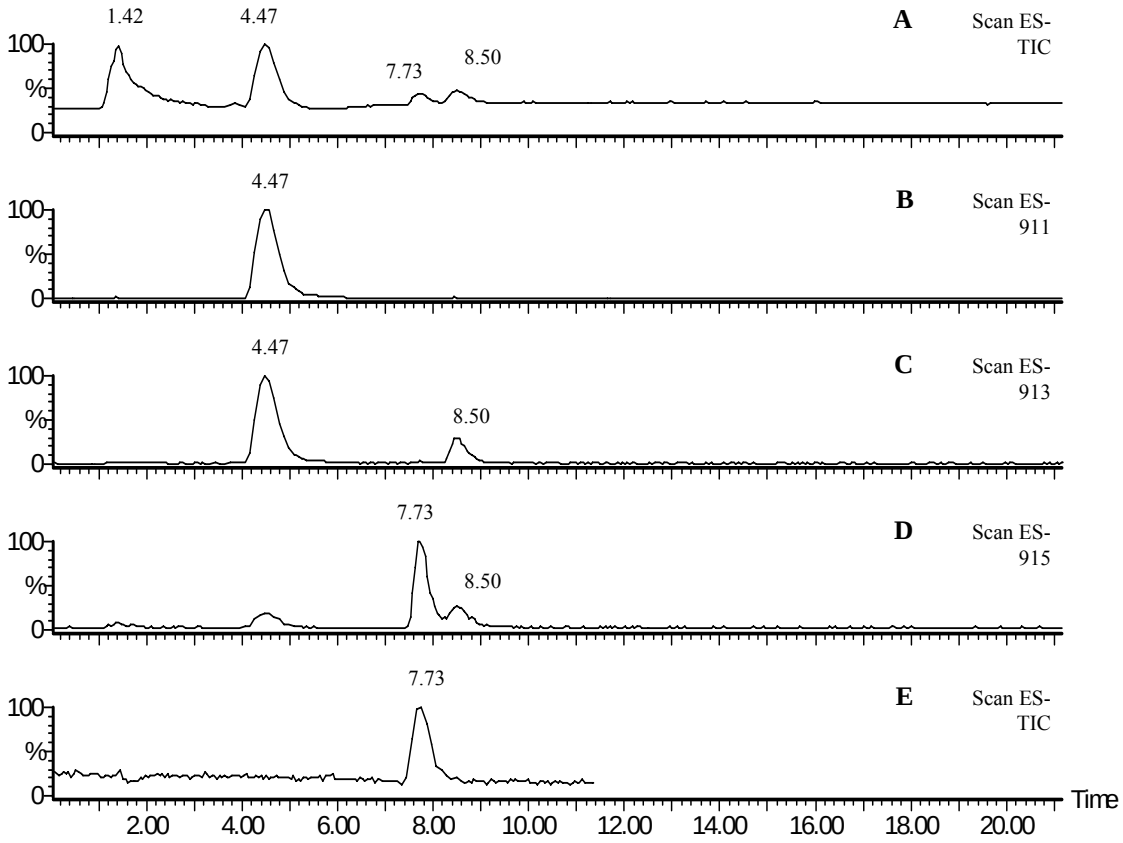

Figure 3.7. Negative mode electrospray LC-MS chromatograms for brevetoxin-2 sample that has undergone incubation with rat microsomes. a) TIC for incubation sample; b) SIC of m/z 911 from the incubation sample. The peak at 4.47 min represents metabolite brevetoxin-2-M1 (identified elsewhere as hydrolysis product with lactone "A" ring opening); c) SIC of m/z 913 from the incubation sample. In this chromatogram, the peak at 8.50 min represents the fluoride adduct of unreacted brevetoxin-2, whereas the peak at 4.47 min is the M+2 peak of brevetoxin-2-M1. d) SIC of m/z 915, metabolite [Brevetoxin-2-M2 + F]$^-$, that elutes at 7.73 min. The peak at 8.50 min is the M+2 peak of unreacted [brevetoxin-2 + F]$^-$. e) In a separate run, TIC for fluoride adduct of brevetoxin-3 standard, its retention time (7.73 min) is the same as that of [brevetoxin-2-M2 + F]$^-$.

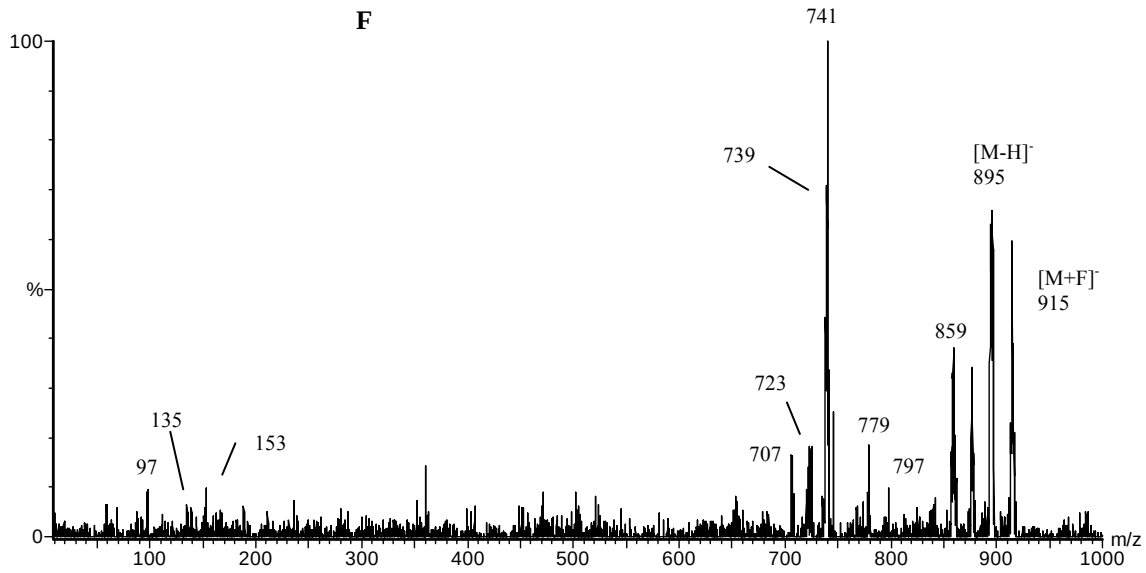

Figure 3.7. Continued f) LC-MS/MS negative mode product ion mass spectrum of m/z 915 at 7.73 min, [Brevetoxin-2-M2 + F]- from 7d above. The spectrum is very similar to that of the fluoride adduct of brevetoxin-3 standard (Fig. 2b). This indicates that Brevetoxin-2-M2 has the same structure as brevetoxin-3**.**

standard at the same LC-MS condition, which is shown in figure 3.7e; Moreover, CID of the fluoride adduct precursor of this metabolite shows a very similar fragmentation pattern to that of fluoride adducts of brevetoxin-3. It therefore confirmed our previous postulation that metabolite brevetoxin-2-M2 is actually brevetoxin-3, a metabolic reduction product of brevetoxin-2.

Conclusion

In this study, an electrospray mass spectrometry method was developed to enhance the CID performance of brevetoxins in negative mode electrospray, as well as to provide a different means to deduce structural information from brevetoxins. In a conventional water/organic solvent system, without the aid of a base, the abundances of brevetoxin ions are not strong enough for tandem MS studies. We have found that brevetoxins may form anionic adducts with fluoride, bicarbonate, chloride, bromide, formate, acetate and nitrate, although upon CID, $[M + Cl]^-$, $[M + Br]^-$, $[M + OAc]^-$, $[M + HCOO]^-$, $[M + NO_3]^-$ adducts only produced respective anions and do not provide structurally-informative fragments. On the other hand, both $[M + F]^-$ and $[M + HCO_3]^-$ adducts underwent fragmentations that yielded product ions that are similar to those of deprotonated brevetoxins, which indicated that the first step of gas phase decomposition of these two adducts is losing a neutral HF or a H_2CO_3 molecule, respectively. In comparing the two adducts, the fluoride adduct showed more informative fragment peaks than its bicarbonate counterpart; it is therefore the anion of choice for anionic adduct approach. The optimal cone voltage for the formation of fluoride adducts is 40 V; further elevating the cone voltage resulted in a decrease of the fluoride adduct signal while the abundance of deprotonated brevetoxins would become the base peak. Thus, this method also allows the production of deprotonated brevetoxins under mild conditions (near neutral pH). Under the same additive concentration and cone voltage, the abundance of deprotonated brevetoxin was higher when adding ammonium fluoride than when adding ammonium hydroxide. The addition of ammonium fluoride combined with the use of suitable cone voltages can significantly improve the ability to obtain structural information by negative mode electrospray tandem mass spectrometry for brevetoxins. Detailed

fragmentation mechanisms were also proposed. With this approach of adding fluoride to the mobile phase of LC-MS/MS, by comparing the retention time and the product ion scan spectrum of a brevetoxins-3 standard with those of an unknown metabolite of brevetoxin-2 in vitro microsomal incubation sample, the metabolite was confirmed to be brevetoxin-3.

References

1. Daugbjerg N, Hansen G, Larsen J, Moestrup O: **Phylogeny of some of the major genera of dinoflagellates based on ultrastructure and partial LSU rDNA sequesnce data**. *Phycologia* 2000, **39**(4):302-317.
2. Risk M, Lin YY, MacFarlane RD, Ramanujam VMS, Smith LL, Trieff NM: **Purification and chemical studies on a major toxin from *Gymnodinium breve.*** In: *Toxic Dinoflagellate Blooms : Proceedings of second International Conference on Toxic Dinoflagellate Blooms.* Edited by Taylor DL, Seliger HH. New York: Elsevier/North Holland; 1979: 335-344.
3. Walker ST: **Fish mortality in the Gulf of Mexico**. *Proc US Natl Mus* 1884, **6**(6):105-109.
4. Kimm-Brinson KL, Ramsdell JS: **The red tide toxin, brevetoxin, induces embryo toxicity and developmental abnormalities.** *Environ Health Perspect* 2001, **109**(4):377-381.
5. Baden DG, Bourdelais AJ, Jacocks H, Michelliza S, Naar J: **Natural and derivative brevetoxins: Historical background, multiplicity, and effects.** *Environ Health Perspect* 2005, **113**(5):621-625.
6. Gunter G, Williams RH, Davis CC, Smith FGW: **Catastropic mass mortality of marine animals and coincident phytoplankton bloom on the west coast of Florida, November 1946 to August 1947**. *Ecol Monogr* 1948, **8**:310-324.
7. Baden DG: **Brevetoxins: Unique polyether dinoflagellate toxins.** *FASEB J* 1989, **3**:1807-1817.

8. Quick JA, Henderson GE: **Evidences of new ichthyointoxicative phenomena in *Gymnodinium breve* red tide**. In: *Proceedings of the First International Conference on Toxic Dinoflagellate Blooms.* Edited by LoCicero VR. New York: Academic Press; 1975: 413-422.

9. Music SI, Howell JT, brumback CL: **Red tides: its public health implication**. *J Fla Med Assoc* 1973, **60**(1):27-39.

10. Baden DG: **Marine food borne dinoflagellate toxins**. *Inter Rev Cytology* 1983, **82**:99-150.

11. Steidinger KA, Joyce EAJ: **Florida red tides**. *Fla State Board Conserv Educ Ser* 1973, **17**:1-26.

12. Fleming LE, Backer LC, Baden DG: **Overview of aerosolized florida red tide toxins: exposures and effects.** *Environ Health Perspect* 2005, **113**(5):618-620.

13. Woodcock AH: **Note concerning human respiratory irritation associated with high concentrations of plankton and mass mortality of marine organisms**. *J Mar Res* 1948, **7**(1):56-62.

14. Backer LC, Fleming LE, Rowan A, Cheng YS, Pierce R: **Recreational exposure to aerosolized brevetoxins during Florida red tide events.** *Harmful Algae* 2003, **2**:19-28.

15. Wang W, Cole RB: **Improved protonation, collision-induced decomposition efficiency and structural assessment for 'red tide' brevetoxins employing nanoelectrospray mass spectrometry.** *J Mass Spectrom* 2006, **41**(8):996-1005.

16. Shimizu Y, Chou H, Bando H, VanDuyne G, Clardy JC: **Structure of Brevetoxin A (Gb-1 toxin), The Most Potent Toxin in Florida Red Tide Organism Gymnodinium breve.** *J Am Soc Chem* 1986, **108**:514-515.

17. Rein KS, Lynn B, Gawley RE, Baden DG: **Brevetoxin B: Chemical modifications, synaptosome binding, toxicity, and an unexpected conformational effect.** *J Org Chem* 1994, **59**:2107-2113.

18. Delaney JE: **Bioassay procedures for shellfish toxins**. In: *Laboratory Procedures for the Examination of Seawater and Shellfish.* Edited by Greenberg AE, Hung DA. Washington DC: American Public Health Association; 1985: 64-80.

19. Poli MA, Musser SM, Dickey RW, Wilers PP, S. H: **Neurotoxinc shellfish poisoning and brevetoxin metabolites: a case study from Florida.** *Toxicon* 2000, **38**(7):981-993.

20. Naar J, Bourdelais A, Tomas C, Kubanek J, Whitney PL, Flewelling L, Steidinger K, Lancaster J, Baden DG: **A competitive ELISA to detect brevetoxins from Karenia brevis (formerly Gymnodinium breve) in seawater, shellfish, and mammalian body fluid.** *Environ Health Perspect* 2002, **110**(2):179-185.

21. Dickey RW, Bencsath FA, Granade HR, Lewis RJ: **Liquid chromatograhic mass spectrometric methods for the determination of marine polyether toxins.** *Bull Soc Pathol Exot* 1992, **85**(5 Pt 2):514-515.

22. Hua Y, Lu W, Henry MS, Pierce RH, Cole RB: **On-line high performance liquid chromatography-electrospray ionization mass spectrometry for the determination of brevetoxins in "red tide" algae.** *Anal Chem* 1995, **67**:1815-1823.

23. Hua Y, Lu W, Henry MS, Pierce RH, Cole RB: **On-line liquid chromatography-electrospray ionization mass spectrometry for determination of the brevetoxin profile in natural "red tide" algae blooms.** *J Chromatography A* 1996, **750**:115-125.

24. Plakas SM, El Said KR, Jester EL, H. RG, Musser SM, Dickey RW: **Confirmation of brevetoxin metabolism in the Eastern oyster (*Crassostrea virginica*) by controlled exposures to pure toxins and to *Karenia brevis* cultures**. *Toxicon* 2002, **40**(6):721-729.

25. Plakas SM, Wang Z, El Said KR, Jester EL, Granade HR, Flewelling L, Scott P, Dickey RW: **Brevetoxin metabolism and elimination in the Eastern oyster (Crassostrea virginica) after controlled exposures to Karenia brevis.** . *Toxicon* 2004, **44**(677-685).

26. Wang Z, Plakas SM, El Said KR, Jester EL, Granade HR, Dickey RW: **LC/MS analysis of brevetoxin metabolites in the Eastern oyster (Crassostrea virginica)**. *Toxicon* 2004, **43**(4):455-465.

27. Wang W, Hua Y, Wang G, Cole RB: **Characterization of rat liver microsomal and hepatocytal metabolites of brevetoxins by liquid chromatography-electrospray tandem mass spectrometry.** *Anal Bioanal Chem* 2005, **383**(1):67-75.

28. Abraham A, Plakas SM, Wang Z, Jester ELE, El Said KR, Granade HR, Henry MS, Blum PC, Pierce RH, Dickey RW: **Characterization of polar brevetoxin derivatives isolated from Karenia brevis cultures and natural blooms.** *Toxicon* 2006, **48**(1):104-115.

29. Hua Y, Cole RB: **Solution reactivity of brevetoxins as monitored by electrospray ionization mass spectrometry and implications for detoxification**. *Chem Res Toxicol* 1999, **12(12)**:1268-1277.

30. Hua Y, Cole RB: **Electrospray ionization tandem mass spectrometry for structural elucidation of protonated brevetoxins in red tide algae.** *Anal Chem* 2000, **72**(2):376-383.

31. Nozawa A, Tsuji K, Ishida H: **Implication of brevetoxin B1 and PbTx-3 in neurotoxic shellfish poisoning in New Zealand by isolation and quantitative determination with liquid chromatography-tandem mass spectrometry** *Toxicon* 2003, **42**(1):91-103.

32. Ishida H, Nozawa A, Nukaya H, Tsuji K: **Comparative concentrations of brevetoxins PbTx-2, PbTx-3, BTX-B1 and BTX-B5 in cockle, Austrovenus stutchburyi, greenshell mussel, Perna canaliculus, and Pacific oyster, Crassostrea gigas, involved neurotoxic shellfish poisoning in New Zealand**. *Toxicon* 2004, **43**(7):779-789.

33. Radwan FFY, Wang Z, Ramsdell JS: **Identification of a Rapid Detoxification Mechanism for Brevetoxin in Rats.** . *Toxicol Sci* 2005, **85**(2):839-846.

34. Cai Y, Cole RB: **Stabilization of Anionic Adducts in Negative Ion Electrospray Mass Spectrometry**. *Anal Chem* 2002, **74**:985-991.

35. Yamashita M, Fenn J: **Negative Ion Production with the Electrospray Ion Source.** *J Phys Chem* 1984, **88**:4671-4675.

36. Cole RB, Zhu J: **Chloride Anion Attachment In Negative Ion Electrospray Ionization Mass Spectrometry.** *Rapid Commun Mass Spectrom* 1999, **13**: 607-611.

37. Zhu J, Cole RB: **Formation and decompositions of chloride adduct ions, [M + Cl]-, in negative ion electrospray ionization mass spectrometry**. *J Am Soc Mass Spectrom* 2000, **11(11)**:932-941.

38. Zhu J, Cole RB: **Ranking of Gas-Phase Acidities and Chloride affinities of Monosaccharides and linkage Specificity in Collision-induced Decompositions of Negative Ion Electrospray-Generated Chloride adducts of Oligosaccharides**. *J Am Soc Mass Spectrom* 2001, **12**:1193-1204.

39. Cai Y, Concha MC, Murray JS, Cole RB: **Evaluation of the Role of Multiple Hydrogen Bonding in Offering Stability to Negative Ion Adducts in Electrospray Mass Spectrometry**. *J Am Soc Mass Spectrom* 2002, **13**(12):1360-1369.

40. Jiang Y, Cole RB: **Oligasaccharide analysis using anion attachment in negative mode electrospray mass spectrometry**. *J Am Soc Mass Spectrom* 2005, **16**(1):60-70.

41. Zhu J, Li YT, Li SC, Cole RB: **Structural characterization of gangliosides isolated from mullet milt using electrospray ionization-tandem mass spectrometry.** *Glycobiology* 1999, **9**(10):985-993.

42. Guan B, Cole RB: **Differentiation of Both Linkage Position and Anomeric Configuration in Underivatized Glucopyranosyl Disaccharides by Anion Attachment with Post-Source Decay in MALDI Linear-Field Reflectron TOF-MS**. *Rapid Comm Mass Spectrom* 2007, **21**:3165-3168.

43. Murae T, Takamatsu Y, Muraoka R, Endoh S, Yamauchi N: **Facile distinction of neutral and acidic tetraether lipids in archaea membrane by halogen atom adduct ions in electrospray ionization mass spectrometry.** *J Mass Spectrom* 2002, **37**:209.

44. Harvey DJ: **Fragmentation of Negative Ions from Carbohydrates: Part 1. Use of Nitrate and Other Anionic Adducts for the Production of Negative Ion Electrospray Spectra from N-linked Carbohydrates**. *J Am Soc Mass Spectrom* 2005, **16**(5):622-630.

45. Sheen JF, Her GR: **Analysis of neutral drugs in human plasma by fluoride attachment in liquid chromatography/negative ion electrospray tandam mass spectrometry.** *Rapid Commun Mass Spectrom* 2004, **18**(17):1911-1918.

46. Larson JW, McMahon TB: **Strong hydrogen bonding in gas-phase anions. An ion cyclotron resonance determination of fluoride binding energetics to Broensted acids**

from gas-phase fluoride exchange equilibrium measurements. *J Am Soc Chem* 1983, **105**:2944 - 2950.

47. Caldwell G, Kebarle P: **The hydrogen bond energies of the bihalide ions XHX- and YHX-**. *Can J Chem* 1985, **63**:1399.

48. Li GP, Reinhart B, Hamilton IP: **The complex of $HF2^-$ and H2O: A theoretical study.** *J Chem Phys* 2001, **115**(13):5883-5890.

49. Mallard WG, Linstrom PJ (eds.): **NIST Chemistry WebBook, NIST Standard Reference Database Number 69**. Gaithersburg MD, 20899 (http://webbook.nist.gov): National Institute of Standards and Technology; February 2000.

VITA

Weiqun Wang was born in Tianjin, China. He graduated from Nankai University in 1989 and obtained his B.S. degree in Chemistry. He then worked as an assistant engineer at Tianjin Automobile Company till 1991. Later he obtained his M.S. in Chemistry in 1994 from Nankai University and worked at Second Hospital of Tianjin Medical University until he came to University of New Orleans in 1999 to pursue his PhD. degree. He earned his M.S. degree in 2004, due to the aftermath of Hurricane Katrina, he started to work at Lexicon Pharmaceuticals in New Jersey in 2006 while manage to complete his PhD program in part time.